UNCLASSIFIED

AD NUMBER
AD383407
CLASSIFICATION CHANGES
TO: **UNCLASSIFIED**
FROM: **CONFIDENTIAL**
LIMITATION CHANGES
TO: **Approved for public release; distribution is unlimited.**
FROM: **Distribution authorized to U.S. Gov't. agencies and their contractors; Critical Technology; JUL 1967. Other requests shall be referred to Air Force Rocket Propulsion Lab., Attn: RPPR/STINFO, Edwards AFB, CA 93523. This document contains export-controlled technical data.**
AUTHORITY
31 Jul 1979, DoDD 5200.10 AFRPL ltr dtd 5 Feb 1986

THIS PAGE IS UNCLASSIFIED

REPRODUCED AT GOVERNMENT EXPENSE

AD 383 407

AUTHORITY:
BERL ltr 5 Feb 64

THIS REPORT HAS BEEN DELIMITED
AND CLEARED FOR PUBLIC RELEASE
UNDER DOD DIRECTIVE 5200.20 AND
NO RESTRICTIONS ARE IMPOSED UPON
ITS USE AND DISCLOSURE.

DISTRIBUTION STATEMENT A

APPROVED FOR PUBLIC RELEASE;
DISTRIBUTION UNLIMITED.

SECURITY MARKING

The classified or limited status of this report applies to each page, unless otherwise marked.
Separate page printouts MUST be marked accordingly.

THIS DOCUMENT CONTAINS INFORMATION AFFECTING THE NATIONAL DEFENSE OF THE UNITED STATES WITHIN THE MEANING OF THE ESPIONAGE LAWS, TITLE 18, U.S.C., SECTIONS 793 AND 794. THE TRANSMISSION OR THE REVELATION OF ITS CONTENTS IN ANY MANNER TO AN UNAUTHORIZED PERSON IS PROHIBITED BY LAW.

NOTICE: When government or other drawings, specifications or other data are used for any purpose other than in connection with a definitely related government procurement operation, the U. S. Government thereby incurs no responsibility, nor any obligation whatsoever; and the fact that the Government may have formulated, furnished, or in any way supplied the said drawings, specifications, or other data is not to be regarded by implication or otherwise as in any manner licensing the holder or any other person or corporation, or conveying any rights or permission to manufacture, use or sell any patented invention that may in any way be related thereto.

CONFIDENTIAL

NO. C55-7C28.
DOCUMENT CONTROL

AD 383407

(TITLE UNCLASSIFIED) EXPERIMENTAL INVESTIGATION OF PREPACKAGED HYBRID PROPELLANT SYSTEMS

J. W. Homers
United Technology Center

FINAL REPORT AFRPL-TR-67-168
July 1967

Group 4
DOWNGRADED AT 3 YEAR INTERVALS
DECLASSIFIED AFTER 12 YEARS
DOD DIR. 5200.10

In addition to security requirements which must be met, this document is subject to special export controls and each transmittal to foreign governments or foreign nationals may be made only with prior approval of AFRPL (RPPR/STINFO), Edwards, California 93523.

This document contains information affecting the national defense of the United States within the meaning of the Espionage Laws, Title 18, U.S.C., Section 793 and 794, the transmission or revelation of which in any manner to an unauthorized person is prohibited by law.

Air Force Rocket Propulsion Laboratory
United States Air Force
Edwards Air Force Base, California

CONFIDENTIAL

NOTICES

When U. S. Government drawings, specifications, or other data are used for any purpose other than a definitely related Government procurement operation, the Government thereby incurs no responsibility nor any obligation whatsoever, and the fact that the Government may have formulated, furnished, or in any way supplied the said drawings, specifications, or other data, is not to be regarded by implication or otherwise, or in any manner licensing the holder or any other person or corporation, or conveying any rights or permission to manufacture, use, or sell any patented invention that may in any way be related thereto.

NO. C55-7C28. [redacted]
DOCUMENT CONTROL

(TITLE UNCLASSIFIED)
EXPERIMENTAL INVESTIGATION OF PREPACKAGED HYBRID PROPELLANT SYSTEMS

J. W. Hamers

Group 4
DOWNGRADED AT 3 YEAR INTERVALS
DECLASSIFIED AFTER 12 YEARS
DOD DIR. 5200.10

In addition to security requirements which must be met, this document is subject to special export controls and each transmittal to foreign governments or foreign nationals may be made only with prior approval of AFRPL (RPPR/STINFO), Edwards, California 93523.

This document contains information affecting the national defense of the United States within the meaning of the Espionage Laws, Title 18, U.S.C., Section 793 and 794, the transmission or revelation of which in any manner to an unauthorized person is prohibited by law.

FOREWORD

(U) The work performed under this project was in response to requirements of AFFTC Project 3058, Program Element No. 62405184, BPSN 623148. The Air Force program monitor is Lt. William Spangler, Air Force Rocket Propulsion Laboratory, Research and Technology Division, Edwards, California.

(U) This report is a technical summary of work conducted under extension of Contract No. AF 04(611)-10789 under which United Technology Center conducted an experimental investigation of prepackaged hybrid propellant systems.

(U) This report covers experimental work conducted at United Technology Center's Sunnyvale, California, research laboratories and United Technology Center's Coyote, California, processing laboratories during the period September 1966 through March 1967. The following professional workers made significant contributions to progress on this program:

R. Brogan
J. W. Hamers
G. A. Kinkel
R. A. Maraschin
D. R. Matthews
J. H. Murray

(U) This report contains classified information extracted from "Experimental Investigation of Prepackaged Hybrid Propulsion Systems (U)," UTC 2141-ITR1, February 1967. (CONFIDENTIAL, Group 4.)

(U) This technical report has been reviewed and is approved.

Lt. William Spangler
Approving Authority

UNCLASSIFIED ABSTRACT

(U) An applied research and development program has been conducted on prepackaged hybrid propellant systems suitable for application to advanced tactical missile requirements.

(U) An 18-in.-diameter flight configuration hybrid motor has been designed, fabricated, and tested. A high density, high specific impulse, hybrid propellant combination has been formulated; and a fuel grain geometry has been developed which will provide nearly constant fuel flow rate and permit nearly complete fuel utilization. Dual-thrust oxidizer injectors have been developed and successfully tested. A simple thrust control system has been designed, which will control the motor thrust at two levels and will permit multiple starts at either thrust level.

(U) The results of the program indicate that high density impulse hybrid propulsion systems are feasible for application to advanced tactical missiles.

PRECEDING PAGE BLANK-NOT FILMED

CONTENTS

CONTENTS (Continued)

ILLUSTRATIONS

ILLUSTRATIONS (Continued)

TABLES

ABBREVIATIONS AND SYMBOLS

Abbreviations

AN	ammonium nitrate
AP	ammonium perchlorate
DTA	differential thermal analysis
HFX 7808	fuel system consisting of 5% boron, 30% TFTA, 30% AP, and 35% R-binder
O/F	gravimetric mixture ratio of oxidizer-to-fuel
OFHC	oxygen-free high conductivity
PBD	polybutadiene binder, hydroxyl terminated
QX/DER	3812 QX binder with DER 332 curative (Dow Chemical Co.)
R-binder	polybutadiene binder, hydroxyl terminated
TAZ	triaminoguanidine azide
TCA	thrust chamber assembly
TDI	toluene diisocynate
TFTA	tetraformaltrisazine
THA	triaminoguanidine azide-hydrazine azide
UTC	United Technology Center

Symbols

A	area, $in.^2$
a	regression rate constant
A_p	instantaneous cross-sectional area of fuel grain port, $in.^2$
C_D	orifice discharge coefficient
D	diameter, in.
ΔP	pressure differential, psi
F_{avg}	average thrust, lb
GH_z	gigahertz, 10^9 cycles/sec

G_o	oxidizer mass flux = $\frac{\dot{w}_{ox_H}}{A_p}$, lb/sec-in.^{2}
I_{sp}	specific impulse, sec
L	length of fuel grain, in.
L_g	grain length
L_{nozzle}	nozzle expansion cone length
m	pressure exponent
ηI_{sp}	specific impulse efficiency
n	oxidizer mass flux exponent
P_b	port burning perimeter, in.
P_c	chamber pressure, psia
$P_{c\ avg}$	average chamber pressure, psia
$\dot{r}$	regression rate (in./sec) or erosion rate, (mil/sec) depending on application
ρ_f	fuel density, lb/in.^{3}
ρI_{sp}	density impulse, gm-sec/cc
S	grain burning surface area, in.^{2}
t_b	burning duration, sec
$\dot{w}_f$	fuel flow rate, lb/sec
$\dot{w}_{ox}$	oxidizer flow rate, lb/sec
$\dot{w}_{ox_H}$	oxidizer flow rate to the head end of the grain
$\dot{w}_p$	total propellant flow rate

Subscripts

a	orifice a	maximum	boost thrust conditions
b	orifice b	minimum	sustain thrust conditions
c	orifice c	t	nozzle throat
e	nozzle exit	p	grain port

PRECEDING PAGE BLANK-NOT FILMED

SECTION I

INTRODUCTION

(U) Under Contract No. AF 04(611)-10789, UTC has been conducting an applied research and development program on prepackaged hybrid propellant systems suitable for application to advanced tactical missile requirements. The scope of the program was to develop a hybrid TCA capable of delivering approximately 200,000 lb-sec of impulse; the impulse to be deliverable from storable prepackaged propellants at either of two thrust levels — 5,000-lb (boost thrust) and 2,500-lb (sustain thrust), with up to two motor restarts after short coasting periods. The program consisted of evaluations of candidate fuel systems and ingredients (for which studies were initiated under Contract No. AF 04(611)-8516), development of flight configuration thrust chamber components including injectors and an oxidizer flow control system, and demonstration testing of complete hybrid TCAs.

(U) The program was divided into four phases: phase I — fuel development, phase II — subscale motor studies, phase III — full-scale motor development, and phase IV — full-scale motor demonstration. Phases I and II were completed during an initial 9-month effort (April 1965 through January 1966); however, technical difficulties in fuel formulation and subscale testing caused the effort to be suspended temporarily with phase III approximately 30% complete and phase IV not initiated. The results of this effort are presented in reference 1, which constitutes a part of this final report. This report is a summary of the work accomplished during the period from September 1966 through March 1967 as a continuation of Contract No. AF 04(611)-10789 in the completion of phases III and IV.

(U) Six full-scale heavyweight TCAs were tested, four of which were used to complete phase III and two in the accomplishment of phase IV. The first two motors were subjected to a series of multiple firings at the two thrust levels of concern to further characterize the fuel system and the grain geometry, and for component evaluation. The second two assemblies incorporated component and flow refinements and were used in firings simulating the final two demonstration tests. The final two assemblies accomplished, with representative duty-cycle firings, phase IV — full-scale motor demonstration.

(U) The program has resulted in the development of all flight configuration TCA components, including oxidizer injectors, oxidizer flow control valves, fuel grain geometry, nozzle, and thrust chamber. Numerous subscale and full-scale motor tests have been conducted with the components and thrust chambers. These tests have shown that a high density hybrid propulsion system is feasible for application to advanced tactical missiles.

SECTION II

SUMMARY

(U) The suitability of prepackaged hybrid propulsion systems for advanced tactical missile applications has been successfully demonstrated through extensive laboratory, subscale motor, and full-scale motor testing. As a part of the studies, an appropriate hybrid propellant combination was selected, developed, and characterized; an oxidizer flow control and injection system was designed and developed; and a unique fuel grain geometry was designed and characterized. Other important areas evaluated included various nozzle configurations, insulation materials, a heavyweight TCA, and a flightweight fiberglass-cased TCA. Combined testing consisted of 16 full-scale tests, 61 5-in. subscale motor tests, 48 3.5-in. subscale motor tests, 79 laboratory research motor tests, and 34 optical bomb tests.

(C) In the initial 9-month effort,[1]* three full-scale tests with the flightweight TCA were conducted as well as 61 5-in. motor tests, 48 3.5-in. tests, 79 laboratory tests, and the optical bomb studies. System studies, followed by laboratory and subscale motor tests, led to the selection of a castable fuel system capable of multiple restarts and consisting of 30% TFTA, 5% boron, 30% AP, and 35% binder to be used in combination with ClF_5 as the oxidizer. Flightweight hybrid TCAs, designed for 1,000 psia chamber pressure during boost thrust (5,000 lb) operation and 500 psia during sustain thrust operation, were fabricated and test fired for durations up to 15 sec. A thrust control system consisting of a dual element solenoid valve, six dual-flow forward oxidizer injectors, and a single aft oxidizer injector was developed to control operation of the TCA at either thrust level while maintaining essentially constant mixture ratio. The flight configuration valve was fabricated and bench flow tested in preparation for full-scale motor tests; the injectors were used in both subscale and full-scale motor firings.

(C) A unique multiple-port fuel grain geometry which provides 92% cross sectional loading and only 7% residual fuel sliver was devised and evaluated in both subscale and full-scale motor studies. The geometry, when matched to the proper fuel, was designed to deliver essentially constant fuel flow rates and thereby a constant mixture ratio while permitting dual-thrust operation.

---

* Superscript numbers denote references appearing on page 85.

(C) During the recent 6-month phase, a heavyweight steel-walled TCA, designed to incorporate the existing internal flight configuration motor design, was used to conduct 13 firings (12 fixed-thrust and one cycled) achieving a specific impulse efficiency near 96% and demonstrating 96% fuel utilization. Six heavyweight TCAs were fabricated during the program; four were employed to characterize the fuel regression behavior and to verify component design concepts, and two to demonstrate TCA operation over representative duty cycles. These studies resulted in: (1) the establishment of a fuel regression-oxidizer mass flux-pressure relationship; (2) evaluation, refinement, and demonstration of flight configuration components; (3) characterization and development of the multiple-port, high volumetric loaded grain geometry; (4) characterization and demonstration of a high density-impulse hybrid propellant combination having very favorable radar attenuation properties; and (5) successful demonstration of overall TCA performance when subjected to duty cycle firings consisting of dual-thrust and on-off operation

(C) The high density-impulse hybrid propellant system has consistently exhibited excellent thrust termination and restart capability with no evidence of fuel degradation. Radar measurements made during motor firings have shown this propellant combination to have low radar attenuation.

(U) Components (oxidizer injectors, insulation, and nozzle) utilizing practical design concepts and material applications have been developed which will withstand the chemical and thermal environment and are capable of repeated thermal cycling (multiple engine starts).

(U) A high volumetric-loaded fuel grain geometry was devised and refined to provide a uniform and predictable burning profile which results in almost complete fuel utilization.

(U) The accomplishments of this program indicate that all facets of full-scale motor development have been explored with results showing the feasibility of hybrid propulsion systems for prepackaged applications.

SECTION III

DESIGN

(U) Experimental efforts and associated support studies to investigate prepackaged hybrid propellant systems for advanced tactical missile applications conducted under the initial 9-month program were continued under the recently completed 6-month program. These investigations have been concerned primarily with the development of the propellant system, the fuel grain geometry, the oxidizer flow control system, the oxidizer injection system, and the TCA portions of the propulsion system.

1. DESIGN CRITERIA

(C) The main objective was to develop a system capable of dual-thrust and multiple start operation. The engine performance and design requirements are summarized in table I. In addition to these requirements, the system must meet the following criteria:

A. The propellant combination must be earth storable, have a relatively high impulse density, and favorable exhaust radar properties.

B. The system must be capable of delivering the impulse in a dual-thrust mode with two motor restarts after short coasting periods.

C. The boost thrust level is 5,000 lb with flexibility to deliver 60% to 100% of the system total impulse during boost.

D. The sustain thrust level is 2,500 lb with flexibility to deliver 0% to 50% of the system total impulse during sustain.

E. The system must demonstrate acceptable fuel utilization and total impulse efficiency.

2. PROPELLANT SYSTEM

(C) Propellant studies conducted in phases I and II resulted in the successful development of four high-density, high-specific impulse fuels which are suitable for prepackaged hybrid propulsion systems. However, one, and

TABLE I

(U) DESIGN REQUIREMENTS

Thrust, delivered (nominal high/nominal low), lb	5,000/2,500
Chamber pressure (nominal high/nominal low), psia	1,000/500
Total impulse, lb-sec	200,000
Number of engine starts	3

possibly two (see section III, part 2b-Fuel Development), are not suited for advanced tactical mission applications requiring on-off operation because of their tendency to sustain combustion on termination of oxidizer flow.* All the fuels contain TFTA, boron, AP, and all are castable. A comprehensive discussion of the fuel development effort is available in reference 1.

(C) The hypergolic propellant combination that was selected for development of the full-scale motor consists of a solid fuel (designated HFX 7808) containing 30% TFTA, 5% boron, 30% AP, and 35% hydroxyl-terminated binder with ClF_5 as the oxidizer. This combination has a theoretical optimum specific impulse of 284 sec (1,000/14.7 psia, O/F = 2.0) and a density impulse of 453 gm-sec/cc. With further development the four component blend has a potential specific impulse of 294 sec and a density impulse of 503 gm-sec/cc.

a. Propellant Criteria

(U) Hybrid propellants, in order to be suitable for application to tactical missile systems, must deliver a relatively high specific impulse, and possess an adequate high temperature

* A nonsustaining fuel is one which permits abrupt termination of thrust and does not continue to consume or degrade itself after oxidizer flow is terminated. Even pure binder can appear to sustain combustion if large quantities of graphite and nonablative insulation materials are used in the construction of the motor. These materials, which absorb heat during the firing, can radiate or conduct energy to the adjacent fuel or insulation materials after the firing. Volatilization of fuel and insulation occurs until the motor components are sufficiently cool. Meanwhile, reaction of the volatiles with air outside the motor gives a false impression of continued internal combustion, the duration of which is dependent on the size and type of heat absorbing materials used.

bulk density to meet weight and volume limitations. The fuel must not sustain combustion on termination of oxidizer flow if on-off operation is to be achieved. In addition, the propellants should provide smooth and reproducible hypergolic ignition and efficient combustion, and should have exhaust products which produce favorable radar characteristics.

(C) Fuels consisting of boron or aluminum, AP, a nitrogen containing additive, and a binder were selected for use with ClF_5, BrF_5, and ClO_3F oxidizers in achieving a propellant system meeting the above requirements. These fuels were selected for development and demonstration in full-scale motors because calculations had shown that they could provide specific impulse values near 295 sec with density impulse values near 503 gm-sec/cc. Other fuels were available which exceed the selected combinations in performance but were not considered because of other disadvantages. For example, higher specific impulse is available with lithium-containing hybrid fuels, but the lithium has relatively low density and unfavorable exhaust radar properties. Extremely high density impulse values can be obtained using high boron loading and BrF_5 oxidizer, but at the expense of correspondingly low specific impulse values.

(U) System design studies were conducted with consideration to the selection of those propellant characteristics which yield maximum vehicle performance consistent with weight and volume restrictions of a typical missile system. The propellant formulations found to offer greatest potential were those which have the highest specific impulse while exhibiting a bulk propellant density sufficient to meet the weight and volume limitations imposed by the mission.

(C) The conclusions derived from this study indicated that the oxidizers selected should be limited to those which primarily produce high specific impulse but with the highest possible density impulse. Therefore, the criteria favored the use of ClF_5 with its generally higher specific impulse rather than BrF_5 with its high density impulse and generally lower specific impulse. The study also indicated that ClF_5/ClO_3F mixtures offer increased vehicle performance over ClF_5 when the oxidizer temperature does not exceed 175° F. However, for systems which operate above that temperature, the reduced bulk density of ClO_3F containing oxidizers severely diminish vehicle performance. Up to 10% ClO_3F may be used

in systems which operate at 175°F, but if oxidizer temperatures up to 195°F are anticipated, only ClF_5 should be considered. The bulk density of propellant systems using ClO_3F can be improved upon by the addition of BrF_5 to the blend, but then the reduction in specific impulse results in vehicle performance which is no better than that obtained using pure ClF_5 as oxidizer.

(U) In addition to performance and propellant bulk density, the selection of a fuel formulation containing four components was further guided by the processability of the propellant blends and the relative cost of ingredients.

b. Fuel Development

(C) The four hybrid fuel systems listed in table II were developed for application to advanced tactical missile propulsion systems. Each of the fuels is suitable for use with ClF_5 oxidizer and will deliver an increase in performance if ClO_3F is added to the oxidizer in small percentages.

TABLE II

(U) PREPACKAGED HYBRID PROPELLANTS DEVELOPED AND TESTED UNDER THIS CONTRACT

	Fuel System*			
	1	2	3	4
TFTA, %	30	22.5	20	15
Boron, %	5	15	9	15
AP, %	30	35	52	40
R-binder, %	35	27.5	19	30
ClF_5 oxidizer†				
I_{sp}, sec	284	288	294	292
ρI_{sp}, gm-sec/cc	453	475	503	491
ClF_5/ClO_3F oxidizer blends				
I_{sp}, sec	289	292	---	---
ρI_{sp}, gm-sec/cc	448	479	---	---
Oxidizer	80% ClF_5/ 20% ClO_3F	90% ClF_5/ 10% ClO_3F	---	---

* Performance figures are for 1,000/14.7 optimum expansion at optimum mixture ratio.

† Performance figures are approximately 6% lower with ClF_3.

(C) Fuel No. 1, which was selected for full-scale motor development, is castable with "as received" ingredients. Fuel No. 2 requires the boron ingredient to be combined in a 1:1 ratio with TFTA in particles called prills, measuring 1/16 in. to 3/16 in. Both fuels were demonstrated to be nonsustaining in subscale motor tests. Fuel No. 3 used the AP in pellet form and was demonstrated to be nonsustaining in certain subscale tests.(1) However, additional fuel studies are required to be assured of nonsustaining combustion characteristics. Fuel No. 4 is castable with "as received" ingredients but is known to be a sustaining fuel system and is therefore not suited for on-off operation. However, its performance and high regression rate make it extremely attractive for an application where variable thrust operation is required and restart capability is not.

(U) These fuels were developed in studies which included investigation of propellant system performance, processing techniques, and combustion characteristics. Each fuel represents the maximum performance obtainable with the four components when present state-of-the-art processing techniques and the resultant fuel combustion characteristics are considered (i.e., some of the formulations require certain prilled or pelletized constituents, compacting, etc.).

c. Propellant Ingredients

(U) Some of the considerations involved in selection of the fuel ingredients are discussed in this section.

(1) Binder

(U) The primary ingredient of any fuel system is its binder, which provides a matrix to hold the fuel. The binder is generally high in carbon content but may vary in content of hydrogen, nitrogen, and oxygen. Of interest in the selection of the binder is the quantity of oxygen from the oxidizer and other fuel sources needed to consume carbon and produce high performance levels. Because of its low conductivity, the binder content also permits limited control of the fuel regression rate.

(U) The binder used during the initial investigation of high density impulse propellants was a hydrocarbon binder designated as R-binder. This binder had already been extensively tested on Contract No. AF 04(611)-8516 and UTC-sponsored programs, and had been demonstrated to be nonsustaining in nearly all formulations.

(C) In general, interhalogen oxidizers are poor oxidizers for carbon-containing fuels and, for good performance, it is desirable to minimize the carbon content and increase the oxygen content of the binder. In order to include an oxidizing element for carbon (thereby improving performance), various oxygen-containing binders were investigated. This investigation resulted in the selection of the QX 3812/DER 332 (Dow Chemical Co., dow epoxy resins) binder. This binder, designated QX/DER was studied extensively during phase I. It contains 61.5% carbon and 20% oxygen as compared to 80% carbon and 10% oxygen in the R-binder. In a typical fuel system oxidized by ClF_5 and ClO_3, the ClO_3F content can be reduced 5% by using the QX/DER binder, and similar reductions are possible in AP loading.

(C) During the subscale motor test program, which was conducted to develop the listed propellant combinations, it was found that nearly all the formulations using QX/DER binder tended to sustain combustion after termination of oxidizer flow. It was also found that a crusty char developed in the fuels containing boron which did not occur when aluminum was substituted for boron. Since laboratory DTA studies had shown that exothermic decomposition of TFTA and QX/DER binder occurred at 266°F (130°C), it was then postulated that this decomposition could be contributing to the sustained combustion characteristics. A review of 5.0-in.-diameter motor data obtained under contract No. AF 04(611)-8516 and 3.5-in.-diameter tests conducted on this contract with R-binder and similar fuel components which did not sustain combustion, indicated that the R-binder could suppress the tendency to sustain. Therefore, it was decided to discontinue further investigation of fuels containing the QX/DER binder and continue work with R-binder systems.

(2) Boron

(C) Boron is the primary additive of the multiple component fuel because of its high density and relatively high heat of reaction with interhalogen oxidizers. Aluminum, however, could be used as an alternate to boron but with a decrease in performance.

(C) Two areas of investigation existed which were important to the successful formulation of boron-containing fuels. The first was the loading level of boron achievable in multiple-component fuels, and the second was the combustion behavior. Boron "as received" can be loaded to approximately 47% of a total blend with R-binder and to a lesser extent (about 20%) when other components are included. Generally, the level of TFTA and boron combined cannot exceed the binder content. Boron loading levels of 20% to 30% are practical, but the boron must be compacted, prilled, or added to AP pellets to achieve extremely high loadings. Higher loading levels using "as received" materials resulted in fuel mixes which were too viscous to be castable. Satisfactory combustion of boron is related to both the fuel regression rate and the boron loading level, i.e., the level of boron in homogeneous fuel blends or the level of boron in the matrix of compacted or large particle containing fuels. Lower percentages of boron (less than 20%) usually burn satisfactorily whereas loading levels greater than 20% burn satisfactorily only if high regression rates are obtained. Without regression rate augmentation, there appears to be a tendency for boron to sinter or char rather than burn where the concentration exceeds 20%. Boron also tends to aggravate existing sustaining problems because of its tendency to form a char layer by absorbing heat and transferring it to the fuel grain after motor shutdown.

(3) Nitrogen Additives (TAZ, THA, TFTA)

Three nitrogen-containing additives were included in the hybrid fuel research investigations: (triaminoguanadine azide (TAZ), its double salt triaminoguanadine azide (THA), and tetraformal trisazine (TFTA). These high nitrogen additives, when substituted for binder in hybrid fuel formulations, serve several purposes. First, they provide a means of maintaining high performance where boron content is limited by supplying significant quantities of working fluid and by their high energy release. Secondly, their density is higher than that of the binders considered, thus improving density impulse. The nitrogen additives

also allow higher AP loading levels for a nonsustaining application by absorbing some of the thermal energy released by the AP during combustion. For example, with the HFX 7808 formulation (including 30% AP and 30% TFTA) used in this test series, the AP loading would have to be limited to approximately 15% without the TFTA ingredient. Finally, the nitrogen additives contain less carbon than the binder, minimizing carbon content in the fuel.

(C) TAZ has the chemical formula CH_9N_9 while THA is $CH_{14}N_{14}$. TFTA has the chemical formula $C_4H_{12}N_6$, and consists of 33.35% carbon, 8.4% hydrogen, and 58.4% nitrogen by weight. Extensive work which has been completed on TFTA is reported in the literature.(2)

(C) Work with THA was discontinued because of its thermal stability limitations. The use of TAZ results in higher performance multicomponent fuels or results in lower AP loading levels. However, the performance advantage is reduced because of the unavailability and relatively high cost of TAZ as compared to TFTA. Comparisons of four-component fuels are made with optimized formulations (i.e., optimum O/F for maximum specific impulse). Since experimental work conducted with TFTA has demonstrated it to be as effective as TAZ, the full-scale motor fuel development included only TFTA. Until a more significant advantage with TAZ can be seen, TFTA is an adequate substitute.

(4) Ammonium Perchlorate

(C) Ammonium perchlorate also has a dual purpose in the multicomponent formulations. Its primary purpose is to provide oxygen to burn the carbon of the binder and TFTA in the combustion process in order to achieve high performance levels; it also significantly augments the regression rate of hybrid fuel formulations because of its high rate of thermal decomposition. In addition, its relatively high density makes it extremely desirable to be included in the formulation.

(U) Ammonium perchlorate can be loaded in binder matrices up to about 85%, depending on particle size. In small particle sizes (40μ to 200μ), AP has been found to produce sustained combustion at levels exceeding 15% loading. However, nonsustaining hybrid fuels have been tested with 40% loading using 600μ to 800μ particle AP.

(C) Maximum performance of fuels containing TFTA, boron, AP, and R-binder occurs when the AP level is approximately 50%. However, with homogenous formulations this level will produce sustained combustion. To produce nonsustaining combustion characteristics, a reduced level of AP loading is required. The ClO_3F can be used to recover the performance lost by reducing AP loading as discussed previously, but only at the expense of reducing oxidizer bulk density.

d. Fuel Characterization

(U) During the previous work,[1] five 1.0-in.-diameter motor tests (accumulated test time of 17 sec) and nine 5.0-in. diameter subscale motor tests (accumulating 172 sec) were conducted with the HFX 7808 formulation. Six full-scale heavyweight motor assemblies fabricated during this program also incorporated the selected HFX 7808 fuel and were used in 13 test firings, accumulating almost 300 sec of firing time. Of these tests, 12 were fixed-thrust with a maximum duration of 40 sec at boost thrust (1,000 psia) and a maximum duration of 40 sec at the sustain level (500 psia). The one cycled firing consisting of 12-sec boost, 20-sec coast, 40-sec sustain, 60-sec coast, and 10-sec boost was performed to demonstrate the dual-thrust and restart capability of the system. The same fuel grain had been previously test fired for 2 sec (terminated prematurely because of an oxidizer leak), thus giving a total of four engine starts on one grain.

(C) All the motor development tests (and also the previous fuel studies) were conducted using ClF_3 as the oxidizer because the substitution was satisfactory for experimental work and resulted in substantial cost savings. The HFX 7808 fuel system when combined with ClF_3 delivers approximately 6% lower performance than when combined with ClF_5. Figure 1 shows theoretical specific impulse versus O/F for HFX 7808 with ClF_5 and ClF_3 under several operating conditions.

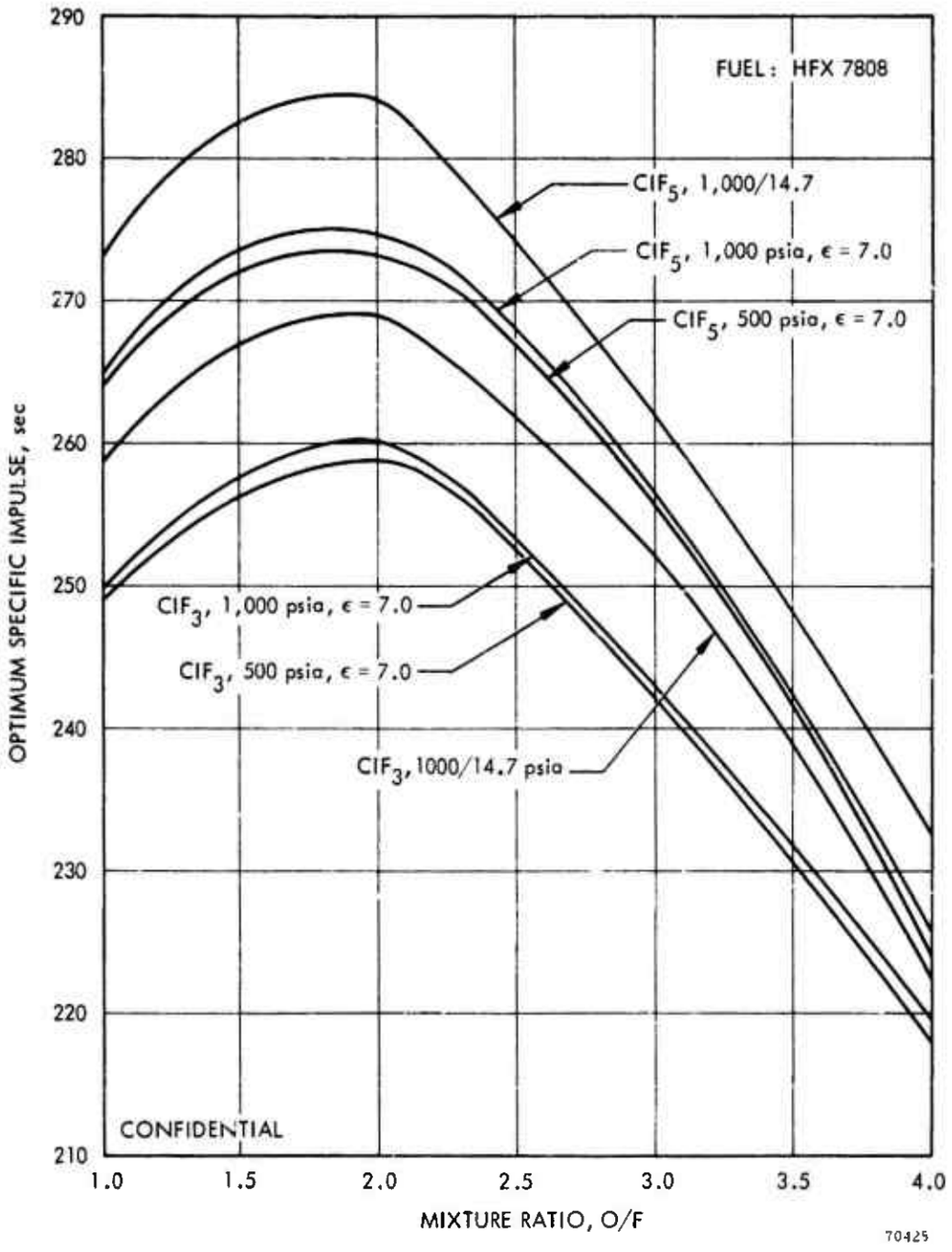

Figure 1. (U) Optimum Specific Impulse vs O/F

(C) The fuel was characterized by smooth and reproducible hypergolic ignition and immediate shutdown upon termination of oxidizer flow with no evidence of fuel surface degradation (sintering or charring). Radar measurements (appendix II) have shown the propellant exhaust to have minimal radar attenuation.

(U) Fuel flow and regression data from the 13 firings have shown that the regression rate of the HFX 7808 can be expressed by $\dot{r} = a\, G_o^n\, P_c^m$ when used with the multiport grain geometry (see section IV of this report). This nonlinear relationship between oxidizer and fuel flow rates dictates the need for aft end injection of supplemental oxidizer to maintain constant mixture ratio for dual-thrust operation.

3. GRAIN GEOMETRY

(U) A multiple-port fuel grain geometry was designed and developed which delivers constant fuel flow rate with respect to burning time at both thrust levels. The geometry is highly volumetric loaded and has demonstrated almost complete fuel utilization in full-scale tests. The multiple-port configuration overcomes design obstacles considered characteristic of hybrid fuels which result from relatively low regression rates as compared to solid rocket propellants.

a. Hybrid Fuel Grain Design

(U) Hybrid fuel grain design is a matter of matching the fuel regression rate and fuel burning surface to deliver constant fuel flow rate as a function of burning time. The controlling factors in grain shape design are the relationships between fuel regression rate, oxidizer flow rate, fuel grain port area, and combustion chamber pressure.

(U) Hybrid fuel flow rate can be expressed:

$$\dot{w}_f = \rho_f\, L\, P_b\, \dot{r} \quad , \tag{1}$$

where:

$\dot{w}_f$ = fuel flow rate, lb/sec

ρ_f = fuel density, $lb/in.^3$

P_b = fuel burning perimeter, in.

L = fuel grain length, in.

$\dot{r}$ = regression rate, in./sec.

(U) The burning surface is a function of the fuel port which changes with time, and the regression rate is usually a function of oxidizer mass flux (G_o = oxidizer flow rate ÷ fuel port cross section, lb/sec-in.^{2}) and possibly of chamber pressure.

(C) Extensive theoretical studies have been conducted on other programs in an attempt to theoretically predict the regression rates of hybrid fuels using convective and radiative heat transfer theory. However, at the point in this program where the system was committed to a final design, the theory was not yet sufficiently developed to handle fuel systems which incorporate ingredients which augment fuel regression rate such as AP, THA, TAZ, and TFTA.

(U) Empirical regression relations have been developed which express the fuel regression rate as a function of chamber pressure and/or oxidizer mass flux. The relations are:

$$\dot{r} = a\, G_o^{\,n} \tag{2}$$

where regression rate is considered to be a function of oxidizer mass flux and:

$$\dot{r} = a\, G_o^{\,n}\, P_c^{\,m} \tag{3}$$

where regression rate is considered to be a function of chamber pressure also. The mass flux, G_o, can be replaced in the equation by $\dot{w}_{oxH}/A_p$ which is the ratio of forward oxidizer flow to fuel port area. The constants and exponents are experimentally determined over the range of motor operation.

(U) The substitution of either equation 2 or 3 into equation 1 will result in

$$\dot{w}_f = a\, \rho_f\, L\, (\dot{w}_{ox})^n \frac{P_b}{(A_p)^n} \tag{4}$$

or

$$\dot{w}_f = a\, \rho_f\, L\, (\dot{w}_{ox})^n \frac{P_b}{(A_p)^n}\, P_c^{\,m} \tag{5}$$

(U) In either case, it is evident that a constant fuel flow rate with burning time will result only when the parameter $P_b/(A_p)^n$ is constant. For example, if a cylindrical fuel port is used with a fuel

which can be characterized with an exponent (n) equal to 0.5, a constant fuel flow rate with burning time is obtained. Since

$$P_b = \pi D \tag{6}$$

and

$$A_p = \frac{\pi D^2}{4} \tag{7}$$

then

$$\frac{P_b}{\left(A_p\right)^n} = \frac{\pi D}{\left(\frac{\pi D^2}{4}\right)^{\frac{1}{2}}} = 2\sqrt{\pi} = \text{constant} \tag{8}$$

The fuel port diameter, D, being the only variable with burning time.

(U) Constant fuel flow rates can also be obtained by conventional solid motor design techniques if the exponent is zero (constant regression rate) and a neutral star grain configuration is used. If the exponent is 0.5, a circular port can be used, and if the exponent is between 0 and 0.5, modified shapes can be used to produce constant fuel flow rate.

b. Grain Shape Studies

(U) The concept of the fuel grain geometry selected for development evolved from 12-in.-diameter motor studies under Contract No. AF 04(611)-8516. These studies and subscale motor studies conducted under this contract are discussed in the following paragraphs to provide background for the development of a fuel grain suitable for tactical missile propulsion systems.

(U) Hybrid fuel regression rates are characteristically low. Therefore, longer grain lengths are required for higher thrust single-port motor designs. Typically, a single-port fuel grain for a 5,000-lb thrust motor would be approximately 80 to 120 in. long depending on the regression rate of the fuel and the optimum propellant mixture ratio.

(C) Twelve-in. motor design studies conducted under Contract No. AF 04(611)-8516 resulted in the development and testing of two multiple-port fuel grain shapes which greatly reduced the required length of a 5,000-lb thrust motor. The fuel grain shapes are a three-port cartwheel design and hubbed nine-port cartwheel grain shape, as shown in figure 2. The resultant reduction in motor L/D is shown in table III in which the benefit of multiple-port fuel grain shapes is clearly indicated.

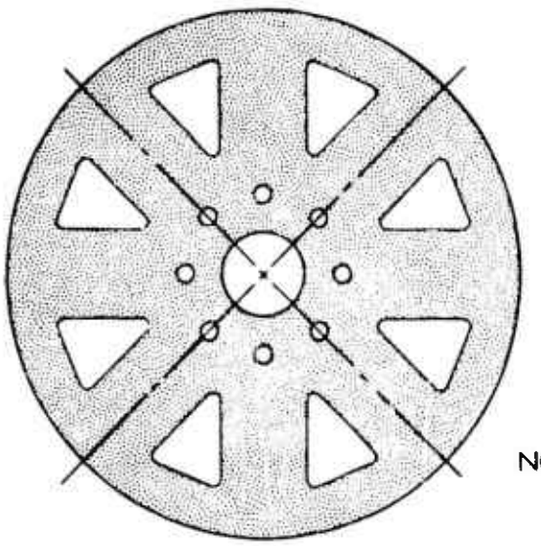

SLIVER 6.3%

LOADING 0.89

NOTE: EIGHT SMALL HOLES INCLUDED TO REDUCE SLIVER LOSS

NINE PORT HUBBED-CARTWHEEL GRAIN DESIGN

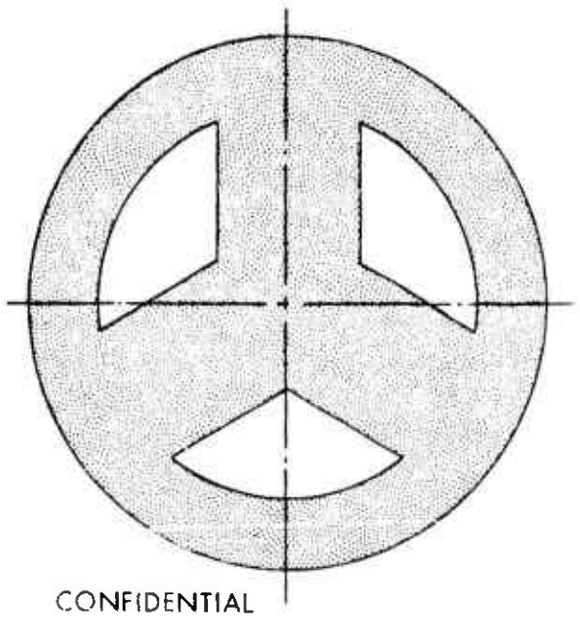

SLIVER 8.5%

LOADING 0.787

CONFIDENTIAL

THREE-PORT CARTWHEEL GRAIN DESIGN

R-60881

Figure 2. (U) Hybrid Fuel Grain Shapes

TABLE III

(U) LENGTH-TO-DIAMETER RATIO
OF TYPICAL 5,000-lb THRUST HYBRID MOTORS

Grain Shape	Motor L/D	Motor Length in.	Motor Diameter in.
Cylindrical single port	7.8	78	10
Three-port cartwheel	2.9	36	12.5
Nine-port cartwheel	1.6	25	15.3

(C) Each of these fuel grains was successfully tested twice during the prior program, and they demonstrated efficient and predictable fuel utilization. These grain shapes had cross-sectional loading fractions of 89% and 80% and sliver fractions of 8.5% and 6.3%, respectively.

(U) A high loading fraction is desirable for maximum system performance, but loading fraction is limited by the smallest port size which is usable. In addition, extremely small port sizes increase the sliver fraction (residual fuel area divided by the chamber area) beyond practical limits and result in poor fuel utilization. The large sliver fractions result from the long radii arcs produced from burning large propellant web thicknesses.

(C) Based on the success of the multiple-port grain shapes tested under Contract No. AF 04(611)-8516, analytical design studies were conducted during phase I which incorporated the concept of using inactive ports in a multiple-port design to promote fuel regression in the direction which normally would result in high fuel sliver volume. The study resulted in the design of the geometry of figure 3 which provides a cross-sectional loading of 93% and a sliver fraction of 6.7%.

c. Geometry Development

(C) The 18-in.-diameter fuel configuration uses six active fuel ports into which oxidizer is sprayed; each active port has seven inactive satellite ports clustered about it which by definition are not supposed to burn until the web between each inactive port is consumed. The successive burning of inactive ports results in constant fuel flow rate (hence, constant O/F) when matched to the proper fuel. Predicted regression profiles are also shown in figure 3, illustrating the change from a circular

FUEL GRAIN LOADING FRACTION - 93%
CALCULATED SLIVER - 6.7%
ACTIVE FUEL PORT AREA - 6.80 in^2
INACTIVE FUEL PORT AREA - 11.88 in^2
FUEL GRAIN CROSS SECTION - 251.2 in^2

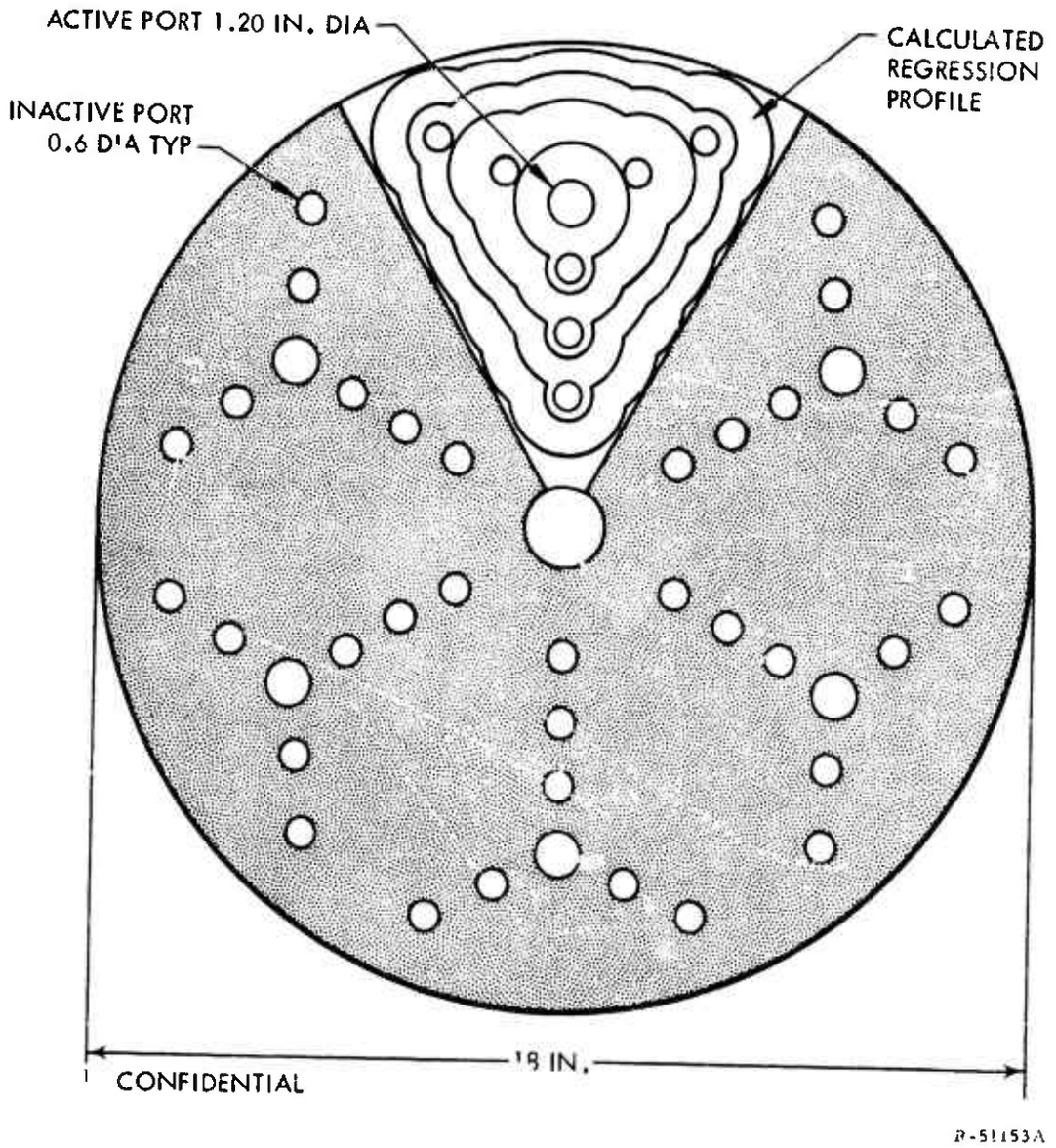

Figure 3. (U) Grain Geometry of Motors 10 and 11

to a near triangular geometry. Appendix I consists of calculations required to determine grain dimensions, oxidizer flow rates, etc.

(U) Four 5-in.-diameter subscale motor tests were conducted during the initial 9-month period of the contract using the selected fuel system (HFX 7808) in a grain configuration similar to one major port of the full-scale motor to obtain regression rate data. Two tests were conducted at the boost thrust oxidizer flow rate and chamber pressure (1,000 psia), and two were conducted at sustain oxidizer flow rate and chamber pressure (500 psia). The test results indicated that high fuel flow rates were obtained during initial consumption of the fuel grain in contrast to the analytically predicted low rates. Measurement of full-scale fuel ports after limited full-scale testing during the same period indicated similar fuel flow behavior to that of the subscale tests; the actual regression behavior produced an initially higher fuel flow than that calculated.

(C) Experimental studies conducted during the recently completed 6-month effort have disclosed that burning of the AP-TFTA-loaded fuel under pressure (500 to 1,000 psia) and temperature (theoretical maximum flame temperature of about 6,500°F) caused the satellite ports (which were open only at the aft end of the grain) to enlarge prematurely (i.e., burn as a solid fuel). This burning was the result of the high AP loading (30%) of the fuel at which level the realm of the "typical hybrid" is left and the pressure-dependent solid influence is seen. Thus, prior to exposure to the oxidizer, the satellite ports contribute fuel flow to supplement that of the primary ports which are functioning as a normal hybrid propellant. In addition to increasing the fuel flow rate, premature enlargement of the satellite ports produced a nonuniform web between the primary ports.

(C) Three modifications were devised to compensate for the nonuniform web burning. The modifications (section IV, part 5 of this report) which were tested and evaluated in four full-scale motor tests resulted in the selection of the final grain geometry of figure 4. This geometry utilizes smaller satellite ports to account for the "solid burning" of the satellites. The burning progression has been found to closely approach the design requirement and has delivered over 96% fuel utilization (by weight) in full-scale tests.

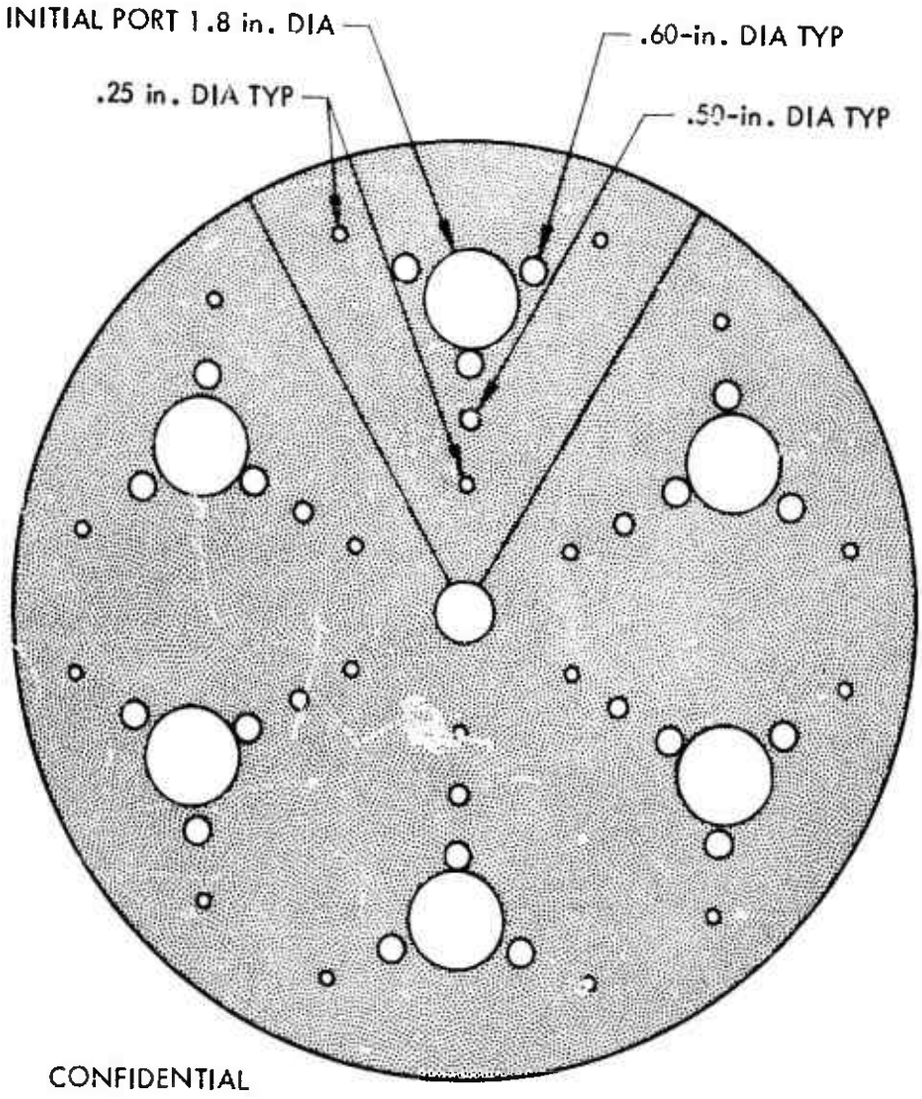

FUEL GRAIN LOADING FRACTION – 91%
ACTIVE FUEL PORT AREA – 15.29 $in.^2$
INACTIVE FUEL PORT AREA – 7.15 $in.^2$
FUEL GRAIN CROSS SECTION - 25'.2 $in.^2$

R-70241A

Figure 4. (U) Grain Geometry of Motors 14 and 15

(C) Preliminary data used to establish the grain dimensions were based on a fuel regression rate given by $\dot{r} = 0.15\ G_o^{0.4} P_c^{0.1}$. Subsequent studies conducted during the present program disclosed that the regression rate is less than previously predicted. (These studies are described in detail in section IV.) The lower rates dictate that the existing grain dimensions be changed or some other grain geometry having an increased fuel surface area be used to achieve the proper fuel flow rates and maintain the optimum mixture ratio over the dual-thrust range.

4. THRUST CONTROL SYSTEM

(U) A thrust control system has been established which will permit operation of the TCA at either thrust level while maintaining constant mixture ratio. The system is comprised of two major subsystems: an oxidizer flow control system, and an oxidizer injection system.

(C) The flow control subsystem consists of a dual-element solenoid valve which provides on-off and dual-thrust operation. The oxidizer injection subsystem consists of six dual-manifold primary injectors and a single aft injector. The flight configuration flow control valve was fabricated and bench-tested in preparation for full-scale motor testing; however, because it was made to mate with the flight configuration forward closure (refer to figure 7), it could not be used with the heavyweight test motor used during this effort. The oxidizer injection system has been extensively utilized in the full-scale test program.

a. Design

(C) A simple thrust control system has been devised which, with one dual-element solenoid valve, can provide dual-thrust operation as well as on-off control. The system shown schematically in figure 5 includes the dual-element valve, six dual-manifold primary injectors, and a single fixed-area aft injector.

(C) During sustain thrust operation, oxidizer is supplied to the motor by the sustain thrust valve element while both valve elements supply oxidizer during boost thrust operation. Oxidizer is supplied to the dual-element valve through a single feedline at a constant pressure of 1,100 psi.

(C) Since boost thrust operating chamber pressure is 1,000 psi and sustain thrust operating pressure is 500 psi, system pressure differentials of 100 psi at boost thrust and 600 psi at sustain thrust are available to control oxidizer flow through the injectors. (All of the injectors are the fixed-area orifice type; therefore, as a result of changes in operating chamber pressure, the flow rates in the aft injector and sustain ports of the primary injector will change in the ratio of $(600/100)^{\frac{1}{2}}$, or 2.45, as thrust changes are made from 5,000 to 2,500 lb.)

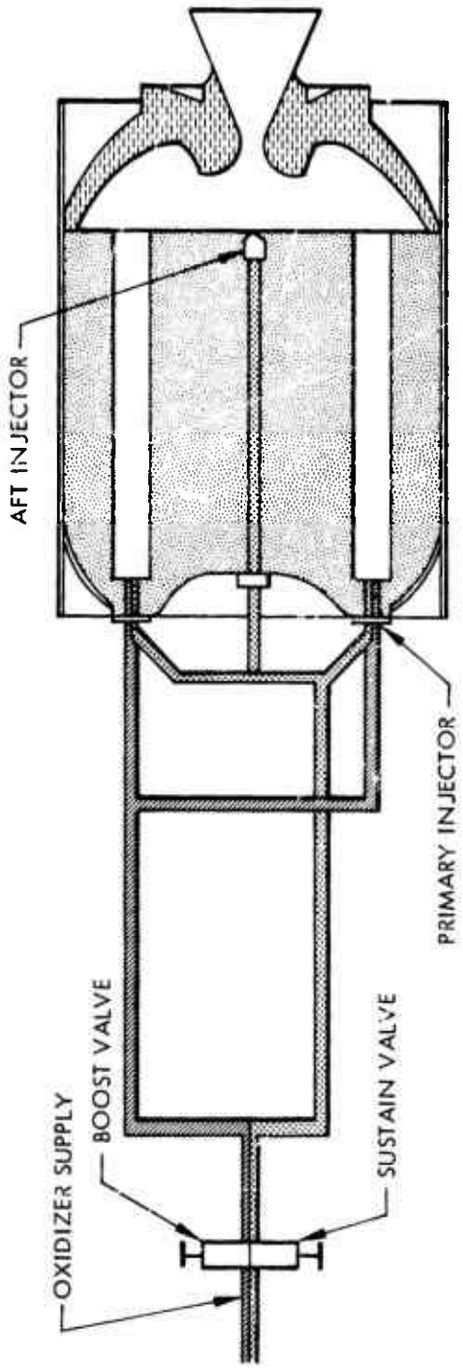

Figure 5. (U) Thrust Control System

(U) The distribution of oxidizer between primary and aft injectors at the boost and sustain thrust levels is a function of the sensitivity of fuel delivery rate to primary oxidizer flow rates and combustion chamber pressure. Experience with fuel of the type being evaluated had shown that it can be characterized reasonably well within the operating limits of this system by an empirical regression rate equation of the form

$$\dot{r} = a\, P_c^{\,m}\, G_o^{\,n} \tag{9}$$

where the operating limits are

P_c less than 1,000 psi

G_o between 0.01 and 2.0 lb/sec-in.^{2}

and

$\dot{r}$ = regression rate, in./sec

a = proportionality constant

P_c = combustion chamber pressure, psi

G_o = oxidizer mass flux (lb/sec-in.) = $\dot{w}_{ox_H} / A_p$

$\dot{w}_{ox_H}$ = primary oxidizer flow rate, lb/sec

A_p = fuel grain port area, in.^{2}

m = pressure exponent

n = oxidizer mass flux exponent.

(C) Experience with the fuel under investigation on this contract indicated that the value of the exponent, n, in the above equation is approximately 0.4 and m is approximately 0.1. Therefore, the ratio of boost-thrust primary oxidizer flow rate to sustain thrust primary flow rate required is almost 5:1 in order to achieve a boost to sustain thrust ratio of 2:1 with a constant mixture ratio.

(U) Since the relationship between the fuel flow rate and primary oxidizer flow rate is nonlinear, supplemental aft injection of oxidizer is needed to maintain a constant mixture ratio. The aft oxidizer boost-level flow rate is selected to provide the proper flow at both thrust levels (minimum flow at boost for survivability yet maintain constant O/F ratio at both levels) with the varying pressure drop. By judicious selection the ratio of aft

oxidizer flow rate at sustain thrust to that at boost thrust can be tailored to fit the ratio (2.45) provided by the system pressure differential change. A similar change in flow rate results in the sustain thrust orifices of the primary injector as the chamber pressure varies with thrust, but this can be accommodated by the oxidizer flow through the boost thrust valve.

b. Oxidizer Flow Control

(U) To meet the operating requirements of dual thrust and random on-off duty cycles, a dual-element thrust control valve, shown in figure 6, has been developed which, when used in the selected thrust control system, will provide on-off and dual-thrust operation from only two 28 v electrical signals.

(U) This valve, which is shown schematically in figure 7, is predominantly aluminum and consists of a common feedline, two pilot solenoids, and two main poppet valves which control oxidizer flow through two discharge manifolds, a boost thrust oxidizer manifold, and a sustain thrust oxidizer manifold.

(U) The valve mounts directly to the forward closure of the flightweight full-scale motor, thus providing a short overall length TCA. It is activated by application of a 28-vdc signal (0.9 amp) to the solenoid which causes the solenoid armature to push the pilot poppet to the opposite seat. Chamber A (see figure 7) is then vented to the valve discharge. The feed system pressure applied to chamber B causes a force unbalance on the poppet, thereby opening the main poppet. Removal of the electrical source causes the pilot poppet to return to the closed position. The feed system pressure is applied again to chamber A, causing the main poppet to close.

(U) The valve weighs only 5 lb and was designed to be amenable with low-cost mass production. No seals are used on the main poppet, and the valve seat is machined into the aluminum valve body. With proper handling and avoidance of foreign particles, this seat should have a service life of 50 cycles minimum and can be refurbished by subsequent lapping. Each pilot-poppet solenoid is removable without otherwise disturbing the valve. Each contains one dynamic seal which permits the use of small low-current solenoids and avoids the necessity of expensive bellows sealed poppets, as normally required for use with fluorinated oxidizers.

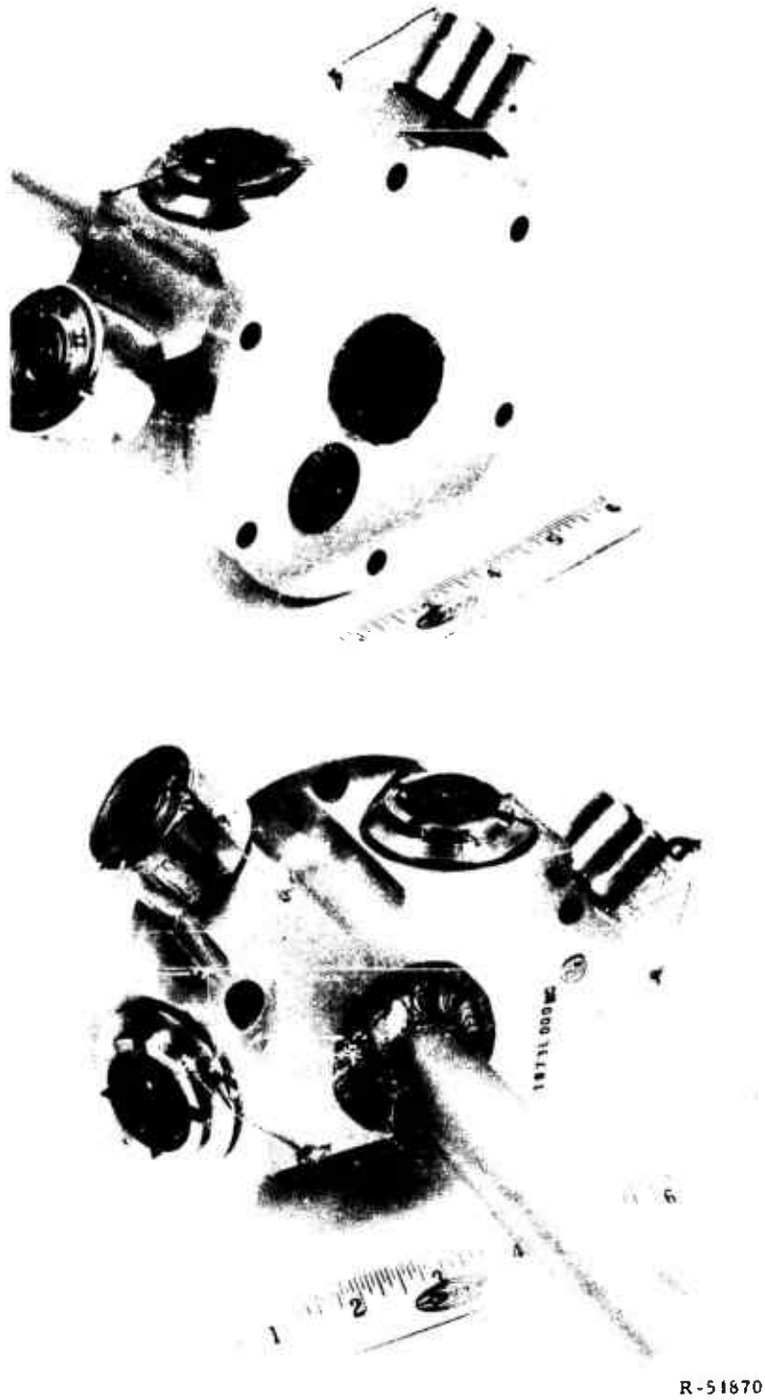

R-51870

Figure 6. (U) Dual-Element Thrust Control Valve

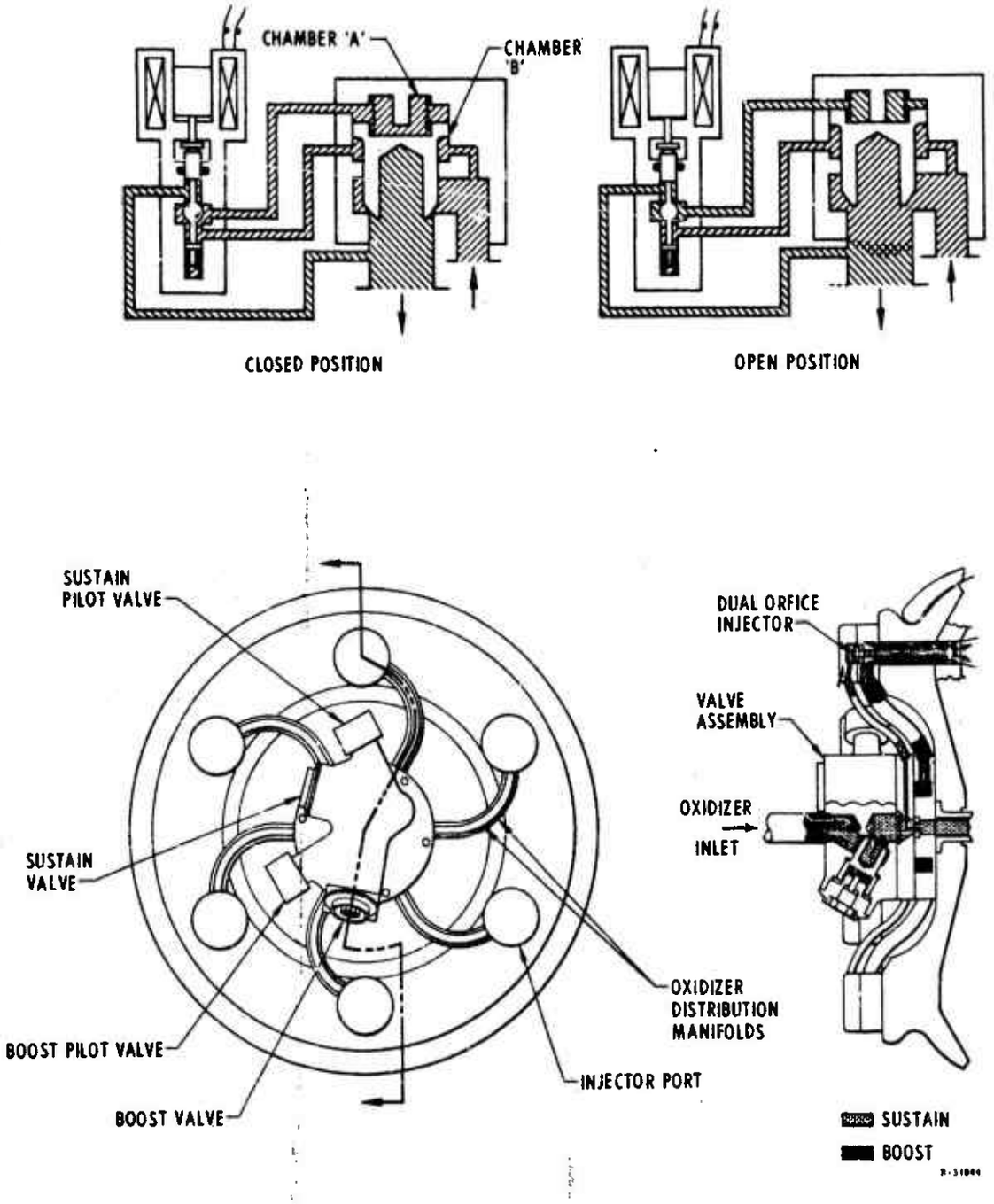

Figure 7. (U) Dual-Element Thrust Control Valve Schematic

(U) The pilot poppet seal is a spring-loaded Teflon packing available under a variety of trade names. Although Teflon is not considered to be compatible with fluorinated oxidizers, it has been used with consistently satisfactory results in situations where the seal operates in a limited duty cycle and is removed from high-velocity oxidizer flow.

(U) Cycling tests conducted by the manufacturer indicate that the valve operates with response times of approximately 100 msec, and at pressures up to 1,500 psi. Water flow calibration tests, hydrostatic tests, and operational tests have been made with the valve.

c. Injection System

(U) Prior to the development of the dual-manifold poppet injector and poppet-type aft injector, an injector development program was conducted to evaluate various injector concepts which had potential application in a dual-thrust hybrid propulsion system. Injector requirements included the capability of delivering two oxidizer flow rates for the boost and sustain thrust levels at forward and aft injector locations. The injectant spray pattern should have a minimum of radial spray momentum to minimize splashblock requirements and effect uniform fuel regression behavior. In addition, the injectors should be capable of multiple motor restarts after short coast periods.

(U) Several additional injector designs were evaluated which had one or more of the desirable features of dual-thrust motor operation. These included an impinging streams injector, a dual-orifice hollow-cone injector, and an orificed poppet injector. Discussion of these studies are available in reference 1.

(1) Forward Injectors

(C) A dual manifold poppet injector has been designed, fabricated, and successfully tested for use with the selected thrust control system in delivering oxidizer throughout a dual-thrust on-off duty cycle. The primary oxidizer injector shown in figure 8 delivers oxidizer at two flow rates and shuts off the oxidizer flow at the injector when flow is terminated upstream. The injector consists of an injector body and a spring-loaded poppet. The poppet stem contains a flow passage and fixed orifices which control oxidizer during sustain thrust operation. The injector

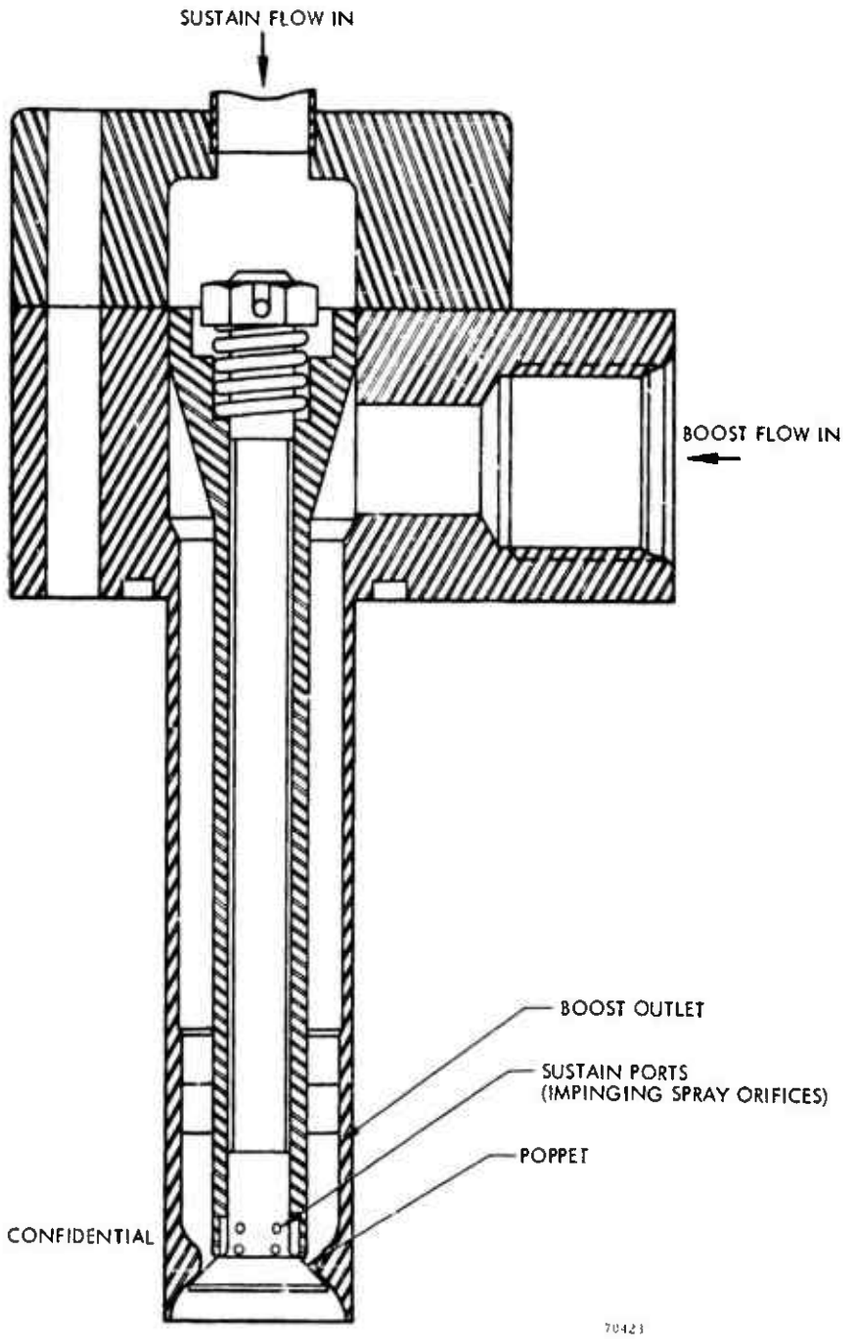

Figure 8. (U) Primary Oxidizer Injector Schematic

body contains an annular flow passage and orifice which controls additional oxidizer flow used during boost thrust operation.

(C) The spring-loaded poppet is designed to open under oxidizer pressure from the sustain thrust valve manifold. The travel of the poppet is limited by an adjustable nut which prevents poppet oscillation. The external surface, on which the poppet seats, serves to direct the oxidizer flow axially into the motor.

(C) Since the poppet is operated by oxidizer pressure, termination of flow upstream will cause it to close, thereby preventing backflow and possible contamination of the feed system with fuel-rich vapors. Contamination of the oxidizer feed system by residual fuel vapors could, on restarting, cause a reaction between contaminants and oxidizers, resulting in damage to the injectors.

(U) This dual-manifold injector has been used extensively in full-scale testing. The injector has performed very satisfactorily under normal test conditions. Further performance description is presented in section IV.

(2) Aft Injector

(U) To complete the complement of injectors required for the selected thrust control scheme, a simple poppet-type aft injector, shown schematically in figure 9, was developed for the full-scale motor. The aft injector has survived four engine starts in a single full-scale motor test.

(C) The aft injector operates on oxidizer fluid pressure, but in this case it also acts as a fixed-area orifice. Flow rate variation through the aft injector is therefore accomplished only by changes in the pressure differential. The aft injector is designed to produce a 120° included-angle radial spray pattern to deliver oxidizer into the motor plenum chamber from its central location. Flow rate changes required for dual-thrust operation are accomplished by changes in injector differential pressure.

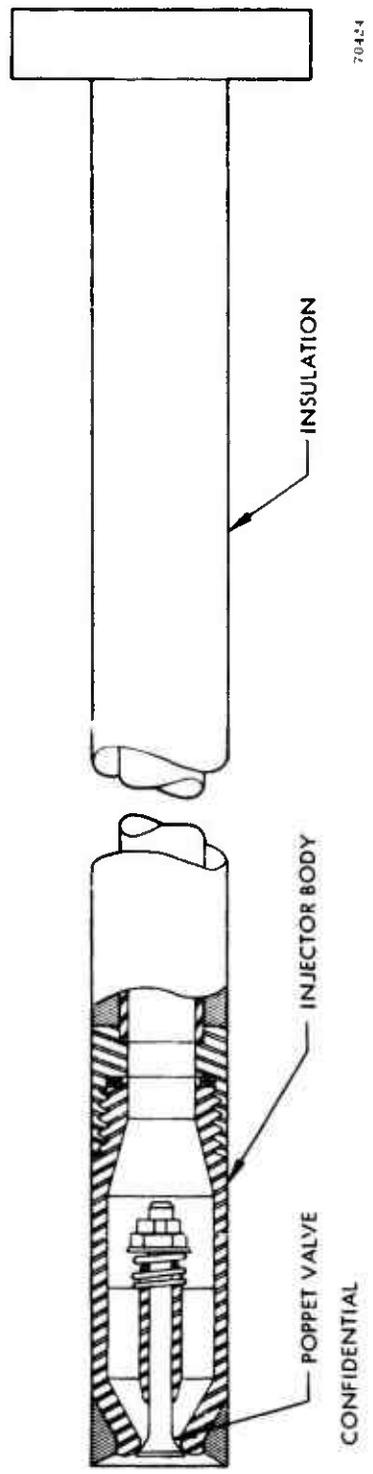

Figure 9. (U) Aft Oxidizer Injector Schematic

5. TEST MOTOR

(U) The test vehicle utilized in the program is the full-scale heavyweight steel-walled TCA illustrated in figure 10. The TCA was designed using the data of table IV to incorporate the fuel system, the fuel grain geometry, and the flight configuration components upon which development had been initiated during the previous 9-month effort. A summary of preliminary design calculations is presented in appendix I

(C) The full-scale system is based on dual-thrust requirements with a maximum thrust of 5,000 lb (delivered) at a chamber pressure of 1,000 psia and a minimum of 2,500 lb at 500 psia chamber pressure. The unit is capable of delivering the total impulse at boost thrust, sustain thrust, or any combination of boost-coast-sustain-coast-boost type of thrust mode.

(C) The HFX 7808/ClF_5 propellant combination was employed using the multiple-port fuel grain geometry. The specific impulse efficiency was assumed to be 94% at maximum chamber pressure. The engine employs the multiple-port grain geometry, aft oxidizer injection, and a submerged nozzle to achieve and maintain mixture ratio and to deliver high performance at the two thrust levels. Excellent shutdown and restart characteristics are ensured by the use of ablative, low heat absorbing materials wherever possible.

(C) The TCA, which contains approximately 200 lb of fuel, incorporates six dual-flow primary oxidizer injectors located in the forward closure, and an aft oxidizer injector which passes through the center of the fuel grain. The aft injector sprays oxidizer into a plenum chamber formed by the aft surface of the fuel grain, the aft closure, and the submerged nozzle.

a. Nozzle

(C) The nozzle design philosophy used was to employ a rapid ablator as the submerged entrance cap to minimize heat input from the cap to the fuel grain and to film-cool the nozzle, while the throat material requirements were dictated by erosion resistance. The designs were subjected to thermal analyses to evaluate their ability to withstand the thermal shock and repeated heat-soak periods characteristic of the duty cycles required. For the purpose of analysis, nylon-phenolic was used as the submerged cap material with graphite-phenolic as the throat section. A motor thrust duty cycle was assumed which would impose the most severe heat loads on the motor components. The thrust duty cycle assumed a 20-sec firing at a chamber pressure of 1,000 psi, a 2-min coast period,

TABLE IV

(U) ENGINE DESIGN DATA

Fuel	HFX 7808
Oxidizer	ClF_5
Fuel grain configuration	Multiple port
Thrust (nominal high/low – delivered), lb	5,000/2,500
Total impulse, lb-sec	200,000
Chamber pressure (maximum/minimum – delivered), psia	1,000/500
Mixture ratio (O/F)	2.5
Design specific impulse efficiency, %	94*
G_o (maximum/minimum), lb/sec-in.^{2}	2.02/0.018
Volumetric loading (fuel grain), %	91
Sliver (fuel grain), %	7
Grain length, in.	20
Grain outside diameter, in.	18
Injector ΔP at boost thrust, psi	100
Injector ΔP at sustain thrust, psi	600
Nozzle throat diameter, in.	2.00
Nozzle expansion ratio	7:1
Nozzle exit half-angle, °	15
Fuel density, lb/in.^{3} (actual)	0.0484
Propellant flame temperature, °F (theoretical)†	6,250

* Performance at maximum thrust
† P_c = 1,000 psia, O/F = 2.5

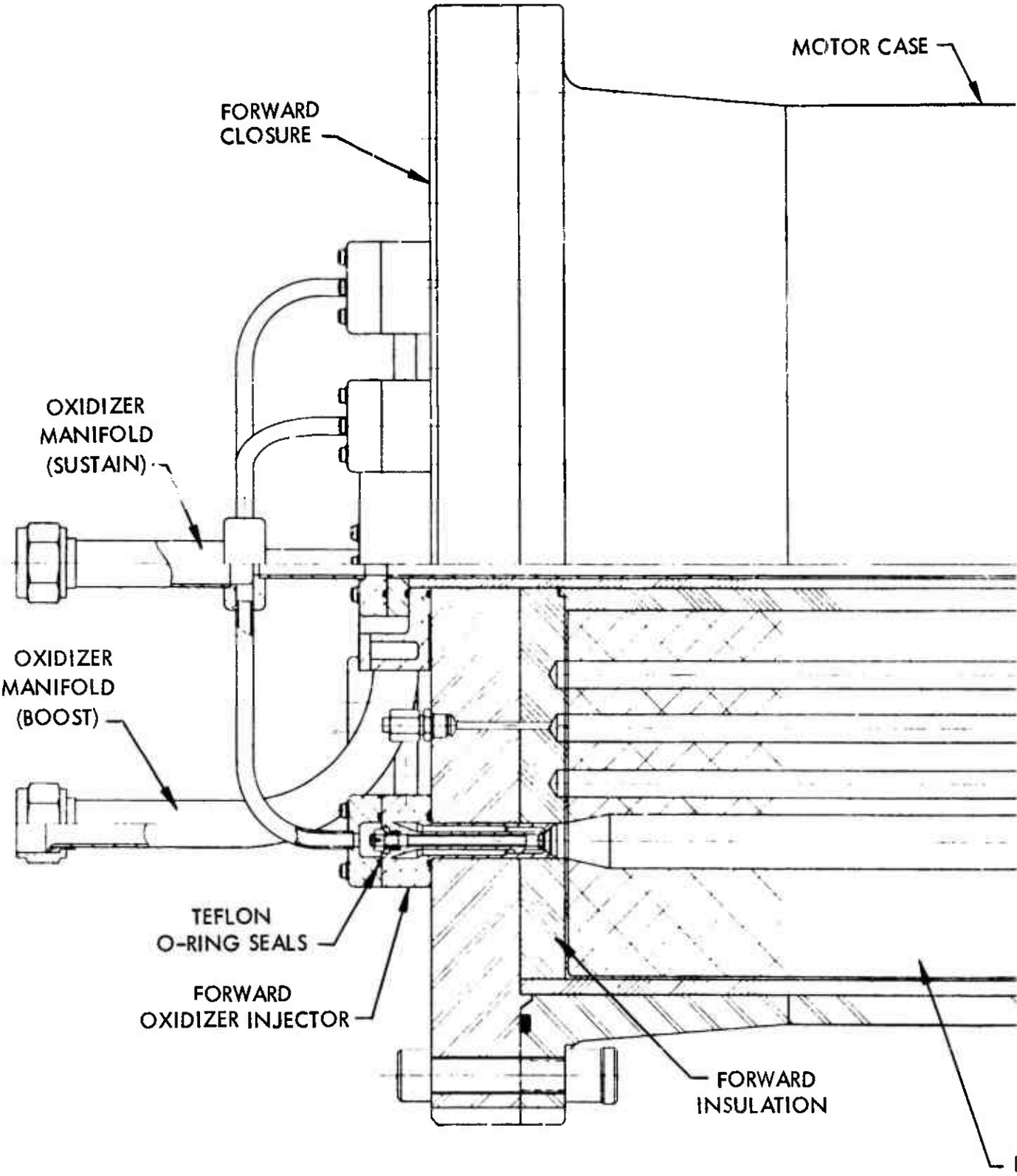
MOTOR CASE
FORWARD CLOSURE
OXIDIZER MANIFOLD (SUSTAIN)
OXIDIZER MANIFOLD (BOOST)
TEFLON O-RING SEALS
FORWARD OXIDIZER INJECTOR
FORWARD INSULATION

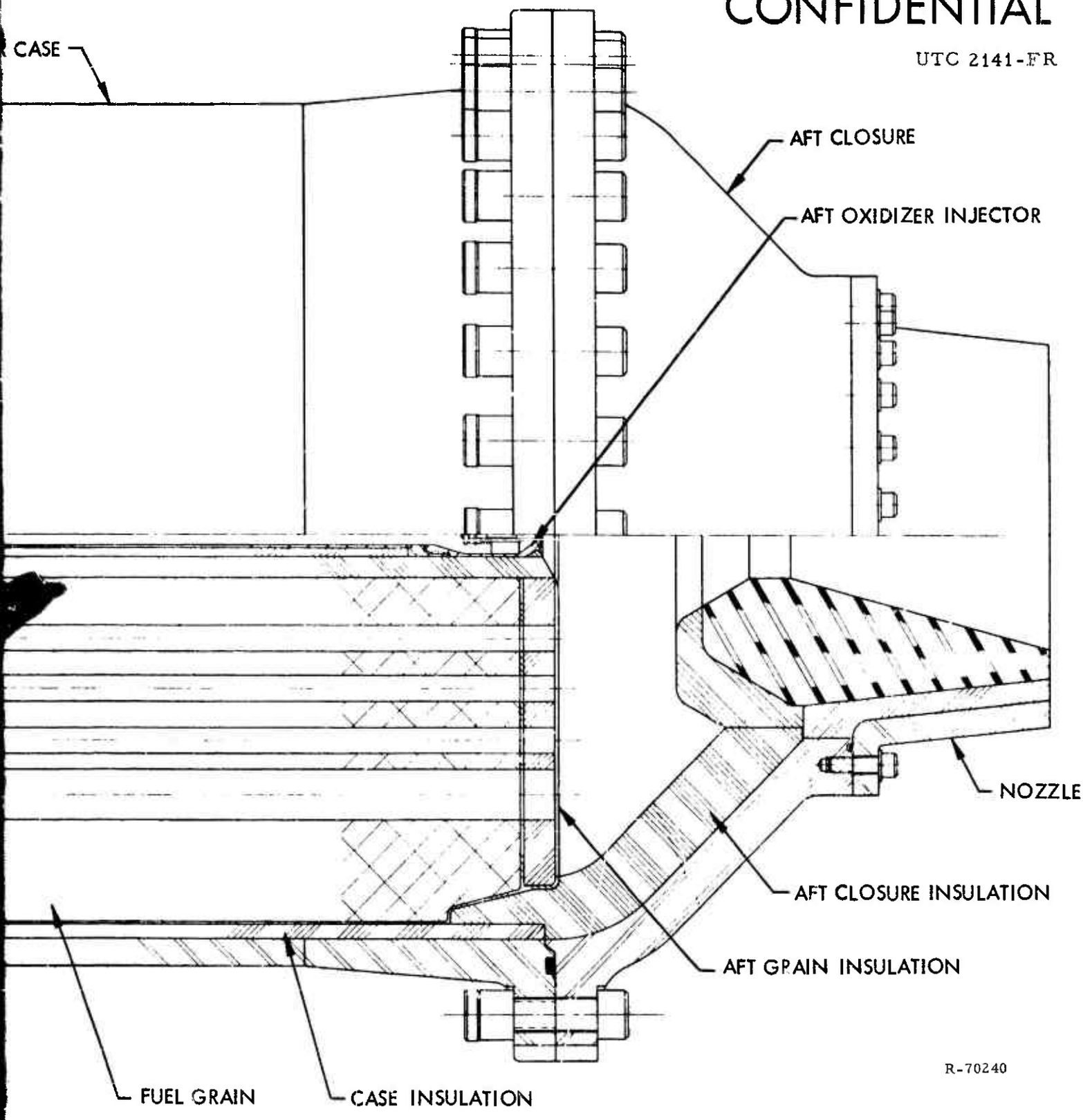

Figure 10. (U) Motor Schematic

a 30-sec firing at a chamber pressure of 500 psi, a 4-min coast period, and finally a 20-sec firing at a chamber pressure of 500 psi. The following additional assumptions were made for use in the thermal analysis:

A. No heats of ablation were considered; the material was assumed to erode at experimentally determined rates.

B. No mass efflux (transpiration) from the wall was considered.

C. No heat of resin pyrolysis was considered.

D. No change in material properties was assumed to occur with the charring process.

E. No convective or radiative cooling was assumed to exist during heat soak.

F. Nylon-phenolic was assumed to ablate at the equilibrium wall temperature (7,000°F). (C)

(U) The effect of these assumptions was to produce the worst possible temperature profile and, hence, a conservative design. As can be seen from the temperature histories in the thermal profile, (figure 11) outside wall temperatures remained under control throughout the duty cycle. Ample material was present in the nozzle to ensure against the occurence of a complete charthrough during the useful life of the nozzle. Minimum wall thicknesses were thus determined from the obtained thermal profiles and applied to the design.

b. Insulation

(U) Studies have shown that the tendency of a hybrid fuel to sustain combustion upon termination of oxidizer flow in some instances is aggravated by the use of graphite and nonablative materials in the construction of the motor. These materials, which absorb heat during the firing, can radiate or conduct energy to the fuel grain and/or adjacent insulation after the firing. Volatilization of the fuel and/or insulation then results until the motor components are sufficiently cool. If only the insulation is affected, the reaction of the insulation volatiles with air outside the motor gives a false impression of continued internal combustion.

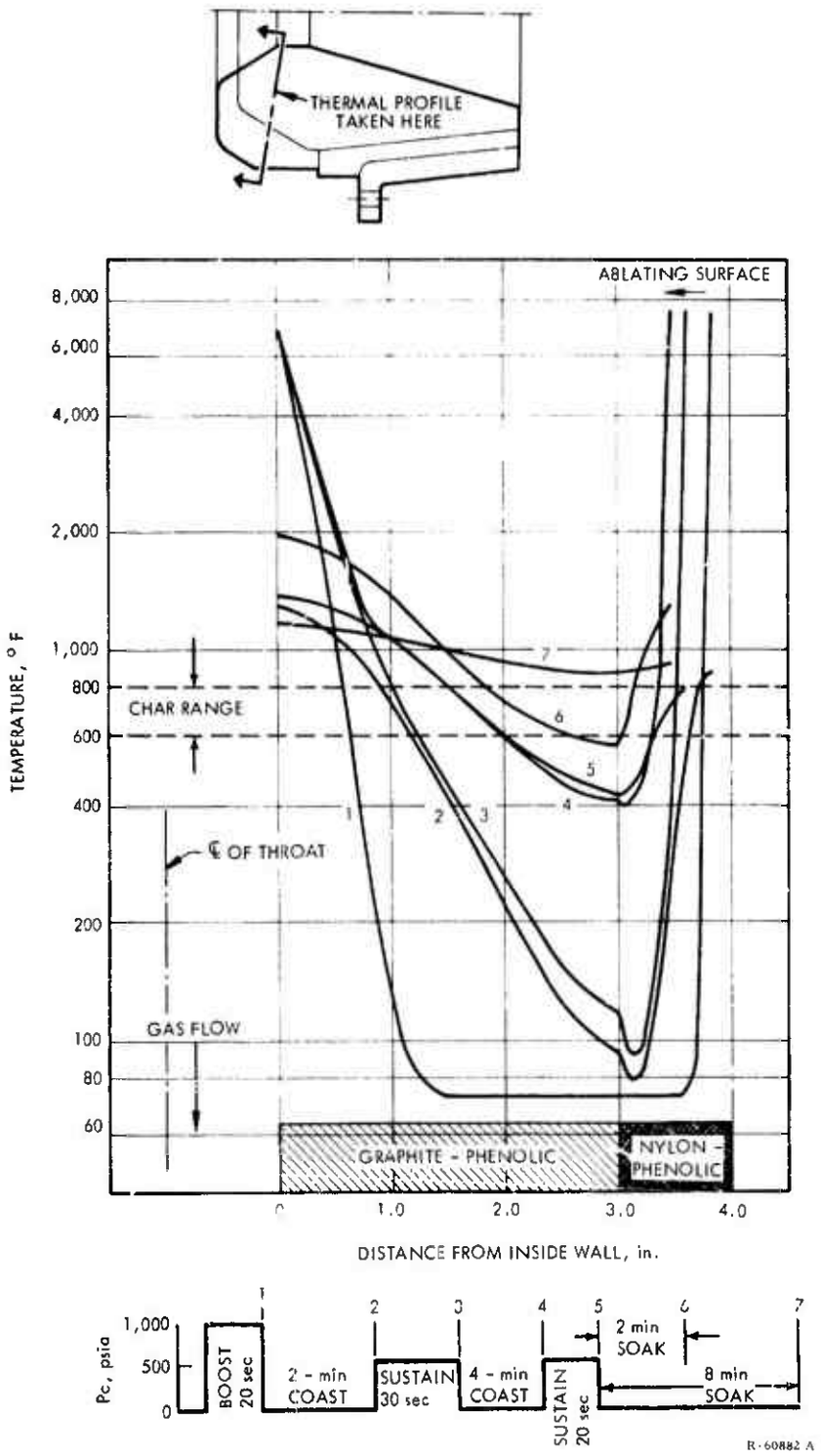

Figure 11. (U) Thermal Profile of Nozzle Throat

(This page is Unclassified)

(U) Nylon-phenolic, a rapid ablator, was thus selected for the aft grain insulation and aft closure insulation applications. This material has shown regression at a moderate rate, producing a uniform, clean surface with very little char.

(U) Based on an ablation rate of approximately 12 mils/sec, the aft grain insulation was fabricated to a 3/4-in. thi kness. Studies conducted under Contracts No. NAS 7-311 and NAS 7-475[3] which used a 25% lithium, 10% lithium hydride, 65% polybutadiene fuel (HFX 2084), had revealed excessive local erosion of the aft closure insulation due to particle and gas impingement from the fuel port (employing a three-port geometry). Therefore, the aft closure insulation for this system was conservatively fabricated 2 in. thick. The local erosion did not occur with the HFX 7808/ClF_3 combination. Hence the insulation was considerably overdesigned.

PRECEDING PAGE BLANK-NOT FILMED

SECTION IV

FULL-SCALE MOTOR DEVELOPMENT AND DEMONSTRATION

(C) Two full-scale motor configurations have been developed: a flight-weight fiberglass-cased design which was developed during the initial program and subjected to limited testing,[1] and a heavyweight design on which extensive testing was recently completed. The motor designs employ a multiple port grain geometry, aft oxidizer injection, and a submerged nozzle to achieve and maintain the desired mixture ratio and deliver high performance at two thrust levels. Excellent shutdown and restart characteristics are ensured by the use of low char, low heat-absorbing materials wherever possible.

(C) Six heavyweight 18-in.-diameter TCAs (figures 10 and 12) were successfully tested in 13 firings (12 fixed-thrust and 1 cycled) achieving performance efficiencies near 96%, and demonstrating 96% fuel utilization. Four assemblies were used to characterize the fuel and verify component design concepts; the remaining two assemblies were used to demonstrate TCA operation over representative duty cycles. The following paragraphs describe the fuel processing techniques, test histories and results, and component evaluations which were accomplished

1. PROCESSING

(U) Rigorous processing procedures were established to circumvent fuel grain porosity and ingredient incompatibility which were observed during the early development of HFX 7808 fuel. New lots of materials were checked for incompatibility (excessive foaming or gassing during cure, resulting in a porous grain) before fabrication of a complete fuel grain was attempted. All constituents were thoroughly dried or degassed. The ingredients were mixed and the fuel was cast under a vacuum atmosphere to minimize dusting.

(U) The fuel was cast into a lined phenolic sleeve for easy removal from the motor case during disassembly (see appendix III). After a 3-day cure at 120° to 130°F, the fuel grain was removed from the oven and stripped of its casting hardware. The final fuel processing procedure consisted of trimming the fuel grain slightly below the aft end of the motor case.

(U) The resultant grains were excellent. The grains were structurally sound; the perforations were smooth and uniform with no evidence of porosity. After it was subjected to multiple firings, the fuel surface appeared as before firing, with no char or indication of degradation.

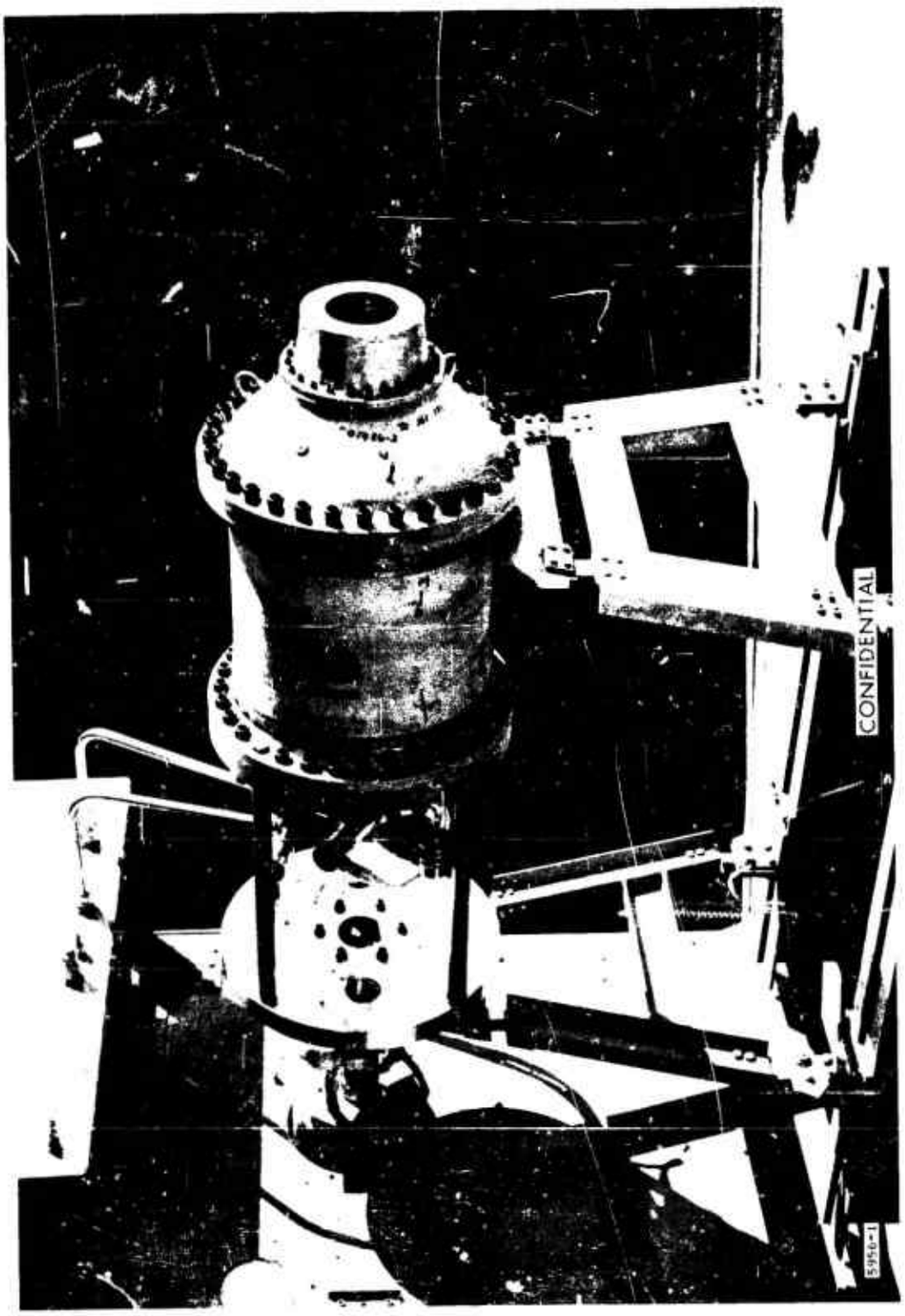

Figure 12. (U) Heavyweight Motor Assembly

2. MOTOR TEST DESCRIPTION

(C) Six full-scale heavyweight motor assemblies were fabricated and tested in 13 firings. The following discussion summarizes the testing of each motor assembly and the various components tested with each assembly. The heavyweight motor assemblies were labeled 10 through 15 following the first nine flightweight assemblies of the previous effort. Figure 13 illustrates the test history of each motor assembly. It should be noted that the decay of the pressure-time curves are due to nozzle erosion except where otherwise indicated.

a. Motor 10

(C) The motor assembly was test fired three times at the sustain thrust level (nominally 500 psia chamber pressure) for a cumulative duration of 54 sec. The objectives of these tests were to further characterize the fuel regression behavior, to observe the growth pattern of the fuel grain perforations, and to evaluate systems and components at the sustain thrust level.

(C) The first firing, scheduled for a 20-sec duration, was terminated after 14 sec due to a small ClF_3 leak at the oxidizer injection manifolding (see figure 10). Shutdown was smooth and immediate. Inspection of the manifolding disclosed a loss of five of the seven Teflon O-rings exposed to ClF_3. Examination of the interior of the motor revealed a uniform profile along the port length, with no tapering. The grain was clean with no char or indication of degradation. The nylon-phenolic aft closure insulation performed well, displaying no irregularities in the ablation pattern and an ablation rate well within design limits. The graphite-phenolic nozzle throat and divergent section showed very little erosion; however, the magnesia-phenolic nozzle entrance cap ablated at a much higher rate than anticipated and was completely gone after 14 sec of operation.

(C) The paper-phenolic forward closure insulation (figure 10) experienced severe local erosion in the vicinity of the forward injectors. The insulation was completely burned away around one injector, damaging the injector and exposing the steel forward closure. Overheating damaged the aft injector poppet along its outer edge.

(C) Further inspection and analyses revealed the following: (1) the Teflon O-ring failures had been caused by scratches on the sealing surfaces which allowed ClF_3 to bleed by and

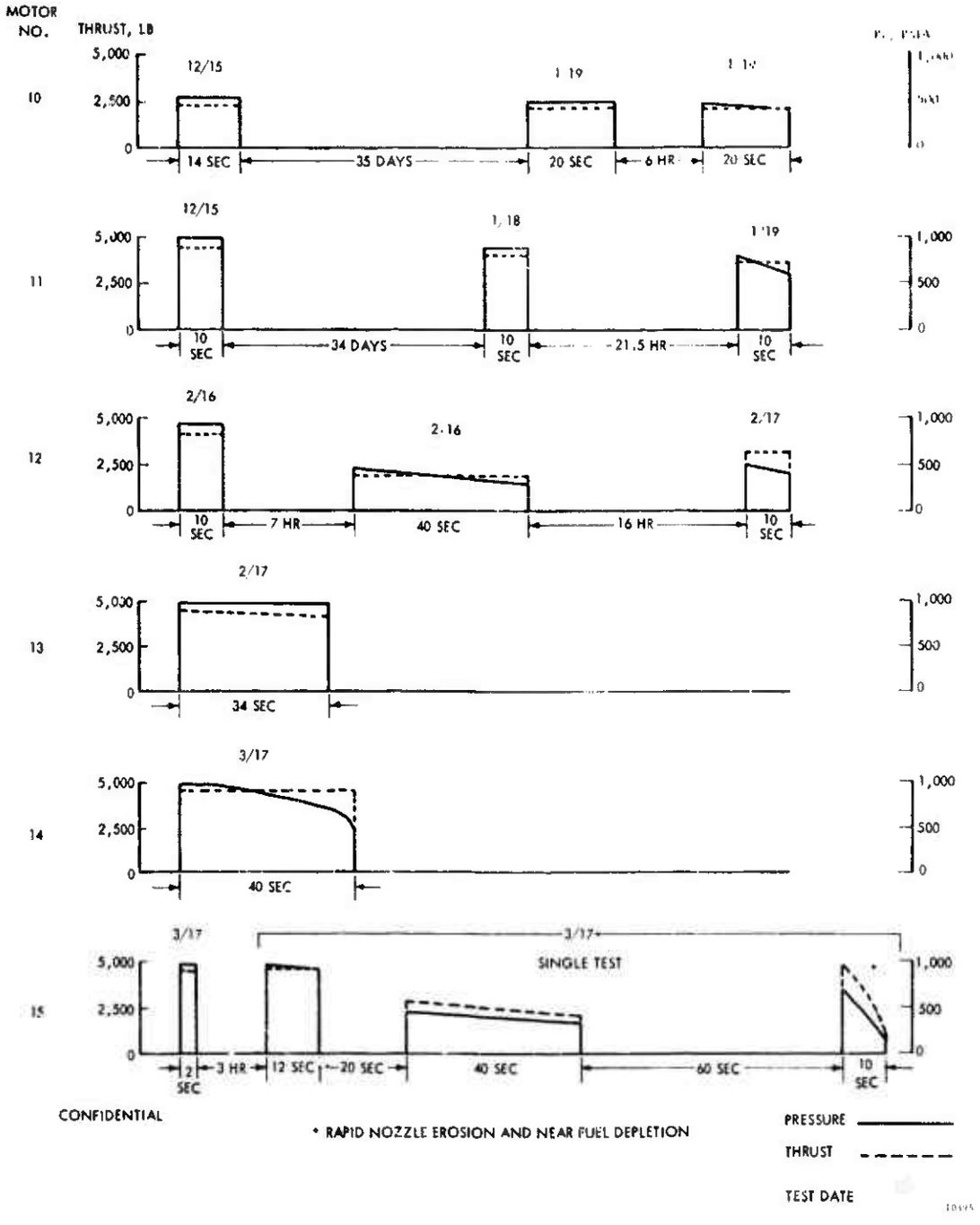

Figure 13. (U) Full-Scale Test History
October 1966 through March 1967

consume the O-rings, and (2) the forward insulation-forward injector damage was a result of excessive radial clearance between the injector bodies and the insulation.

(C) Prior to further testing of motor 10, the O-ring sealing surfaces were repaired, radial clearance around the forward injectors eliminated, and the aluminum aft injector poppet replaced with a copper poppet.

(C) The motor was successfully refired two times for 20-sec durations. The forward insulation-forward injector damage did not recur, O-ring leakage was slight, and the same aft injector survived both firings. The aft closure insulation, nozzle throat, and divergent sections continued to perform well.

(C) Termination of the firings was smooth and immediate. The fuel grain continued to maintain a clean surface with no evidence of char or degradation.

b. Motor 11

(C) Three firings were performed with motor 11 at the boost thrust level (1,000 psia chamber pressure) accumulating 30 sec of firing time. The objectives of these tests were to characterize the fuel regression, observe the grain geometry progression with successive firings, and evaluate the individual components at the boost thrust level.

(C) The motor was initially test fired for 10 sec. The aft insulation again performed well as did the integral nozzle throat and exit section, and the grain surface was uniform with no sign of thermal degradation. The same problem areas occurred as in the first test of motor 10. All six forward injectors were damaged severely, the magnesia-phenolic nozzle entrance cap had regressed excessively, and the aft injector poppet valve was similarly damaged.

(C) Before continuing the series, the radial clearance around the forward injectors was corrected as in motor 10; the aluminum aft injector poppet valve was replaced with a copper valve. In addition, the magnesia-phenolic nozzle entrance cap was replaced with one fabricated of silica-phenolic.

(C) The aft injector was lost during the next 10-sec firing. The failure was attributed to the loss of a Teflon O-ring at the aft injector-feed tube joint with subsequent oxidizer leakage

and reaction upstream of the injector. Since ClF_3 had severely damaged the aft injector insulation, the aft injector was omitted from the assembly during the final 10-sec firing of the motor. The substitution of silica-phenolic for magnesia-phenolic in the nozzle entrance cap resulted in lower erosion rates, although overall performance of the cap remained lower than desired.

(C) Analysis of the fuel grain geometry data gathered from the six tests (motors 10 and 11) disclosed that: (1) the basic concept of using satellite ports to convert the initial circular main port to a triangular shape was valid, (2) prior to merging with the main ports, the fuel within the satellite ports was burning without oxidizer flow at an average rate of 15 mil/sec, and (3) the overall fuel regression rate was lower than anticipated.

(C) Burning of the AP-TFTA-loaded fuel under pressure and temperature caused the satellite ports to enlarge prematurely, resulting in rapid enlargement of the corners of the triangular cross section. This effect, coupled with a lower regression rate along the sides of the port, produced a nonuniform web between ports. The web was thinner at the center and periphery of the motor than at its midpoint. This nonuniformity could eventually cause the web to burn through at its extremities, leaving the central portion of the web unsupported.

(C) In the fuel grains for the next two motors (motors 12 and 13), three different modifications to the port configuration were applied to compensate for the nonuniform burning. Both motor grain geometries were identical to eliminate the possibility of pressure and duty cycle variations from confusing data evaluation.

c. Motor 12

(C) Motor 12 underwent a duty cycle test consisting of firings for 10 sec at full thrust, 40 sec at 50% thrust, and 10 sec at full thrust. The motor was disassembled, examined, and weighed between firings. The primary functions of the test series were to evaluate grain geometry modifications, to simulate a cycled firing, and for further component evaluation.

(C) During the first firing, the aft injector and one forward injector were damaged. Postfire examination indicated that a reaction between foreign matter within the forward injector and the oxidizer resulted in internal damage to the injector. The aft injector damage was the result of excessive submergence

of the aft injector within its insulator tube, a condition which severely disrupted the oxidizer spray pattern. The damaged injectors were replaced between firings and the excessive submergence of the aft injector was corrected. No further injector problems were encountered for the remainder of the test series.

(C) All insulation within the motor continued to exhibit performance and durability in excess of design predictions. A silica-phenolic nozzle entrance cap was employed and it exhibited excessive erosion rates as in the previous test series. The nozzle throat, which was a graphite cloth/high-char phenolic system, eroded from 2.000 to approximately 2.677 in. in diameter.

(C) A principal objective of this test series was to evaluate modifications to the grain port configuration resulting from analysis of data from motors 10 and 11. Three different modifications (see part 5 in this section) were made to correct variations between the predicted and actual burning profile of the fuel port. Each modification was made to two adjacent main ports of the fuel grain. Analysis of the fuel grain after each firing indicated that all modifications gave improvements but that enlargement of the main ports coupled with reduction of the satellite ports produced a burning profile more closely approaching the design requirement. This modification was incorporated in motors 14 and 15 for the final demonstration test series.

d. Motor 13

(C) Motor 13 was fired for 34 sec at full thrust to simulate a 90% duration full-thrust test, to further evaluate grain geometry modifications, and to evaluate individual components.

(C) All components performed satisfactorily. The nozzle entrance cap, fabricated of carbon-phenolic, remained very uniform and experienced essentially zero erosion while the graphite-phenolic throat eroded less than 1 mil/sec.

(C) Most of the fuel grain progression data were obtained from motor 12 since it had been subjected to multiple firings; however, comparison of the final firing profiles of motors 12 and 13 revealed that essentially the same fuel regression pattern had occurred.

e. Motor 14

(C) Motor 14 was intended to demonstrate a full-thrust, full-duration firing; fuel utilization; and component durability. Thus, the motor was fired for 40 sec at the boost level with consumption of 93% (by weight) of the solid fuel.

(C) All components performed well with the exception of the nozzle throat, which achieved a 10.5 mils/sec erosion rate. The nozzle entrance cap and throat sections were fabricated of materials similar to those of motor 13; however, slightly different materials were employed here to gain as much material application data as possible. All injectors were intact, test termination was mooth and abrupt, and what little fuel remained was clean and uncharred.

f. Motor 15

(C) Motor 15 was scheduled to demonstrate a duty cycle consisting of 12-sec boost, 20-sec coast, 40 sec at the sustain thrust level, 60-sec coast, and 12-sec boost without purge following oxidizer cutoff. Approximately 2 sec into the duty cycle an oxidizer leak occurred at one oxidizer injector (as a result of a CTF reaction at a contaminated fitting), causing the the firing to be terminated. Minor repairs were made without removing the motor from the test stand. The duty cycle was then performed less 2 sec at the end of the cycle (12-sec boost, 20-sec coast, 40-sec sustain, 60-sec coast, and 10-sec boost) achieving 96% (residual to initial fuel weight ratio x 100) fuel utilization. Even without purge, the fuel grain ceased burning promptly after each oxidizer cutoff and demonstrated the non-sustaining behavior of the fuel. The aft injector survived all four starts but was slightly damaged near the end of the cycle due to the loss of a section of the surrounding insulation. Nozzle throat erosion was about 7 mils/sec.

3. MOTOR PERFORMANCE SUMMARY

(C) Performance data for the 12 fixed thrust and 1 duty-cycled full-scale heavyweight motor firings are presented in table V. Because ClF_3 rather than the ClF_5 oxidizer was used, delivered specific impulse is accordingly lower (about 6%) than anticipated with ClF_5.

(C) Several conclusions can be drawn by correlating specific test conditions with the performance figures given in the table. In general, performance efficiences are relatvely high and consistent. Tests which indicate

TABLE V

(U) FULL-SCALE MOTOR PERFORMANCE DATA

(1) Motor Firing	t_b sec	P_c average psia	F average lb	Oxidizer Flow lb/sec	O/F	I_{sp} sec	ηI_{sp}
10-1	14	546	2,258	7.91	2.42	202	0.825
10-2	20	494	2,116	7.91	3.27	205	0.908
10-3	20	440	2,021	7.93	3.51	198	0.909
11-1	10	1,000(2)	4,446	13.98	2.50	227	0.873
11-2	10	892	4,065	13.92	3.40	226	0.958
11-3(3)	10	703	3,733	13.24	3.23	215	0.911
12-1	10	948	4,139	14.23	3.37	224	0.936
12-2	40	353	1,868	7.78	3.91	191	0.936
12-3	10	460	3,413	14.89	4.96	190	0.928
13-1	34	968	4,264	13.91	3.02	230	0.932
14-1	40	800	4,458	16.12	3.53	216	0.948
15-1	2	980	4,310	15.00	3.33(5)	221	0.934
15-2(4)	12	950	4,350	14.80	3.21(5)	224	0.937
	40	424	2,184	8.67	3.77(5)	199	0.892
	10	470	3,458	27.10(6)	←Depletion of Fuel→		

(1) The first number indicates the motor and the second number indicates the firing. For example, 10-3 indicates the third firing of motor 10.
(2) Approximate (P_c taps plugged during firing)
(3) No aft injection
(4) Duty cycled firing
(5) Fuel flow rate is estimated from previous data. The motor was not weighed between firings.
(6) Due to fuel depletion P_c decayed, increasing the ΔP across the injector. Since the flows were ΔP-controlled, the flow rate increased accordingly.

efficiencies lower than 90% (tests 10-1 and 11-1) are those during which the aft injectors were damaged and the submerged nozzle entrance sections were nearly consumed.

(C) Tests conducted at the higher pressure levels (900 to 1,000 psia) and at similar conditions deliver higher efficiency levels than tests conducted at the lower pressure levels (500 psia). For example, test 11-3, which was conducted at approximately 700 psia, delivered performance comparable to tests 10-2 and 10-3 (approximately 500 psia) even though no aft injection of oxidizer was used in test 11-3.

(C) It is also worthwhile to compare test 11-2 and 11-3. The approximate 4.5% efficiency differential is accredited to the use of aft injection in test 11-2 as opposed to no aft injection in test 11-3.

(C) It is interesting to note the range and magnitude of mixture ratios which were achieved. The delivered O/F ratios are typically higher than the design of 2.5 because the fuel regression is lower than anticipated. The wide range of ratios is due to the variation in oxidizer flow rates, the use of three different fuel grain geometries (see part 5 of this section), the relative test durations (since fuel flow rate varies with port growth and port growth increases with time), the pressure dependency of the fuel regression rate, and the inclusion of the flow contribution from the insulation, nozzle, etc., as fuel flow.

(C) Particularly low O/F ratios (tests 10-1 and 11-1) have been attributed to a fuel flow contribution from the satellite fuel ports "solid burning" (i.e., burning as a solid fuel). Before exposure to the oxidizer, the satellite ports regress at a rate of approximately 0.015 in./sec. Thus, while the first 25% of the grain is being consumed, the satellite ports contribute fuel flow to supplement that of the primary ports which are functioning as a hybrid fuel. Tests 10-1 and 11-1 represent this initial period and accordingly reflect reduced mixture ratio levels. Test 12-1 also represents the same initial period but with a modified fuel grain geometry in which the satellite port effects were lessened by reduction or elimination of the satellite burning surfaces. Later tests with the same fuel grain (test 12-2 and 12-3) indicate an O/F ratio increase in accordance with the above theory.

(U) The high O/F (4.96) of test 12-3 is due to a combination of effects. Nozzle erosion caused the pressure to drop; since the fuel regression rate is pressure sensitive, the regression rate, and hence, the fuel flow rate, dropped accordingly.

4. COMPONENT EVALUATION

(U) Forward and aft oxidizer injectors, insulation for five different applications, and an exhaust nozzle have been developed and successfully demonstrated. All components were subjected to repetitive thermal cycling through multiple engine starts, extensive durations in the combustion atmosphere, and a variety of test conditions. A summary of the individual component histories follows.

a. Forward Injectors

(C) Six dual-manifold, fixed-area poppet injectors were used to deliver two oxidizer flow levels to the forward end of the TCA. A discussion of the injector design has been presented in section III of this report.

(C) Testing of the injectors revealed several associated problem areas. The first difficulty consisted of extensive oxidizer leakage at the joint between the oxidizer manifolding and the forward injectors (refer to figure 10). The leakage was associated with the Teflon O-rings used to seal liquid ClF_3 from the atmosphere. During the first two tests approximately 70% of the O-rings were consumed, giving the oxidizer a free path to the atmosphere. Posttest inspection of the injectors indicated that the O-ring sealing surface had been gouged during a drilling operation. Therefore, the oxidizer leaked past and consumed the Teflon O-ring. The injectors were resurfaced prior to further testing.

(C) Later tests still incurred random O-ring failures; however, the loss rate was only about 5% and has been attributed to contamination of the O-ring during assembly. While the resulting oxidizer leak was insignificant in terms of decreasing the oxidizer flow to the motor, the high reactivity of the ClF_3 makes it hazardous to instrumentation in the vicinity of the leak. Elimination of this leakage can be achieved through the use of metal O-rings (aluminum or copper) or the use of joints designed to be self-sealing (AN type or tapered seat).

(C) Figure 14 compares six severely damaged injectors to a new one. The injectors were damaged during the program's first 10-sec, 1,000 psia firing. Similar damage occurred in the first 14-sec, 500 psia firing of a second motor. The injector damage was caused by an annular clearance (0.030 in.) between the injector body and the forward insulation (figure 15).

Figure 14. (U) Damaged Forward Injectors

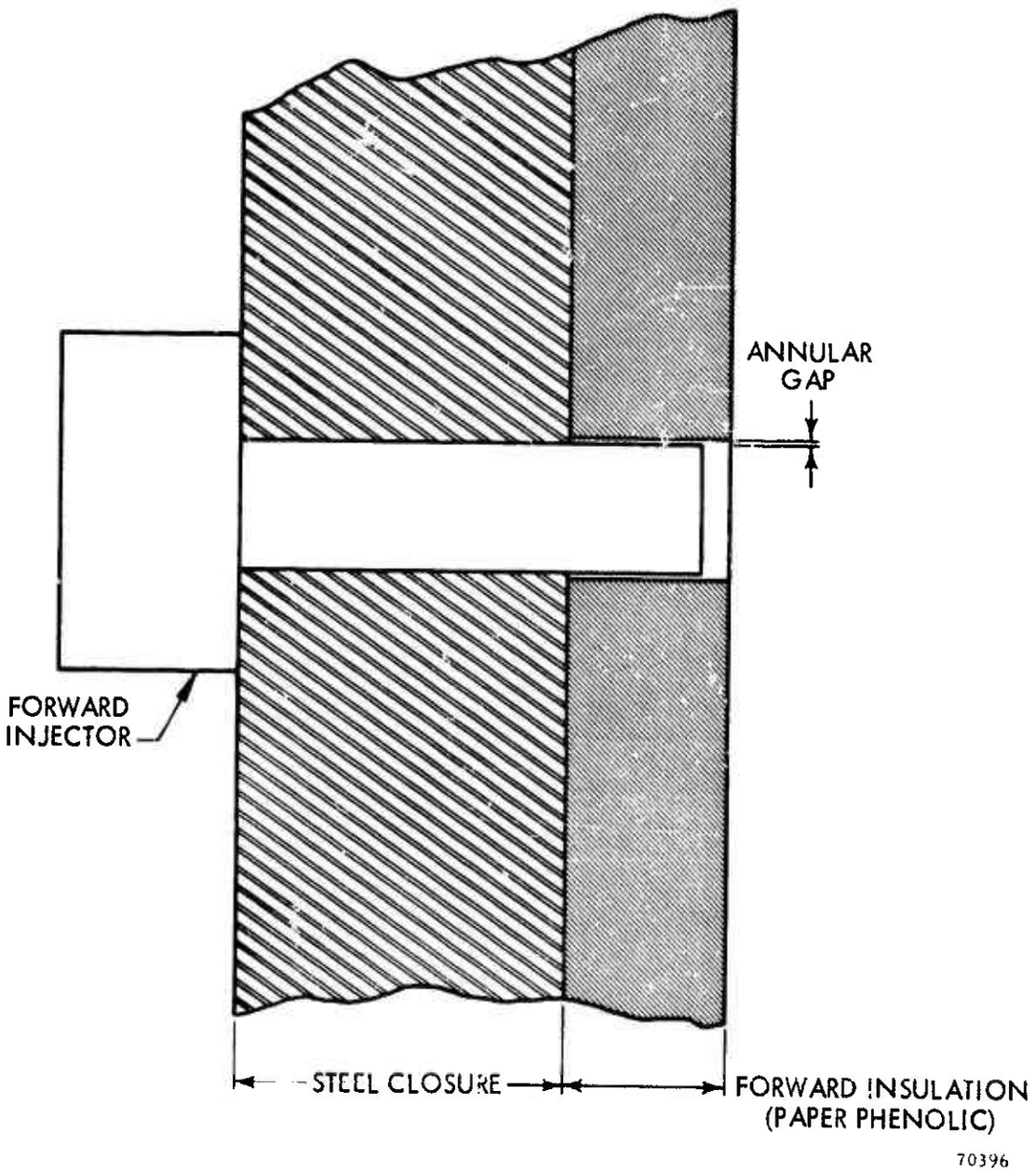

Figure 15. (U) Injector Fit in Forward Insulation

(This page is Unclassified)

The clearance, which was the result of a tolerance buildup in the design, allowed hot gases to circulate around and burn through the injector body. The damaged injector permitted ClF_3 to further consume the paper-phenolic forward insulation (see figure 16). The forward insulation was remachined, the eroded sections replaced with 5-in.-diameter inserts of silica and graphite-phenolic, and the inserts drilled and reamed to snuggly fit each injector, thereby eliminating the annular clearance. Subsequent injector damage of this type did not recur. Later insulations used 2-in.-diameter inserts (figure 17) of silica-phenolic (Fiberite MX 2625) with equal success; the point being that the problem was not one of a material application since in this instance the paper-phenolic was also exposed to the combustion environment and performed as well as the silica.

(C) On two occasions the periphery of the injector poppet head was partially eroded. This erosion has been attributed to oxidizer reaction with foreign matter lodged in the poppet seat. After many firings the aluminum poppet and/or the injector body occasionally became slightly warped due to repeated thermal cycling. When warped, the poppet will not seat properly and may allow particles and/or gases to back up into the injector after termination of the oxidizer flow. When the flow is reinitiated, a reaction will occur.

(C) Approximately four sets of forward injectors were used to accomplish 13 firings. Refurbishment (straightening, cleaning, and recalibration) of the injectors was necessary only once, indicating the degree of injector durability which has been achieved.

b. Aft Injector

(C) A single centrally located poppet type aft injector (refer to figure 10) delivered supplementary oxidizer flow to the aft plenum section of the TCA to achieve the desired mixture ratio. This injector, incorporating an aluminum body and a copper poppet valve, has survived four consecutive engine starts encompassing two pressure and flow levels. A design discussion of this type of injector is presented in section III of this report.

(C) Both of the initial 500 and 1,000 psia level firings resulted in erosion of the poppet periphery almost to the poppet seat as shown in figure 18. This erosion had the effect of disrupting the

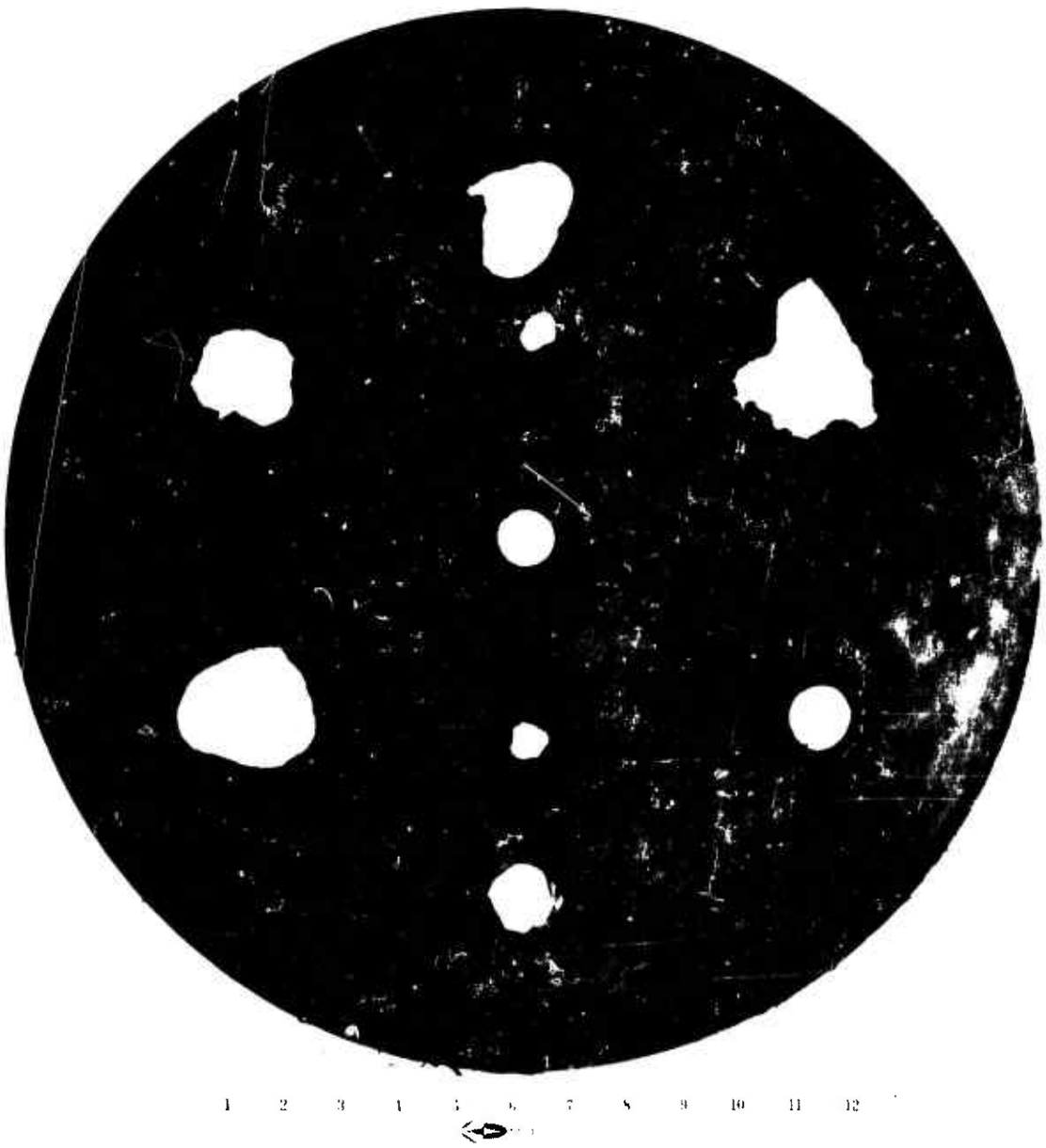

Figure 16. (U) Damaged Forward Insulation After Test 11-1

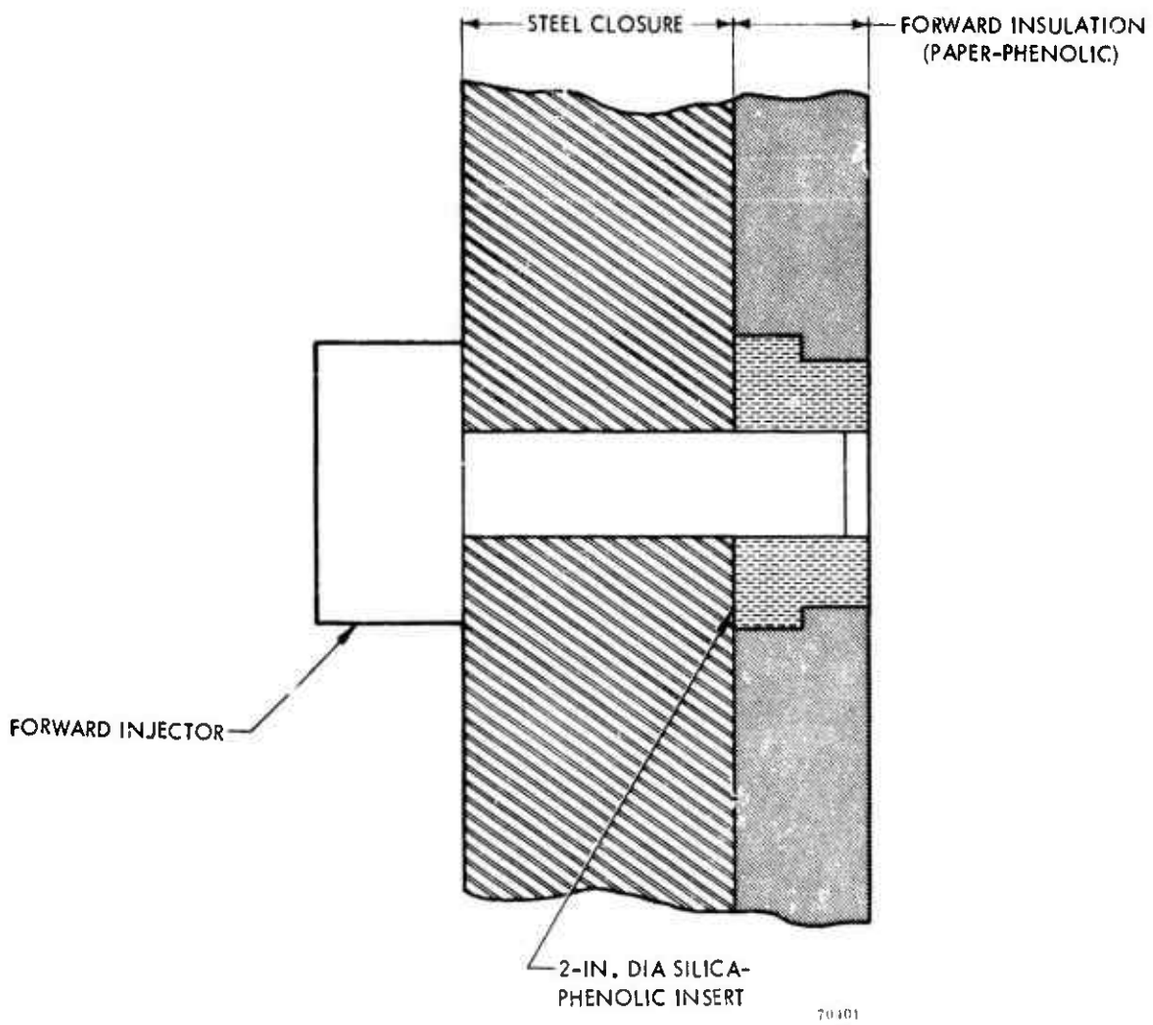

Figure 17. (U) Modified Forward Insulation

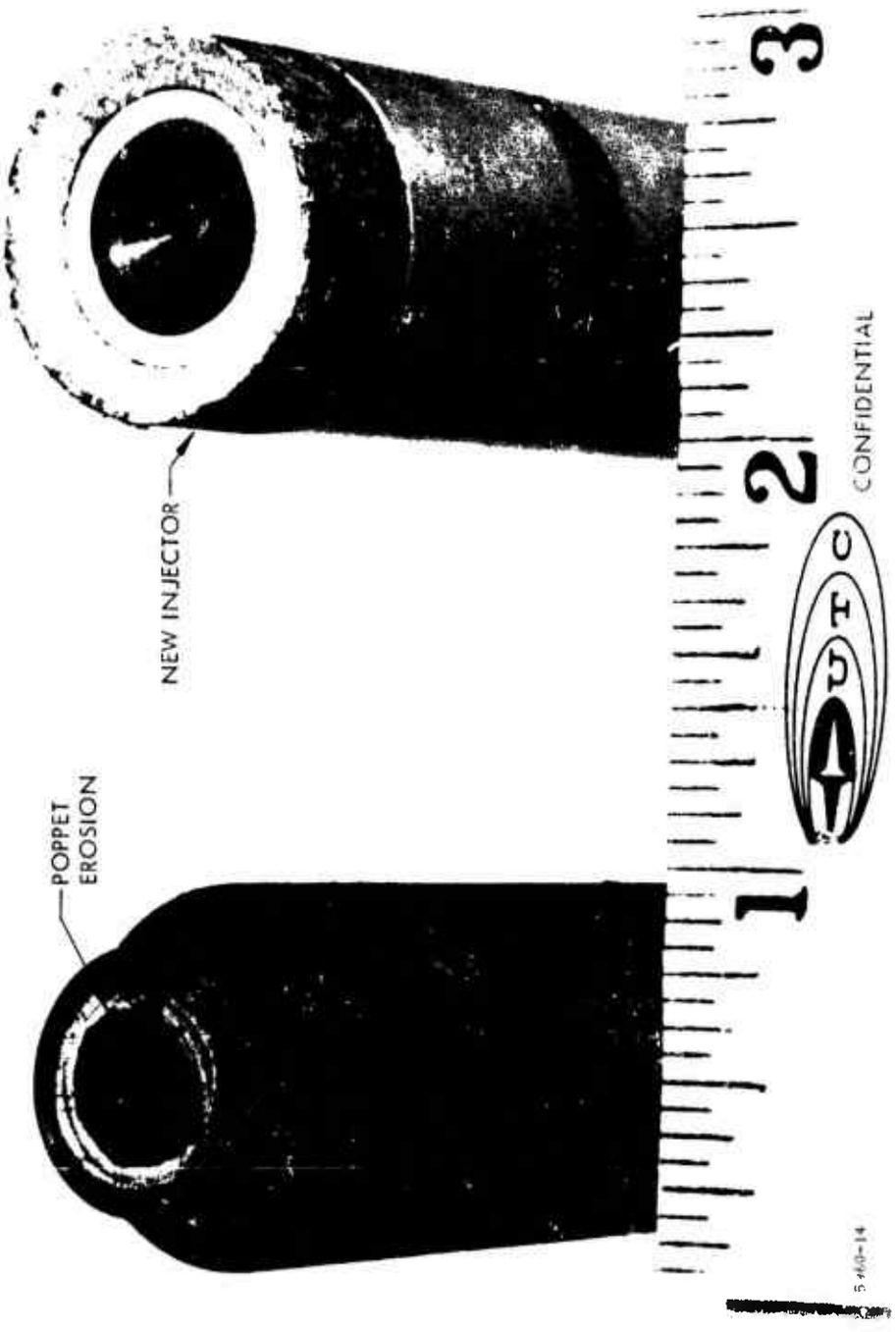

Figure 18. (U) Damaged Aft Injector

uniform 120° oxidizer spray pattern which in turn caused a reduction in combustion efficiency. The damaged poppet valves, which were fabricated of hard-anodized 6061-T6 aluminum, were then replaced with oxygen-free, high-conductivity copper poppet valves. Copper has the advantage of a higher melt temperature than the aluminum, and a lower operating temperature due to its higher thermal conductivity.

(C) Table VI presents the test history of the aft injectors. After substitution of copper for aluminum poppet valves, marked success can be seen. Aft injectors were successfully fired and refired without damage at the 500 psia level (tests 10-2 and 10-3), fired at the 500 psia level and refired at 1,000 psia (tests 12-2 and 12-3), tested for long durations at 1,000 psia (test 14, figure 19), and subjected to multiple starts encompassing combinations of both pressure and flow levels.

c. Nozzles

(C) Two nozzle configurations were used in the full-scale heavyweight motor testing of the program; both utilized submerged entrance sections and ablative throats. The geometries are illustrated in figure 20 and differ primarily in that design A employs an integral throat and exit section while design B uses separate throat and exit sections, thereby allowing different materials to be used for each application.

(C) Five entrance cap materials, four throat materials, and two exit cone materials were tested in six nozzle assemblies. Results of these tests and the relative test conditions are shown in table VII. Erosion rates for the cap and throat materials are also given. Material descriptions are presented in table VIII.

(C) Prior to fabrication of the first nozzles, short-fiber magnesia-phenolic (WBC 5217) was substituted for nylon-phenolic as the entrance cap. Magnesia-phenolic had shown possession of ablative and thermal properties similar to nylon-phenolic but with improved physical properties.[3] Subsequent tests with this material demonstrated erosion rates of approximately 30 mil/sec; an excessive rate for this application.

TABLE VI

(U) AFT INJECTOR TEST HISTORY

Test	P_c psia	t_b sec	Type of Poppet	Comments
10-1	546	14	Aluminum 6061-T6	Poppet periphery eroded
10-2	494	20	OFHC Copper	Survived
10-3	440	20	OFHC Copper	Refire of 10-2, survived
11-1	1,000	10	Aluminum 6061-T6	Poppet periphery eroded
11-2	892	10	OFHC Copper	Injector damaged due to O-ring failure
11-3	703	10	---	Injector omitted — lack of adequate insulation
12-1	948	10	OFHC Copper	Injector damaged due to recession in insulation
12-2	353	40	OFHC Copper	Survived
12-3	460	10	OFHC Copper	Refire of 12-2, survived
13	968	34	OFHC Copper	Survived
14	900	40	OFHC Copper	Survived
15	(1)	(1)	OFHC Copper	Survived four starts, damaged near end of duty cycle due to insulation failure

(1) Duty Cycle:
2 sec on — 975 psia
2 hours off
12 sec on — 940 psia
20 sec off
40 sec on — 450 psia
60 sec off
10 sec on — 500 psia

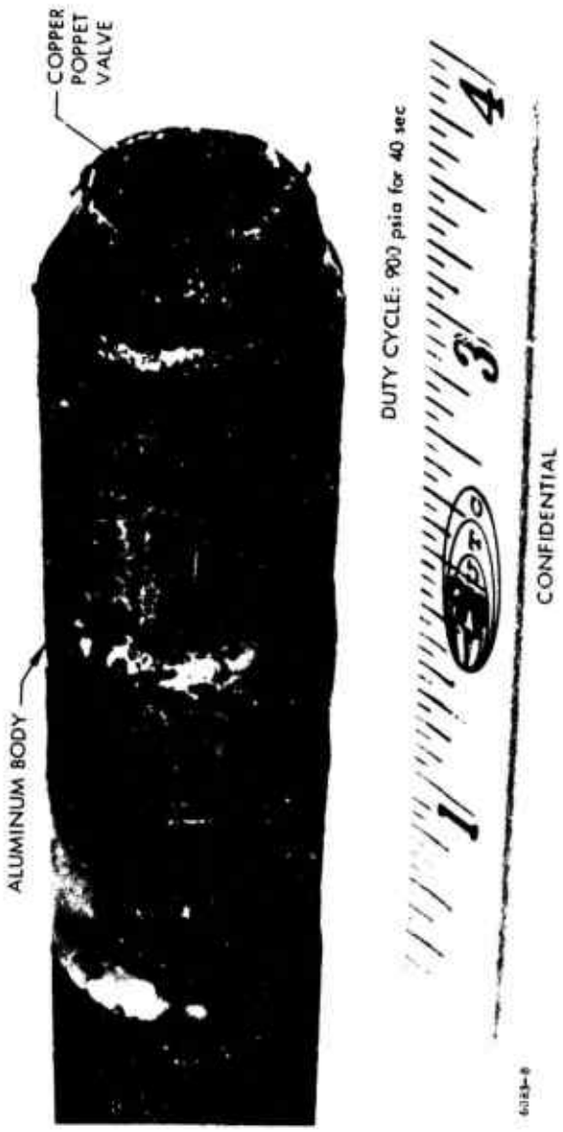

Figure 19. (U) Aft Injector of Motor 14 (Postfire)

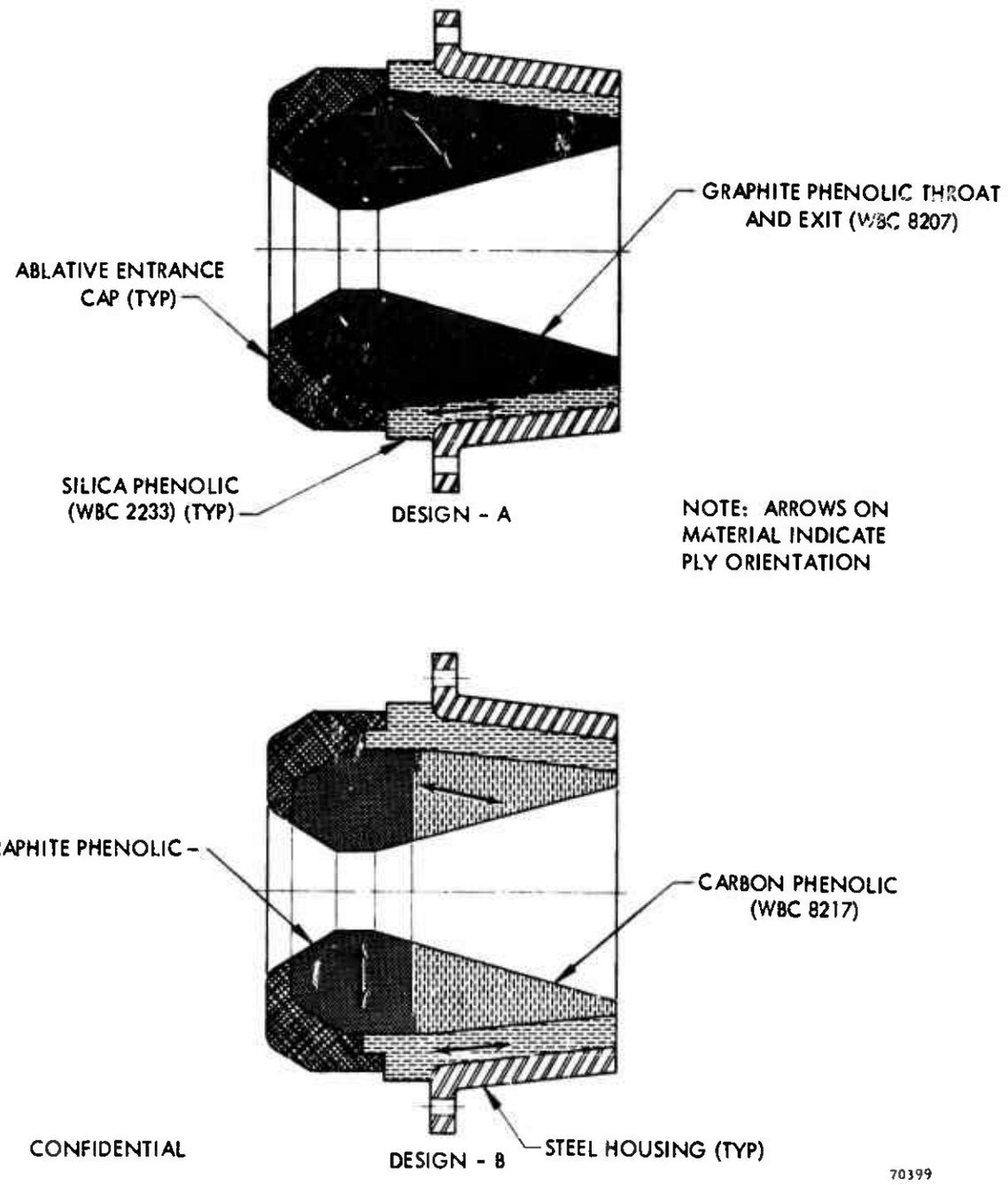

Figure 20. (U) Full-Scale Nozzle Configurations

(This page is Unclassified)

TABLE VII

(U) SUMMARY OF NOZZLE DATA

Test	P_c average psia	t_b sec	Design[1]	Entrance Cap Material	Cap $\dot{r}$ mil/sec	Throat Material	Throat[2] Diameter Initial in.	Throat[2] Diameter Final in.	ΔD_t in.	Throat $\dot{r}$ mil/sec	Exit[3] Material
10-1[4]	546	14	A	WBC5217	30	WBC8207	1.948 1.955	1.930 1.935	-0.018 -0.020	(5) (5)	WBC8207
10-2[4]	494	20	A	WBC5217	30	WBC8207	1.935 1.930	2.020 1.997	0.085 0.067	2.2 1.7	WBC8207
10-3[4]	440	20	A	WBC5217	30	WBC8207	1.997 2.020	2.150 2.185	0.153 0.167	3.9 4.4	WBC8207
11-1[6]	1,000 (assumed)	10	A	WBC5217	30	WBC8207	2.000 2.000	1.925 1.950	-0.075 -0.050	(5) (5)	WBC8207
11-2[6]	892	10	A	WBC2233	22	WBC8207	1.950 1.925	2.024 2.007	0.074 0.082	3.7 4.1	WBC8207
11-3[6]	703	10	A	WBC2233	20 – 25	WBC8207	2.024 2.018	2.240 2.235	0.216 0.217	10.9 10.9	WBC8207
12-1[7]	948	10	A	WBC2233	22	WBC8207	2.000 2.000	1.960 1.930	-0.040 -0.070	(5) (5)	WBC8207
12-2[7]	353	40	A	WBC2233	22	WBC8207	1.960 1.930	2.447 2.373	0.413 0.417	5.2 5.2	WBC8207
12-3[7]	460	10	A	WBC2233	22	WBC8207	2.373 2.447	2.535 2.818	0.162 0.371	8.1 18.6	WBC8207
13	968	34	B	WBC8204	0	WBC8268	2.002 2.002	2.014 2.055	0.012 0.053	0.2 0.8	WBC8217
14	900	40	B	WBC8251	1 – 8	WBC8249	2.000 2.000	2.623 2.835	0.623 0.835	7.8 10.5	WBC8217
15	(8)	(8)	B	WBC8217	0	WBC8269	1.996 1.996	2.876 2.767	0.880 0.771	6.9 6.0	WBC8217

(1) See figure 20
(2) Two measurements taken 90° apart
(3) ϵ = 7.0
(4) Same nozzle
(5) Diameter decrease due to expansion
(6) Same nozzle (cap replaced after 11-1 with WBC2233)
(7) Same nozzle
(8) Duty cycle: 2 sec on – 975 psia, 2 hours off; 40 sec on – 450 psia, 60 sec off; 12 sec on – 940 psia, 20 sec off; 10 sec on – 500 psia

TABLE VIII

(U) MATERIAL DESCRIPTION

Material*	Application	Form	Material Description
WBC 5217	Entrance cap	Molding compound	WBC 2223 high char phenolic reinforced with TX fibers (magnesia)
WBC 2233	Entrance cap, Throat backup	Molding compound Tapewrap	WBC 2223 high char phenolic resin reinforced with high silica fabric
WBC 8204	Entrance cap	Molding compound	WBC 2242 polyfunctional aldehyde phenolic resin reinforced with carbon fabric
WBC 8251	Entrance cap	Molding compound	WBC 2223 high char phenolic resin reinforced with carbon-silica fabric
WBC 8217	Entrance cap, Exit cone	Molding compound Flat laminate	WBC 2223 high char phenolic resin on carbon fabric
WBC 8207	Throat, Exit cone	Flat laminate Flat laminate	WBC 2223 high char phenolic resin reinforced with graphite fabric
WBC 8268	Throat	Flat laminate	WBC 2271 phenolic resin on graphite cloth
WBC 8249	Throat	Flat laminate	WBC 2223 high char phenolic resin with ACX filler on graphite cloth
WBC 8269	Throat	Flat laminate	WBC 2273 phenolic resin on graphite cloth

* Designation of Western Backing Corporation (WBC), Culver City, California.

CONFIDENTIAL
(This page is Unclassified)

Silica-phenolic was then selected to replace the magnesia caps. Tests with this material indicated a slightly improved erosion rate (20 to 25 mil/sec, figure 21, motor 12). Later tests employed caps of carbon silica-phenolic and carbon-phenolic materials. The carbon-silica cap (WBC 8251) eroded at rates between 1 to 8 mil/sec but was not uniform (figure 21, motor 14). Both carbon-phenolics, WBC 8204 and WBC 8217 (figure 21, motors 13 and 15, respectively) experienced essentially zero erosion when submitted to relatively rigorous duty cycles. However, the 8217 material did exhibit severe grooving and undercutting of the plys, probably due to effluxing of the resin products when subjected to such a rigorous duty cycle (as indicated in table VII). The WBC 8204 material produced a smooth and even surface. The shutdown characteristics of the fuel grain did not appear to be impaired by the use of these heat storing materials.

(C) The first three nozzles used were fabricated to design A (see figure 20), using an integral throat and exit section fabricated of WBC 8207. The first short duration firings with this material resulted in a reduction in the throat diameter which was caused by expansion of the material. Subsequent tests with the same nozzles revealed throat erosion rates ranging from approximately 2 to 19 mil/sec depending upon the severity of the test and the number of starts the nozzle had experienced. It is interesting to note that although the nozzle of motor 10 was exposed to almost double the test duration of the nozzle of motor 11 (table VII), the erosion rates of motor 10 are the lesser. This is due to an approximate doubling of flows and pressures from motor 10 to motor 11.

(C) The final three nozzle assemblies were fabricated to design B. Three graphite-phenolics were used for the throat sections, each differing in the type of resin system employed (table VII). Of all four nozzle materials tested, WBC 8268 demonstrated the best erosion resistance. This material was tested at approximately 1,000 psia for 34 sec and eroded at less than 1 mil/sec. The other graphite-phenolics, WBC 8249 and WBC 8269, delivered rates of 7 to 10 and 6 to 7 mil/sec, respectively, and became somewhat elliptical.

(C) WBC 8207 and WBC 8217 performed well in the exit section. As can be seen from figure 21, char depths of the throat and exit sections were not sufficient to affect the silica backup material.

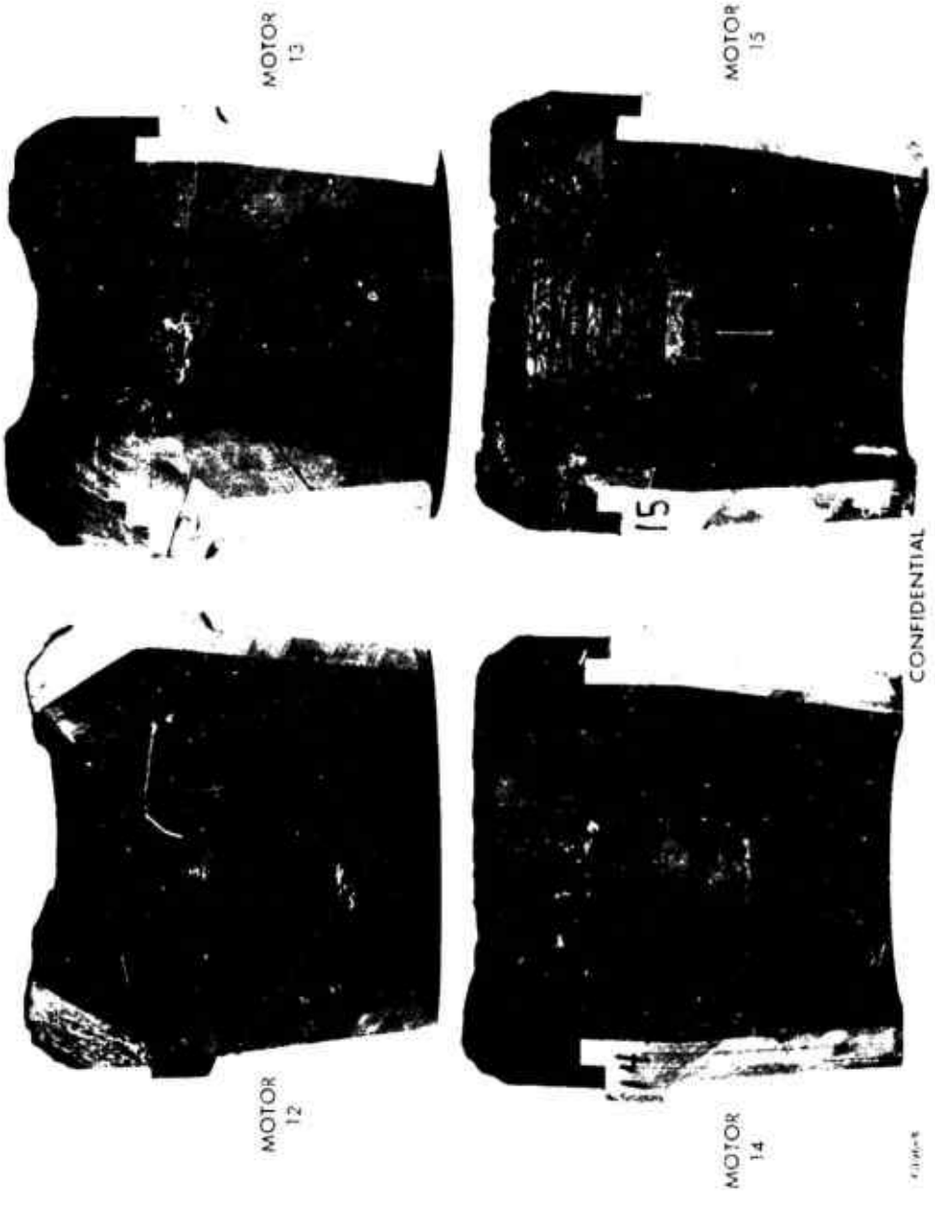

Figure 21. (U) Nozzle Sections

d. Insulation

(C) The insulation requirements can be subdivided into two categories: those applications which were subjected to the combustion environment, and those which were not (refer to figure 10 for identification). The forward closure insulation, the insulation tube surrounding the aft injector, and the sleeve into which the fuel grain was cast were not intended to see the combustion environment and were therefore fabricated of paper-phenolic, a readily available and inexpensive material. The aft grain insulation and the aft closure insulation (which were exposed to combustion) were fabricated of an ablative, low-char material, nylon-phenolic, to minimize heat feedback to the fuel grain.

(1) Forward Closure Insulation

(C) As previously mentioned in part a. of this section, an annular clearance between the forward insulation and the injector body (illustrated in figure 15) allowed hot gases to circulate around and burn through the injector bodies. Oxidizer from the damaged injectors then consumed portions of the insulation (figure 16) in the vicinity of the injectors.

(C) The damaged portions of the insulation were machined away and 5-in.-diameter inserts of carbon-phenolic (WBC 8217) and silica-phenolic (WBC 2233) installed. The method of motor assembly was modified to provide a close tolerance fit between the injectors and the insulation insert. This modification consisted of drilling and reaming the inserts to snuggly fit the injectors after the motor was assembled, thereby eliminating the annulus. Damage of this nature did not recur in subsequent testing.

(U) Later insulation pieces were fitted with 2-in.-diameter inserts of silica-phenolic (Fiberite—MX 2625) as shown in figure 17. As the grain was consumed, paper-phenolic exposed to the combustion environment performed as well as the silica inserts, indicating that the problem was not one of material incompatibility.

(2) Aft Injector Insulation

(C) A 2-in.-diameter cylinder of paper-phenolic was used to protect the aft injector located in the center of the fuel grain. Early in the testing it became evident that the end of the insulating tube exposed to the combustion gases was being partially consumed, exposing the injector body. During the next tests (conducted with motors 12 and 13), the ends of the tubes were replaced with 2-in. sections fabricated of carbon-phenolic (WBC 8217). During assembly zinc chromate putty was packed between the injector body and the 2-in. section to prevent gas circulation between the components. These modifications performed very well and gave ample protection to the injector.

(U) Because of material availability, later tests (conducted with motors 14 and 15) employed sections of silica-phenolic for the same application. The silica sections did not withstand the conditions as well as the carbon material and were partially consumed.

(C) Judging from the overall results, it is evident that the full length of the insulating tube should be fabricated of carbon-phenolic for the best protection, but the thickness of the insulation can be considerably reduced (at least 50%). Allowance should also be made for packing a sealant (zinc chromate putty has performed very well) around the injector to prevent gas circulation.

(3) Case Insulation

(U) The fuel grain was cast into a 1/4-in.-thick paper-phenolic sleeve providing an easily removable cartridge for convenience in disassembly. The sleeve also protected the steel motor case when the fuel was depleted. Paper-phenolic functioned satisfactorily in this application.

(U) This insulation component would not be used in a lightweight system. However, local application of high erosion-resistant insulation (asbestos-loaded epoxy was used during the final test series) might be needed to protect the case wall against injector effects.

(4) Aft Grain Insulation

(C) The purpose of the aft grain insulation is to inhibit end burning of the solid fuel grain during motor operation and to protect the grain from radiated heat during shutdown. Nylon-phenolic was selected for this application because of its low heat retention and favorable ablative characteristics.

(U) The nylon-phenolic material (WBC 2208), fabricated with 1/2-in. by 1/2-in. chopped nylon squares and a standard phenolic resin, maintains a uniform, clean surface with very little char. Figure 22 illustrates a typical posttest profile of the nylon aft grain insulation. The regression rates shown are representative of the tests of this program and are consistent with rates achieved during other programs (NAS 7-311 and NAS 7-475).[3]

(C) During the first tests with motors 10 and 11, the perforations in the aft grain insulation opened at a lesser rate than the fuel ports (shown in figures 23 and 24). If this were allowed to continue, as the fuel was expended, the insulation would present more of an obstruction to the flow, become less supported, and may eventually break up, possibly plugging the nozzle. Prior to the second firings of motors 10 and 11, the perforations in the insulation were opened to match the grain. Posttest inspection again indicated a very slight opening of the perforations as compared to the fuel grain perforations. The aft grain insulation was omitted from the final firings of motors 10 and 11 with no apparent adverse effects.

(C) The thickness of the insulation used in motors 12 and 13 was decreased from 0.75-in. to 0.40-in. to assist the regression of the perforations. Posttest inspection revealed that reduction of the insulation thickness did not aid the desired regression. At this time it was evident that degradation of the fuel grain due to internal heat radiation at shutdown was not a problem. Therefore, a 1/4-in.-thick section

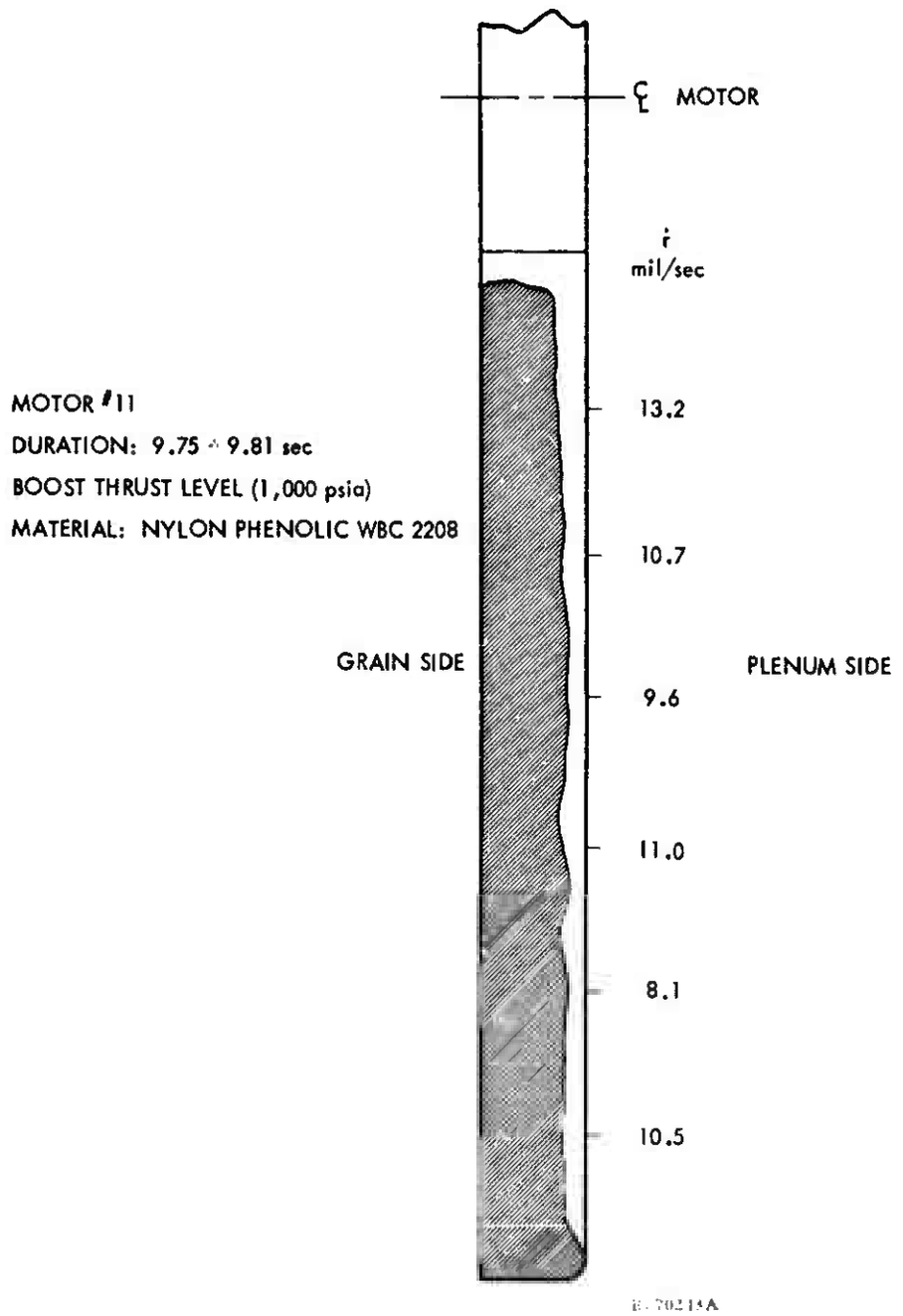

Figure 22. (U) Aft Grain Insulation – Postfire Profile

(This page is Unclassified)

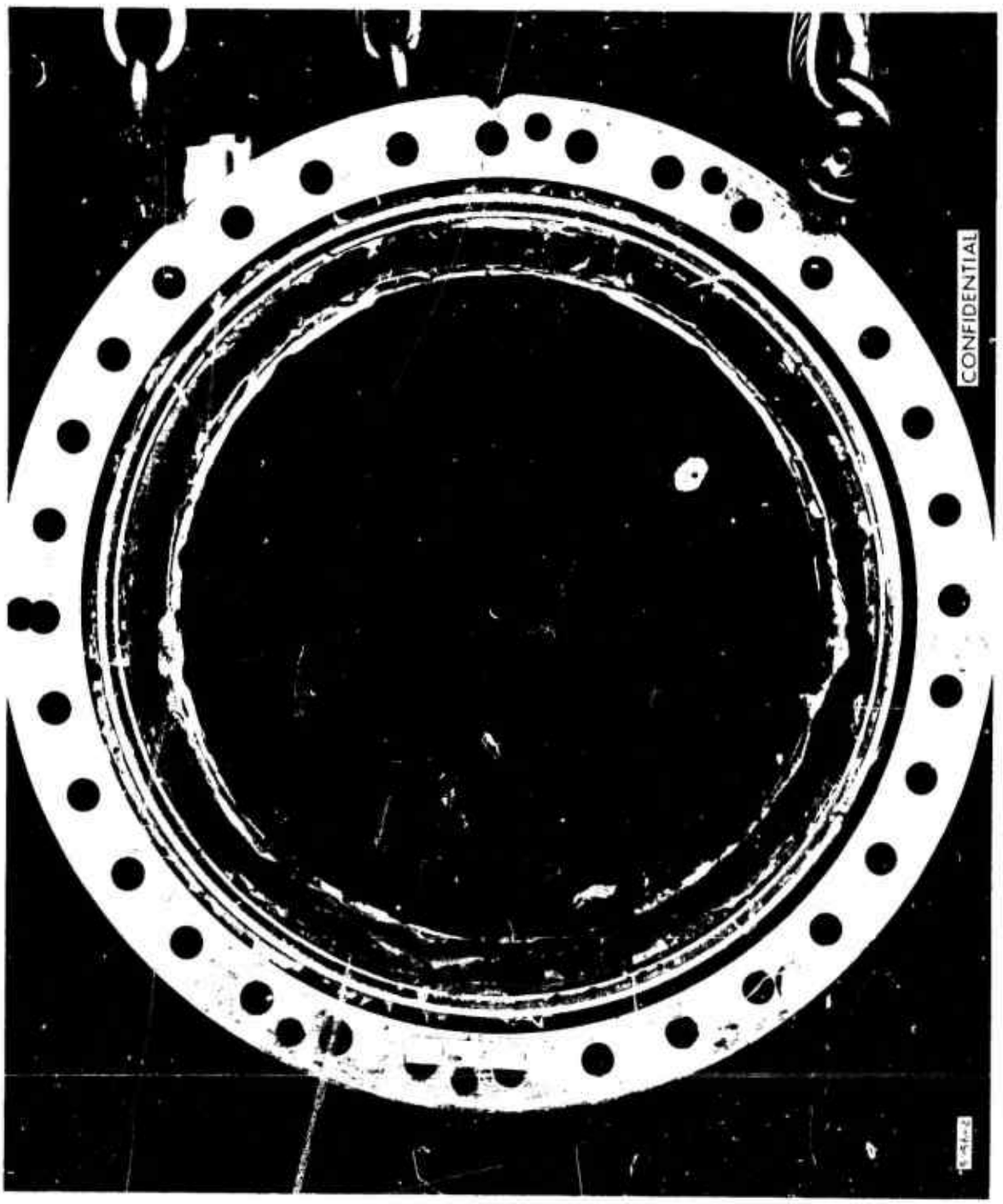

Figure 23. (U) Aft Grain Insulation

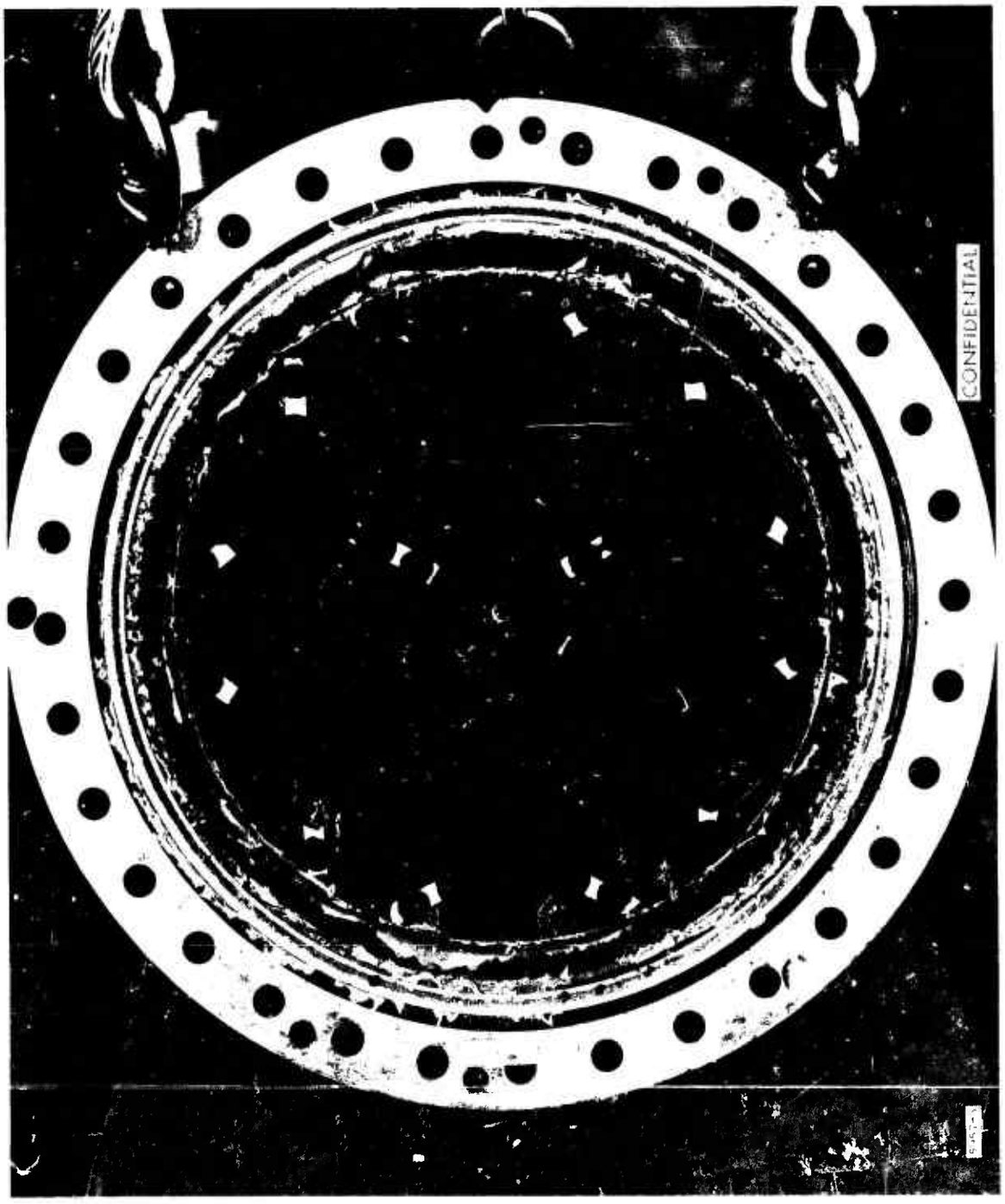

Figure 24. (U) Aft End of Grain

of asbestos-loaded epoxy was cast in place of the aft grain insulation of the final two motors. Unfortunately, essentially all of the fuel grain was consumed in testing of these motors as well as the epoxy aft grain insulation. Therefore, no observations of the insulation performance could be made.

(5) Aft Closure Insulation

(U) The function of the aft closure insulation is to protect the aft closure from the severe combustion environment. Nylon-phenolic was also selected for this application because of its low heat retention and favorable ablative characteristics. In addition to retaining little heat, a highly ablative material has the additional advantage of providing film cooling for the nozzle when used in this application.

(U) The nylon-phenolic employed, WBC 2208, was of the same chopped square form as that used for the aft grain insulation, part (4) of this section. Testing has shown the material to ablate uniformly and at a moderate rate well within the design limit. Figure 25 is a representative profile taken after a typical duty cycle. The material does not appear to be influenced by repeated thermal cycling (start, stop, heat soak, etc.). Nylon-phenolic performed very well in this application and, as can be seen from the postfire profile, was somewhat overdesigned.

5. FULL-SCALE GRAIN GEOMETRY

(C) The grain geometry of motors 10 and 11, illustrated in figure 3, has been discussed previously in section III of this report. The 18-in.-diameter geometry uses six 1.2-in.-diameter active fuel ports into which oxidizer is sprayed. Each active port has seven 0.6-in.-diameter inactive "satellite" ports clustered about it which are not intended to burn until the web between each inactive port and active port is consumed. The successive burning of inactive ports is intended to result in an essentially constant fuel flow rate when used with the HFX 7808 fuel. Predicted regression profiles are also shown in figure 3, illustrating the expected geometry change from a circular to a near triangular geometry.

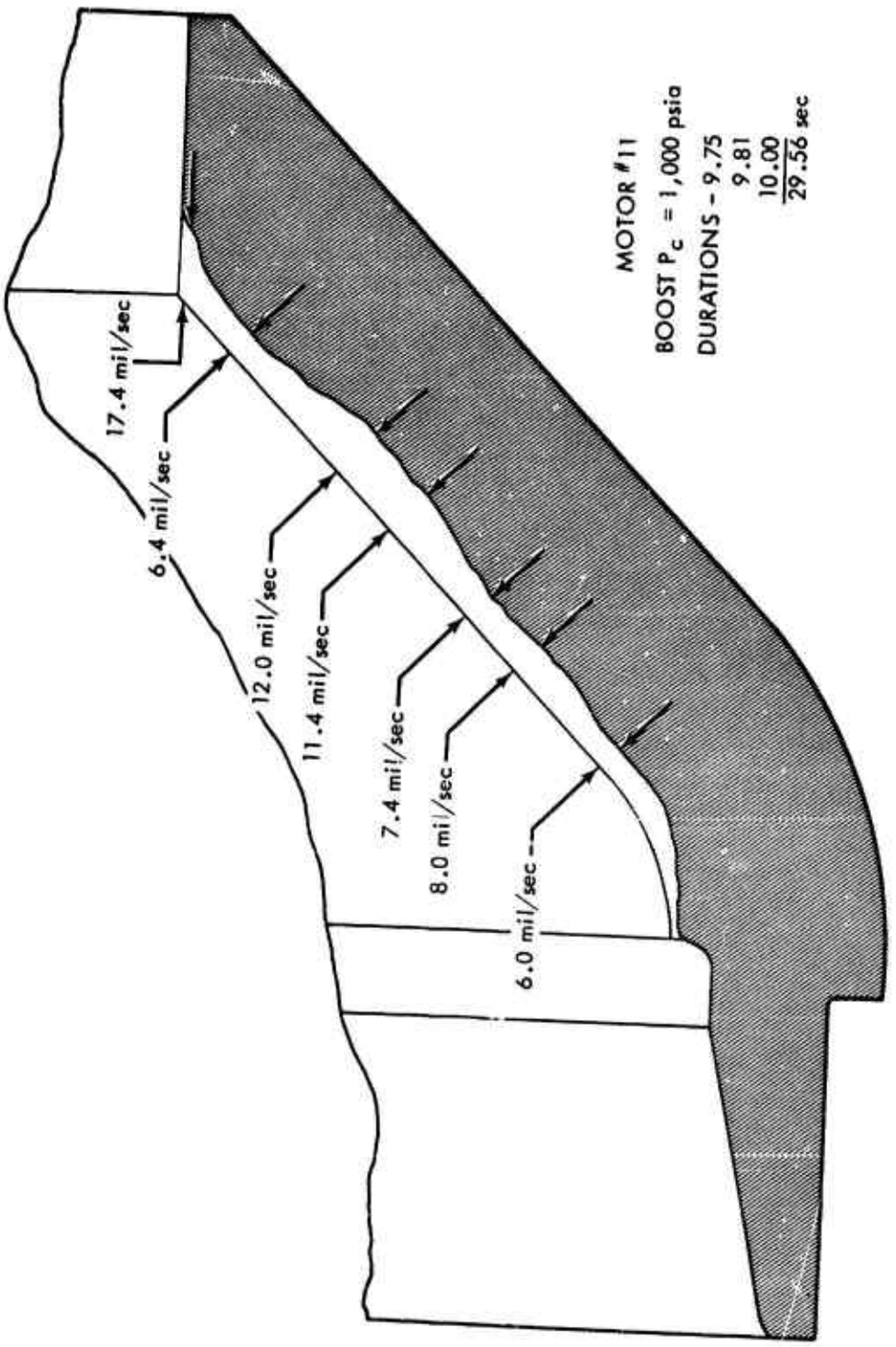

Figure 25. (U) Cross Section of Aft Closure Insulation

(C) Motors 10 and 11 were subjected to multiple firings at the sustain and boost thrust levels, respectively, to observe the port geometry progression with each successive test. Following each test, the fuel port profile was recorded for comparison with the predicted profile. Early in the series it became evident that significant variation between the predicted and actual burning fuel port profile was occurring. The discrepancy was most evident as a nonuniform web between the ports.

(C) Figure 26 illustrates the fuel port profiles of motor 11 after each of three successive 10-sec, 1,000 psia firings. This illustration shows the web between adjacent ports to be very thick in the center, yet nearly converging with the adjacent ports near the corners. Study of these profiles and those taken from the three sustain level tests (motor 10) disclosed that (1) the overall fuel regression rate was lower than anticipated, (2) prior to merging with the main ports, the fuel within the satellite ports was burning without oxidizer at an average rate of 15 mil/sec, and (3) the concept of using satellite ports to convert an initially circular main port to a near triangular shape appeared to be valid.

(C) The burning of the AP-TFTA-loaded fuel under pressure and temperature caused the satellite ports to enlarge prematurely, resulting in a more rapid enlargement in the corners of the triangular cross section. This effect, coupled with a lower regression rate along the sides of the port, produced the nonuniform web between ports. This nonuniformity could eventually cause the web to burn through at its extremities, leaving the central portion of the web unsupported.

(C) In the fuel grains for the next two motors (motors 12 and 13), three different modifications to the port configuration were applied to compensate for the nonuniform burning. Since the basic grain geometry employs six active ports, all three approaches were tested in each grain (one modification applied to two adjacent ports) to determine an optimum solution. Both motor grain geometries were identical to eliminate the possibility of pressure and duty cycle variations from confusing data evaluation.

(C) Figure 27 illustrates the application of the modifications. In two grain sectors (segment A) the geometry was unchanged, but the satellite port surfaces were inhibited to prevent premature burning by coating the port surfaces with an inert compound (essentially composed of the fuel binder). In two additional sectors (segment B) the central port diameters were enlarged to 1.8 in. and the three outermost satellite ports eliminated to compensate for the satellite burning. In the last two sectors (segment C) the central port diameters were enlarged to 1.8 in. and the outside satellite port diameters reduced in diameter to account for the premature burning.

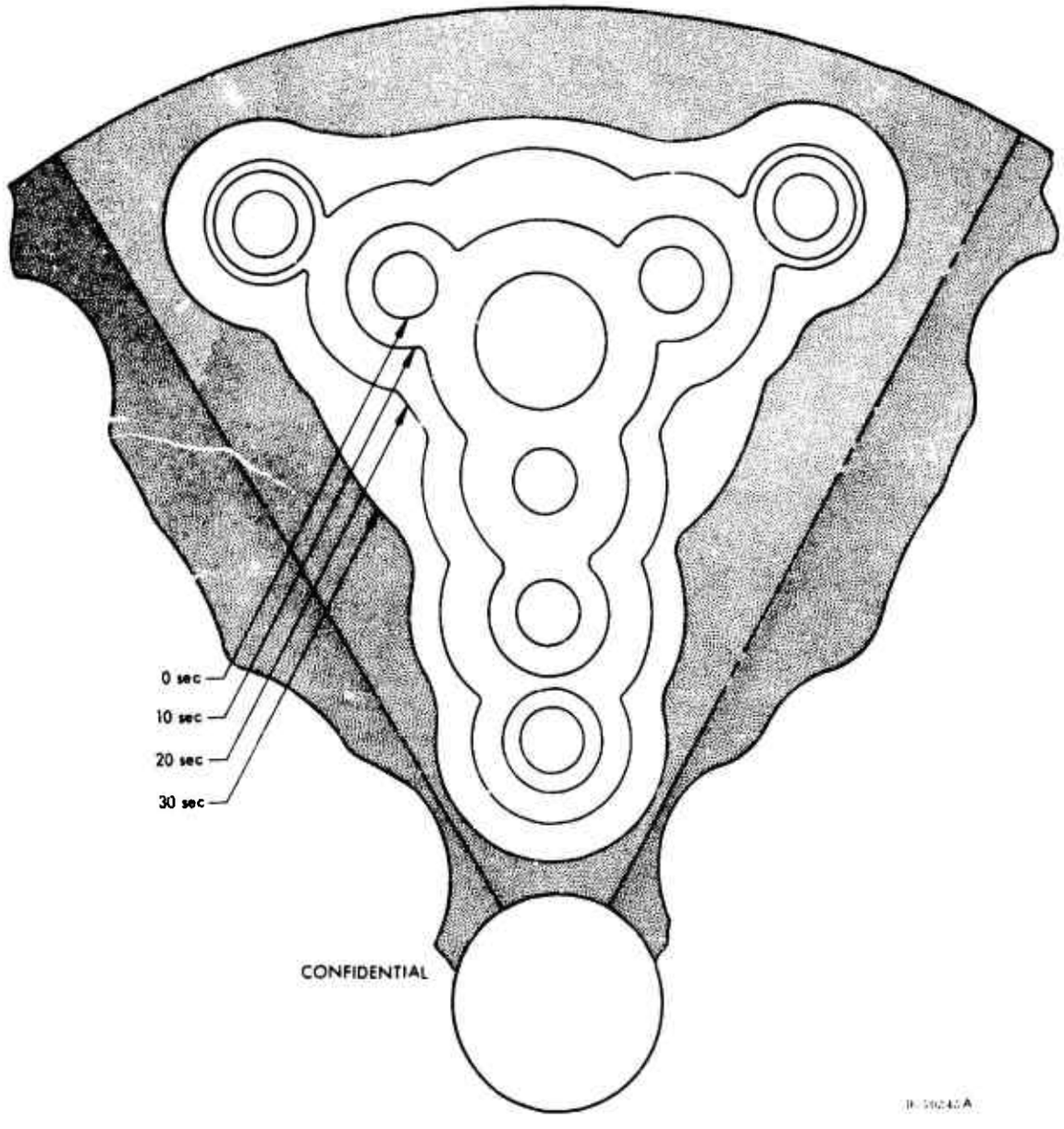

Figure 26. (U) Actual Port Profile of Motor 11

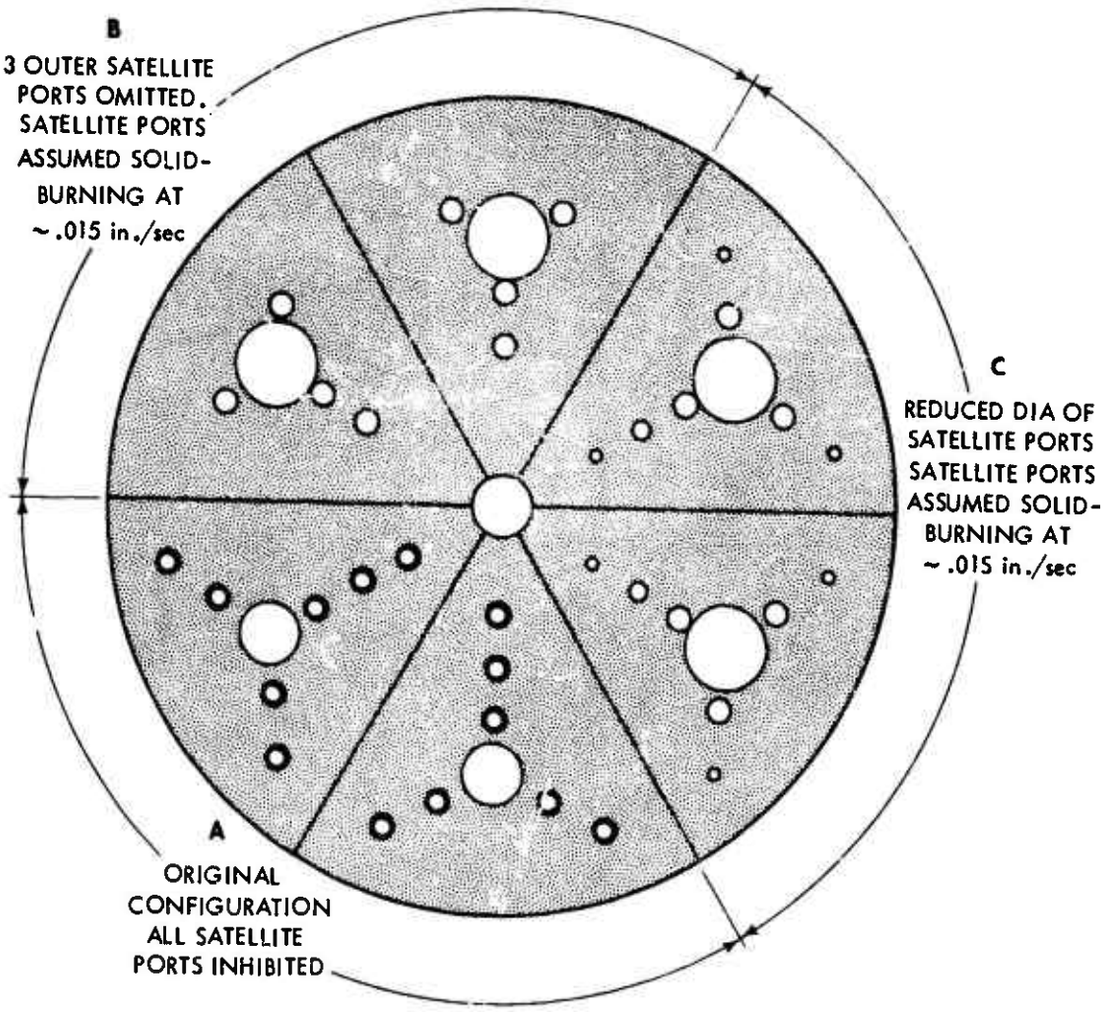

Figure 27. (U) Grain Geometry of Motors 12 and 13

(C) Figure 28 illustrates the profiles of motor 12 after each of three consecutive firings (10 sec at 1,000 psia, 40 sec at 500 psia, and 10 sec at 1,000 psia). Analyses of these profiles and the profile from motor 13 (34 sec at 1,000 psia) indicated that all modifications gave improvements but that the enlargement of the main ports, coupled with reduction of the satellite ports (segment C, figure 28), produced a burning profile most closely approaching the design requirement. .

(C) Several additional conclusions were drawn from figure 28. Coating the satellite ports with a thin layer of a binder type material was only slightly effective in inhibiting the satellite ports from burning (compare segment A of figure 28 with figure 26). The effectiveness of this correction could be improved by applying a thicker coating and/or using a more effective compound; however, such a means of correction is undesirable in an end product. Coating the port adds additional procedures, complexity, and weight to the system. Enlarging the main ports and eliminating the three outermost satellite ports (segment G, figure 28) produced a more uniform web but also considerably increased the fuel sliver at the extremities of the web. Enlarging the main ports and reducing the outermost satellite ports proved to be an effective means of accounting for the burning of the satellite ports. Figure 28 (segment C) indicates the remaining web to be uniform and supported at the wall. This modification was incorporated in motors 14 and 15 (as shown in figure 29) for the final demonstration test series. Motor 14 was test fired for 40 sec at the boost thrust, level consuming 93% (by weight) of the solid fuel. Motor 15 was subjected to a rigorous duty cycle as previously indicated and demonstrated 96% fuel utilization. Figure 30 illustrates the residual fuel of motor 15.

6. FUEL BALLISTICS ANALYSIS

(C) Data analyses from 11 full-scale fixed-thrust test firings have shown that the HFX 7808 fuel regression rate can be adequately expressed by the function, $\dot{r} = a G_o^n P_c^m$, where a, n, and m are constants characteristic of the system, G_o is the oxidizer mass flux, and P_c represents the chamber pressure. The equation employed in the determination of the fuel grain dimensions and the oxidizer flow schedule was of the form $\dot{r} = 0.5\, G_o^{0.5} (P_c/1{,}000)^{0.1}$. This assumed relationship was based on prior experience with similar four-component fuel systems and assumes no oxidizer dependency (i.e., ClF_3 versus ClF_5 will have no influence on regression rate, performance, etc. This has been verified by a multitude of experimental data with various oxidizers and fuels).

(C) Recent tests have resulted in a revised equation of the form, $\dot{r} = 0.13\, G_o^{0.5} P_c/1{,}000)^{0.1}$ which reflects lower regression and fuel flow rates. As a consequence of these lower rates, the fuel surface area must be increased to achieve an optimum O/F. This may be accomplished by lengthening the fuel grain or changing the grain shape. Since the motor hardware was fabricated and modification would have required more time than available, these changes cculd not be accomplished during this program.

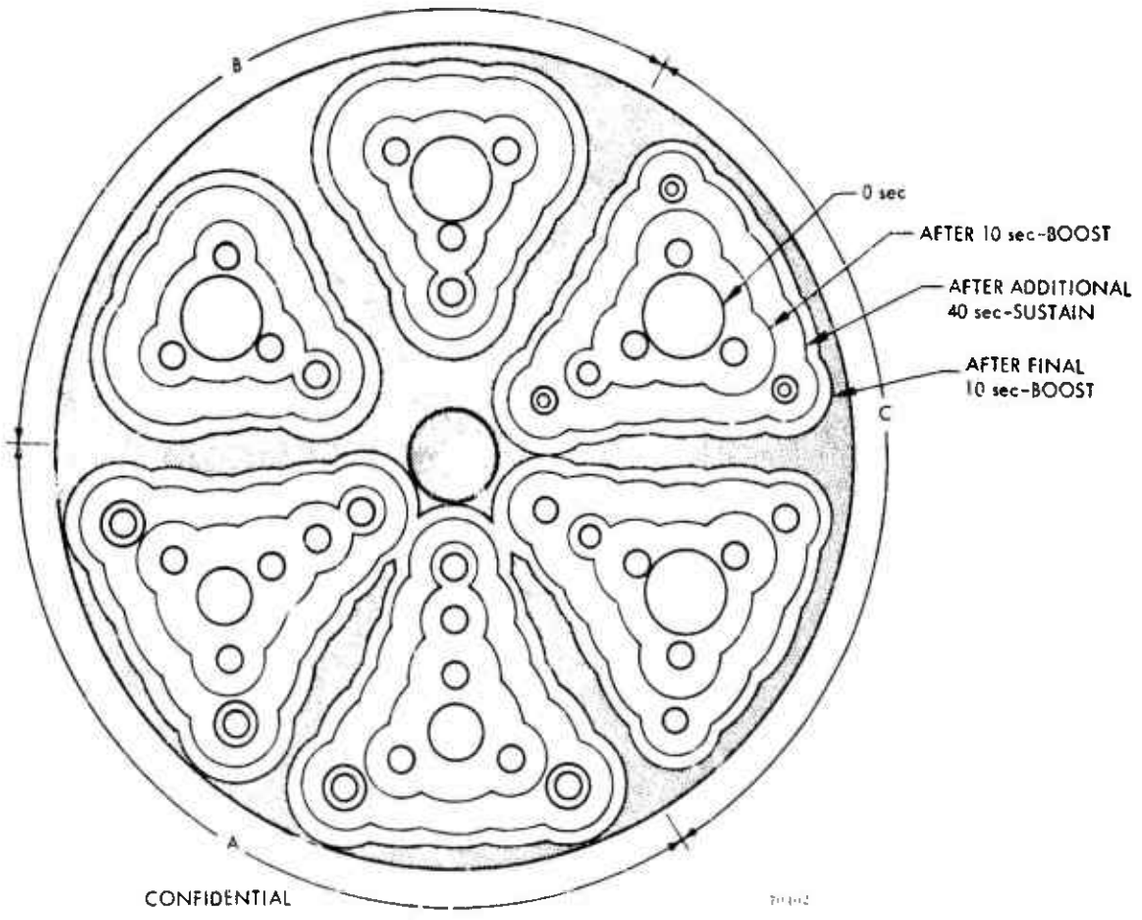

Figure 28. (U) Postfire Grain Profiles of Motor 12

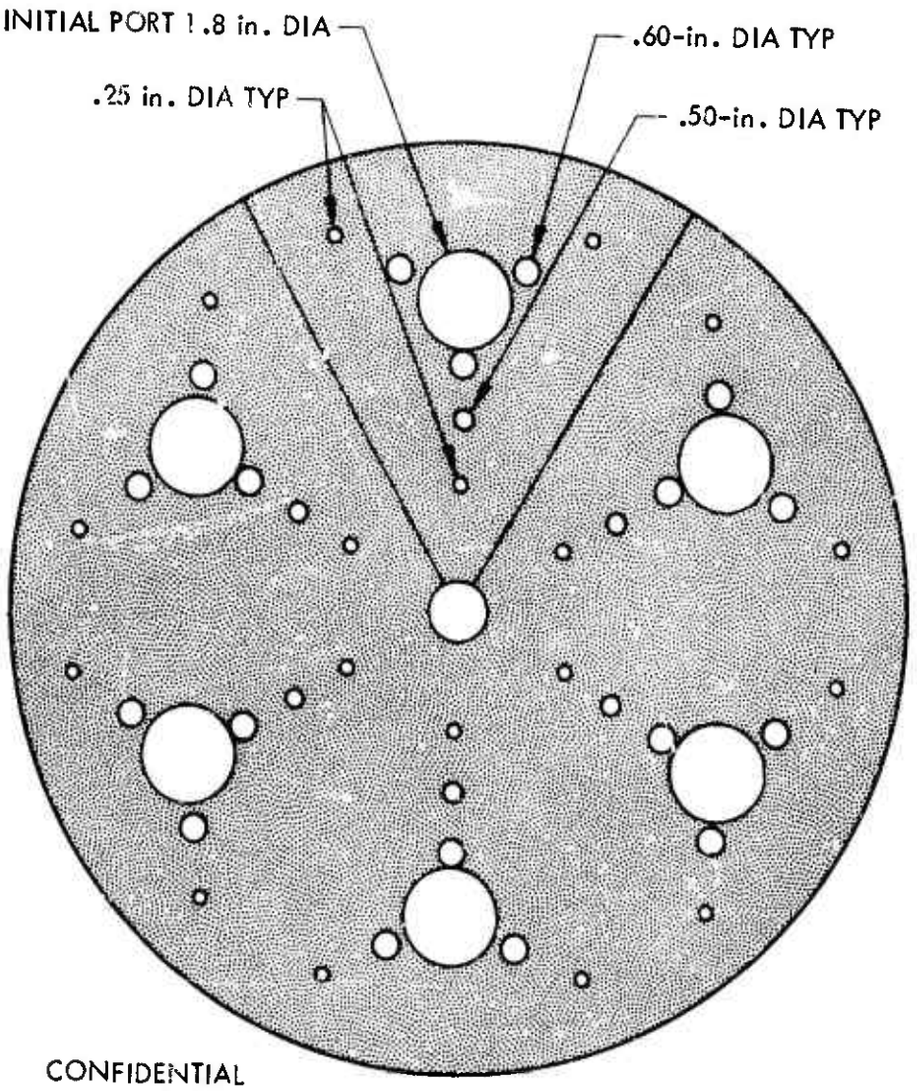

FUEL GRAIN LOADING FRACTION – 91%
ACTIVE FUEL PORT AREA – 15.29 $in.^2$
INACTIVE FUEL PORT AREA – 7.15 $in.^2$
FUEL GRAIN CROSS SECTION – 251.2 $in.^2$

E-70244 A

Figure 29. (U) Grain Geometry of Motors 14 and 15

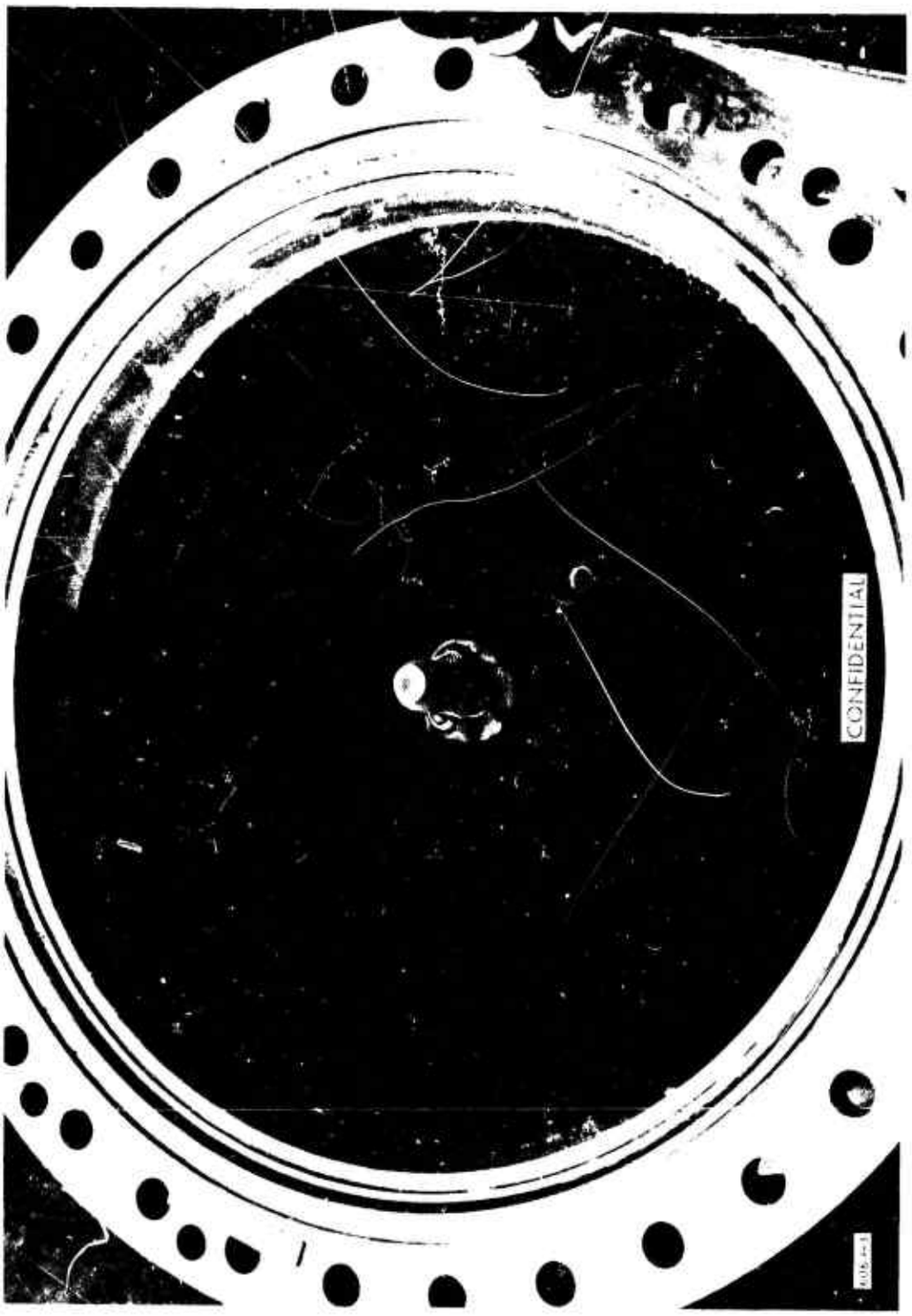

Figure 30. (U) Posttest Internal Grain of Motor 15

(U) The derived regression relation is based upon delivered fuel flow rates. The experimental fuel flow rate ($\dot{w}_f$) is an average determined by weighing the fuel grain before and after firing and dividing the fuel weight loss by the test duration. Insulation and other consumable component weight losses were separated for purposes of this analysis. Because fixed-thrust firing data are much more accurate than data obtained from varied thrust firings, only the fixed-thrust firing data were used in the analyses.

a. Procedure

(U) Fuel flow rate can be expressed by the empirical relationship

$$\dot{w}_f = \rho_f S_b \dot{r} \tag{10}$$

where

$$S_b = L_G P_b$$

and

$$\dot{r} = a G_o^n \left(\frac{P_c}{1,000}\right)^m = a \left(\frac{\dot{w}_{ox_H}}{A_p}\right)^n \left(\frac{P_c}{1,000}\right)^m \tag{11}$$

Therefore,

$$\dot{w}_f = \rho_f L_G a \left(\dot{w}_{ox_H}\right)^n \frac{P_b}{\left(A_p\right)^n} \left(\frac{P_c}{1,000}\right)^m \tag{12}$$

where ρ_f, L_G, a, $\left(\dot{w}_{ox_H}\right)^n$, and $\left(P_c/1,000\right)^m$ are constant for a fixed-thrust test and $P_b/(A_p)^n$ is a time-dependent characteristic of the grain geometry.

(U) For systems where radiation is minor, n has been experimentally found to be approximately 0.5. The parameter $P_b/\sqrt{A_p}$ then varies as shown in figure 31 for the initial multiport grain design where no satellite port "solid burning" was assumed. An average value of $P_b/\sqrt{A_p}$ can be determined from this figure and the parameters ρ_f, L_G, and $\left(P_b/\sqrt{A_p}\right)_{avg}$ then expressed as a constant, K. The fuel flow rate equation now reads

$$\dot{w}_f = a K \sqrt{\dot{w}_{ox_H}} \left(P_c/1,000\right)^m \tag{13}$$

or rearranging,

$$\frac{\dot{w}_f}{K\sqrt{\dot{w}_{ox_H}}} = a \left(\frac{P_c}{1,000}\right)^m \tag{14}$$

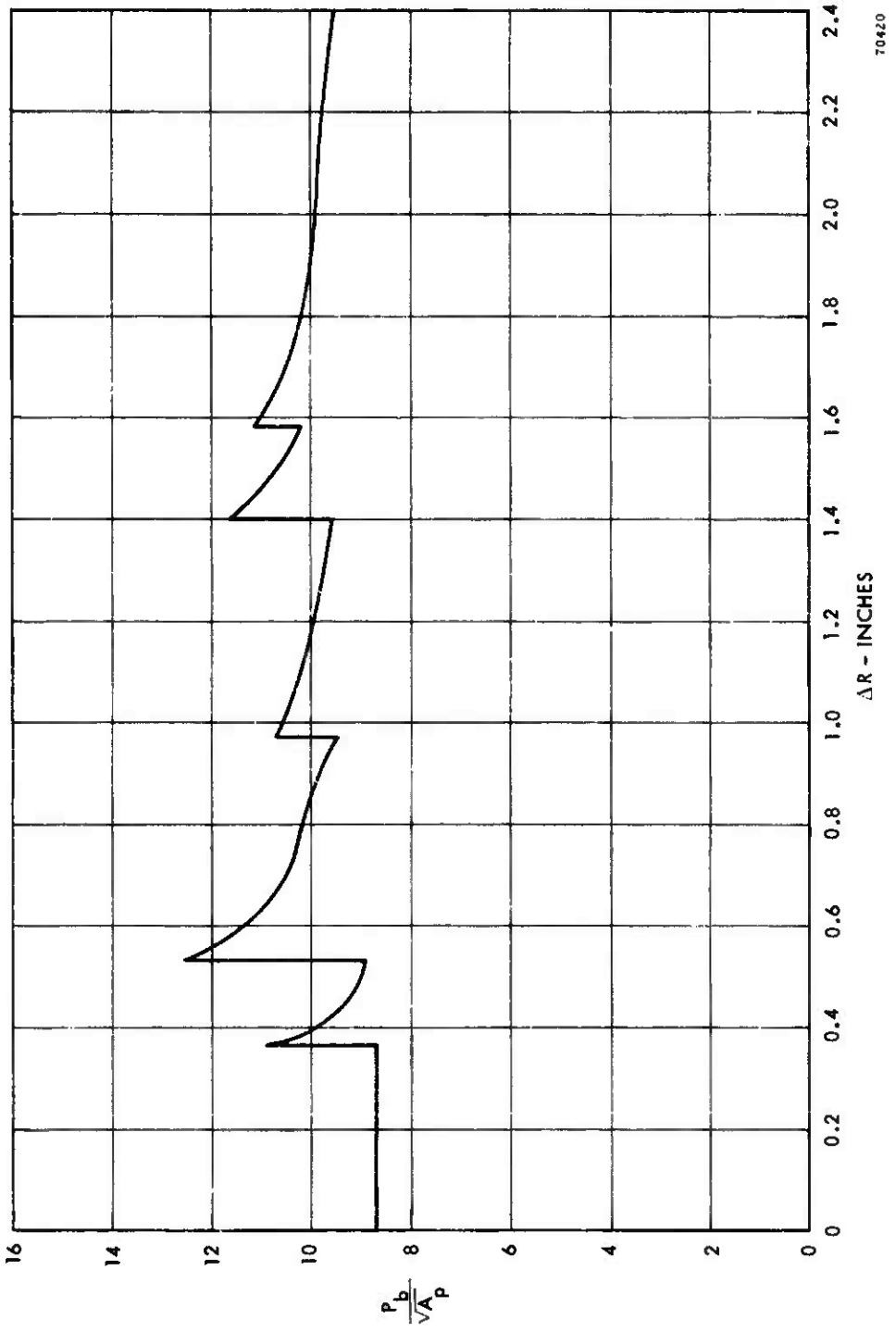

Figure 31. (U) $P_b/\sqrt{A_p}$ as a Function of Web Consumed

(U) The expression $\dot{w}_f/\left(K\sqrt{\dot{w}_{ox_H}}\right)$ can be determined from specific test data and plotted versus the appropriate $(P_c/1,000)$ on logarithmic scale. The plot represents equation 14 expressed in logarithmic terms,

$$\text{Ln}\ \frac{\dot{w}_f}{K\sqrt{\dot{w}_{ox_H}}} = \text{Ln}\ r = \text{Ln}\ a + m\ \text{Ln}\left(\frac{P_c}{1,000}\right) \qquad (15)$$

where a is the intercept at $(P_c/1,000) = 1.0$ and m is the slope of the curve.

(C) Such an analysis was conducted using the experimental data of this program. From the resultant plot illustrated in figure 32, a and m have been determined to be approximately 0.13 and 0.1, respectively.

(C) Variables which were primarily responsible for the scatter of the data points are as follows:

A. Three different fuel grain geometries were used which employed various fuel port diameters. Since fuel flow rate is a function of the grain geometry (A_p and P_b), each change will be accordingly reflected. Six data points were taken using the initial grain geometry (previous section), four points were taken using a geometry which incorporated three modifications, and one data point was taken using the final configuration.

B. An average $P_b/\sqrt{A_p}$ was used, whereas the expression is predicted to vary similar to figure 31. The $P_b/\sqrt{A_p}$ profile will also change with each new geometry.

C. An average fuel flow rate was used; fuel flow is predicted to vary similar to the $P_b/\sqrt{A_p}$ expression and is also influenced by changes in chamber pressure which occur during the test.

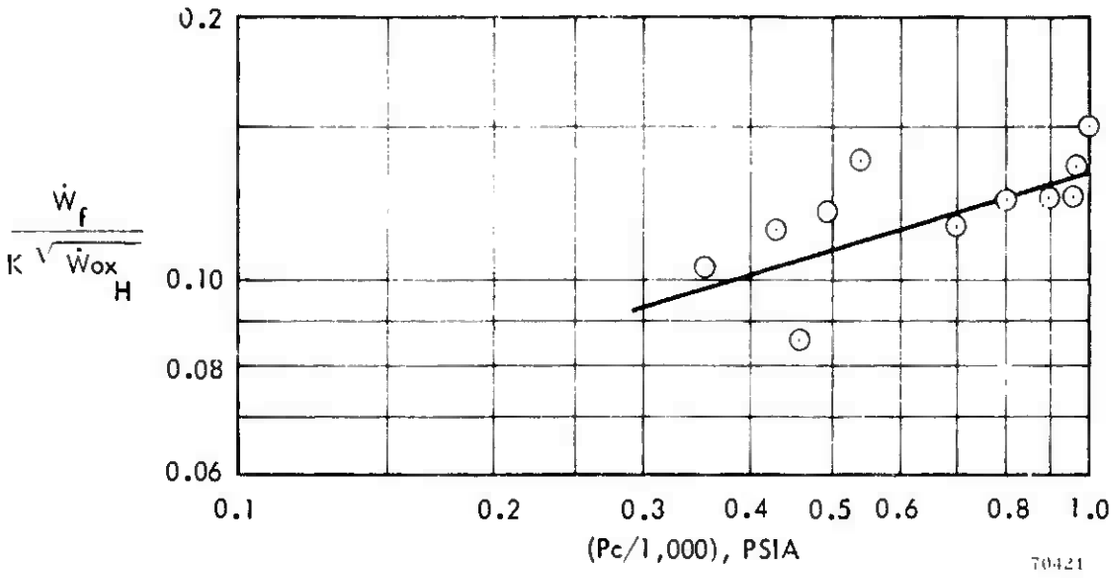

Figure 32. (U) Determination of a and m

D. "Solid burning" of the satellite ports contributed fuel flow to supplement that of the main ports prior to exposure of the satellite ports to the main port. Therefore, fuel flow was higher during the initial burning of the fuel grain.

E. Injector effects, although slight, caused local areas of abnormal fuel regression during several tests.

(U) An effort was made to verify the derived equation using existing hybrid ballistics computer programs in combination with the experimental data. However, due to the complexity of the problem and the vast number of variables, such an analysis was beyond the program scope.

REFERENCES

1. Vickland, C. W., "Experimental Investigation of Prepackaged Hybrid Propulsion Systems (U)," UTC 2141-ITR1, United Technology Center, February 1967. (CONFIDENTIAL)

2. Stolle, R., BER, 40:1505, 1907. Hoffman, K., and D. Storm, BER, 45:1728, 1912. Nevreiter, J. Am. Chem. Soc., 81:2910, 1959. Food Machinery Corporation, Classified Lit, 1960.

3. Hamers, J. W., P. D. La Force, "Technological Development of a Throttling Hybrid Propulsion System (U)," UTC 2215-FR. United Technology Center, 4 January 1967. (CONFIDENTIAL)

PRECEDING PAGE BLANK-NOT FILMED

APPENDIX I

THRUST CHAMBER ASSEMBLY (INTERNAL SIZING)

(C) As specified in the contract, the TCA is to be suitable for eventual application to a 900 lb "round-of-ammunition" type propulsion system having the following characteristics:

A. Capable of boost-coast-sustain-coast-boost or sustain (total of three starts)

B. Boost thrust of 5,000 lb with the flexibility to deliver 60% to 100% of the system total impulse during boost

C. Sustain thrust of 2,500 lb with the flexibility to deliver 0% to 50% of the system total impulse during sustain

D. System total impulse of approximately 200,000 lb-sec.

In addition, data from systems studies at UTC and elsewhere have indicated the following parameters for the propulsion unit:

Boost chamber pressure = 1,000 psia
Area ratio = 8.0:1
Motor diameter = 18 in. (desired)

(U) The design calculations which were used to size the preliminary TCA and the assumptions made follow.

1. PROPELLANT SYSTEM DATA

(C) The selected propellant system consisted of TFTA/AP/B/PBD-TDI (30/30/5/35) fuel oxidized with ClF_5. This propellant system has a theoretical specific impulse of 284 sec at the design mixture ratio of 2.0.

(C) The theoretical density of the selected fuel is calculated from the known ingredient densities as follows

$$\frac{100}{\rho f} = \frac{30}{\rho_{TFTA}} + \frac{30}{\rho_{AP}} + \frac{5}{\rho_{B}} + \frac{35}{\rho_{PBD\text{-}TDI}}$$

where the ingredient densities are

TFTA	1.30 g/cc
AP	1.96 g/cc
B	2.33 g/cc
PBD-TDI	1.00 g/cc

(C) This calculation results in a theoretical fuel density of 1.324 g/cc or 0.0478 lb/in.^{3} However, theoretical fuel densities are rarely achieved as the result of small voids which remain between the ingredient particles during processing. For this purpose, a conservative fuel density efficiency value of 95% has been assumed. This yields an actual density of 0.0454 lb/in.^{3}

(C) The oxidizer density used in the calculations corresponds to 77°F and has a value of 1.78 g/cc or 0.0643 lb/in.^{3}

(C) The sea-level delivered specific impulse values used in the calculations were based on a 94% efficiency. The values are 276 sec for the boost phase and 267 sec for the sustain phase with an area ratio of 8.0:1.

2. FLOW RATE CALCULATIONS

(U) Calculations to determine the fuel flow rates and the oxidizer flow rate distribution for each thrust level are presented in this section.

(U) The simplest design will usually consist of one in which the oxidizer flow is controlled by constant area orifices in an arrangement as illustrated in figure 33.

(C) This can be accomplished by proper design of the orifices so that proper flow is achieved at both thrust levels taking into account the change in flow resulting from pressure drop changes. The following parameters have been assumed in the design:

Maximum/minimum thrust = 5,000/2,500 lb
Maximum/minimum pressure = 1,000/515 psia
Boost I_{sp} (delivered) = 276 sec
Sustain I_{sp} (delivered) = 267 sec
Orifice discharge coefficient, C_D = 0.61
Oxidizer density = 0.0643 lb/in.^{3}
Mixture ratio = 2.0
Regression rate relationship: $\dot{r} = 0.15\ G_o^{0.4}\ (P_c/1,000)^{0.1}$

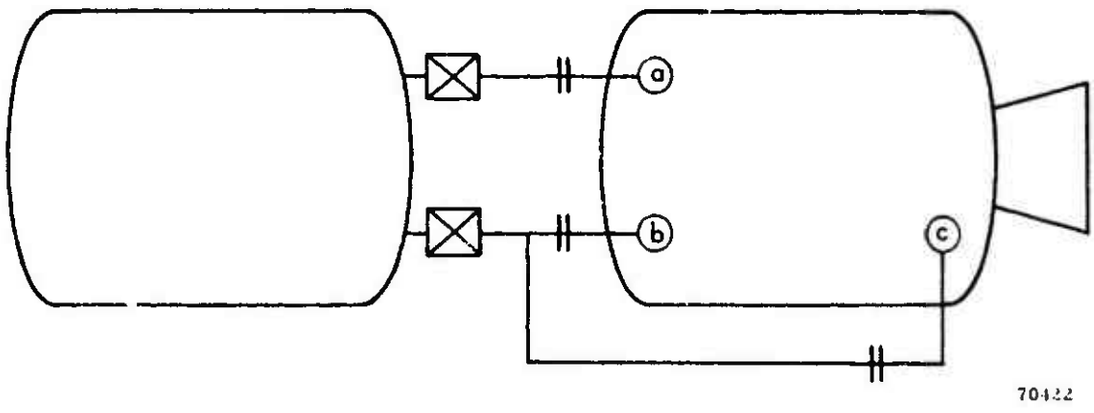

Figure 33. Oxidizer Flow Distribution

(C) The calculations were carried out in the following sequence

A. (C) The propellant flow rate and total oxidizer and fuel flow rates at both thrust levels are determined from thrust, specific impulse and mixture ratio as follows:

$$\dot{w}_p = F/I_{sp}$$

$\dot{w}_p$ maximum = 5,000/276 = 18.11 lb/sec

$\dot{w}_p$ minimum = 2,500/267 = 9.36 lb/sec

$$\dot{w}_f = \frac{\dot{w}_p}{O/F + 1}$$

$\dot{w}_f$ maximum = 18.11/(2 + 1) = 6.04 lb/sec

$\dot{w}_f$ minimum = 9.36/(2 + 1) = 3.12 lb/sec

$$\dot{w}_{ox} = \dot{w}_p - \dot{w}_f$$

$$\dot{w}_{ox}\ \text{maximum} = 18.11 - 6.04 = 12.07\ \text{lb/sec}$$

$$\dot{w}_{ox}\ \text{minimum} = 9.36 - 3.12 = 6.24\ \text{lb/sec}$$

B. (C) The ratio of the oxidizer flow to the head end at the maximum thrust to minimum thrust is determined from the regression rate equation to be

$$\frac{\dot{w}_f\ \text{maximum}}{\dot{w}_f\ \text{minimum}} = \left(\frac{\dot{w}_{ox_H}\ \text{maximum}}{\dot{w}_{ox_H}\ \text{minimum}}\right)^{0.4} \left(\frac{P_c\ \text{maximum}}{P_c\ \text{minimum}}\right)^{0.1} \tag{16}$$

or

$$\frac{\dot{w}_{ox_H}\ \text{maximum}}{\dot{w}_{ox_H}\ \text{minimum}} = \left(\frac{6.04}{3.12}\right)^{2.5} \left(\frac{515}{1,000}\right)^{0.25} = 4.36 \tag{17}$$

C. (U) The orifice equation may be simplified as follows:

$$\dot{w}_{ox} = C_D A\sqrt{2\, g\, \rho \Delta P}$$

$$= 0.61 A\sqrt{2\, g\, (0.0643)\, (\Delta P)\, (12)} \tag{18}$$

$$= 4.30 A\sqrt{\Delta P}$$

D. (U) The combination of steps B and C results in

$$\frac{\dot{w}_{ox_H}\ \text{maximum}}{\dot{w}_{ox_H}\ \text{minimum}} = 4.36 = \frac{4.30\sqrt{100}\ (A_a + A_b)}{4.30\sqrt{585}\ A_b} \tag{19}$$

This assumes a minimum ΔP of 100 psi which applies to the boost phase. The equation reduces to

$$A_b = A_a/9.56 \tag{20}$$

E. (U) Satisfying the maximum thrust condition results in

$$\dot{w}_{ox}\ \text{maximum} = \dot{w}_{ox_a} + \dot{w}_{ox_b} + \dot{w}_{ox_c} = 12.07\ \text{lb/sec}$$

$$4.30(A_a + A_b + A_c)\sqrt{100} = 12.07\ \text{lb/sec} \tag{21}$$

$$A_a + A_b + A_c = 0.281\ \text{in.}^2$$

F. (U) Satisfying the minimum thrust condition results in

$$\dot{w}_{ox}\ \text{minimum} = \dot{w}_{ox_b} + \dot{w}_{ox_c} = 6.24 \tag{22}$$

and

$$6.24 = 4.30\,(A_b + A_c)\sqrt{585} \tag{23}$$

$$A_b + A_c = 0.0600\ \text{in.}^2$$

G. (C) The simultaneous solution of the results of steps D, E, and F may be summarized as follows:

Orifice	Orifice Area in.^2	Oxidizer Flow Rate (lb/sec)	
		Maximum Thrust	Minimum Thrust
a	0.220	9.46	0
b	0.023	0.99	2.39
c	0.037	1.59	3.85

3. NOZZLE SIZING

(U) The basic nozzle dimensions are calculated in this section. The theoretical characteristic exhaust for the selected propellant is 5,690 ft/sec. Based on a combustion efficiency of 97%, the delivered value is estimated to be 5,520 ft/sec. The nozzle throat area and diameter are

$$A_t = \frac{c^* \dot{w}_p}{P_c g} = \frac{(5,520)(18.11)}{(1,000)(32.2)} = 3.10\ \text{in.}^2 \tag{24}$$

$$D_t = 1.98\ \text{in.} \tag{25}$$

The exit area and diameter are

$$A_e = \epsilon A_t = (8.0)(3.10) = 24.8 \text{ in.}^2 \tag{26}$$

$$D_e = 5.60 \text{ in.} \tag{27}$$

The length of the conical expansion cone (15° half angle) is

$$L_{nozzle} = \frac{(D_e - D_t)/2}{\tan 15°} = \frac{(5.60 - 1.98)/2}{0.268} \tag{28}$$

$$= 6.75 \text{ in.}$$

4. GRAIN DESIGN

(C) Since the necessary flow rates have been established, all parameters necessary for preliminary grain design calculations are available. The grain design calculations will be based on the boost thrust condition; however, it can be shown that the same results would be obtained had the sustain condition been used.

(C) The fuel flow rate from a hybrid fuel grain may be expressed as

$$\dot{w}_f = \dot{r} S \rho_f \tag{29}$$

and since

$$\dot{r} = a G_o^n P_c^m \tag{30}$$

then

$$f = \frac{a\left(\dot{w}_{ox_H}\right)^n P_c^m P_b L_g \rho_f}{\left(A_p\right)^n} \tag{31}$$

All of the above parameters are known except for P_b, L_g, and A_p.

(C) The grain length can be closely estimated from overall propulsion system considerations which indicated a desire for a 900 lb propulsion system with a diameter of 18 in. Design studies conducted at UTC and elsewhere indicate that a unit of this type will have a mass fraction of about 0.75. Based on the 900 lb total weight, a propellant weight of 680 lb is estimated. Using the mixture ratio and fuel density as specified in part 1, the usable fuel weight and volume are found to be 226 lb and 4,980 in.^{3}

Since an 18-in.-diameter grain has been selected, the total grain cross-sectional area is 254 in.^{2} Reasonably good grain designs can be expected to yield 85% of the total cross-sectional area for usable fuel. On this basis, the following grain properties are assumed: (C)

Usable fuel area-to-chamber area ratio	=	0.85
Port area-to-chamber area ratio	=	0.10*
Sliver area-to-chamber area ratio	=	0.05

The grain length, therefore, becomes

$$L_g = \frac{(4,980)}{(254)(0.85)} = 23.0 \text{ in.} \tag{32}$$

(U) Substituting these values into the fuel flow rate equation developed above yields

$$6.04 = \frac{(0.15)(10.91)^{0.4}\,(1,000/1,000)^{0.1}\,P_b\,(23.0)(0.0454)}{(A_p)^{0.4}} \tag{33}$$

or

$$\frac{P_b}{(A_p)^{0.4}} = 12.94 \tag{34}$$

Table IX lists the values of $P_b/A_p^{0.4}$ properties for circular multiple-port grain configurations for the initial condition of A_p/A_c of 0.1. As can be seen in this table, the required geometry parameter falls very close to the six-port configuration. This design was selected for full-scale motor detailed design.

---

* At this point, the port area should be checked to ensure that the design is on a sound basis. First, the port area-to-nozzle throat area should be checked to see that it is above ~1.5:1. The ratio for this design is 24.4/1.55 or 16.4, which is well above the suggested minimum. Second, the maximum oxidizer mass flux should be checked to ensure that it is not unreasonably high. Unstable hybrid operation (flooding, etc.) can occur when the maximum (initial) G_o is in excess of ~2 to 4. The maximum G_o for this design is 10.45/25.4 or 0.41 lb/sec-in.^{2} This value is well within the safe region of operation.

TABLE IX

(U) CIRCULAR PORT GRAIN PROPERTIES

(A_p/A_c = 0.10)

Number of Ports	$P_b/(A_p)^{.44}$
1	5.49
2	7.77
3	9.52
4	10.99
5	12.29
6	13.46
7	14.54
8	15.55
9	16.49
10	17.38

APPENDIX II

RADAR MEASUREMENTS

(U) Spectral measurements were made of the radiation from the exhaust plume of motors 10 and 11. The measurements did not show the presence of alkali metal species which have been prominently observed in previous spectra of solid and hybrid propellants using AP, and which contribute significantly to radar interference.

(C) These findings prompted measurements of the radar propagation through the plume during the firing of motors 12 and 13. A simple microwave transmission system was assembled from x-band interferometer components and mounted to an improvised stand (figures 34 and 35). The four firings of these two motors were monitored and a typical result is shown in figure 36. The beam axis was transverse to the plume and coincidental with the first shock diamond. No attenuation was detected during the steady-state portions of the tests. A summary of test conditions is given in table X.

(C) A small amount of intermittent attenuation was observed during start and shutdown transients, and in one test a 0.006 db/cm value at 10 cps accompanied a steady chamber pressure ripple of the same frequency. These mainly serve to indicate that the equipment was working properly. In every test the klystron power drifted by approximately +0.006 db. Since the uncooled tube was only a few feet from the plume, the drift is attributed to differential expansion of the cavity. After each test the output returned to its pretest value. Based on periodic measurements, the microwave frequency was 9.04±0.02 GHz. During the steady-state test portions, the oscillogram trace noise did not differ from that present without the plume. The minimum attenuation measurable was about 0.01 db corresponding to 0.0006 db/cm.

(C) To verify the adequacy of the microwave equipment used, a UTP-3096 (16% aluminum, 68% ammonium perchlorate, and 16% binder) motor firing was monitored. The attenuation was substantially the same as reported previously for similar propellants and as measured at UTC with other equipment: about 3 to 5 db over a transverse plume path length of approximately 8 cm (approximately 0.5 db/cm), about the region of the first shock. In the

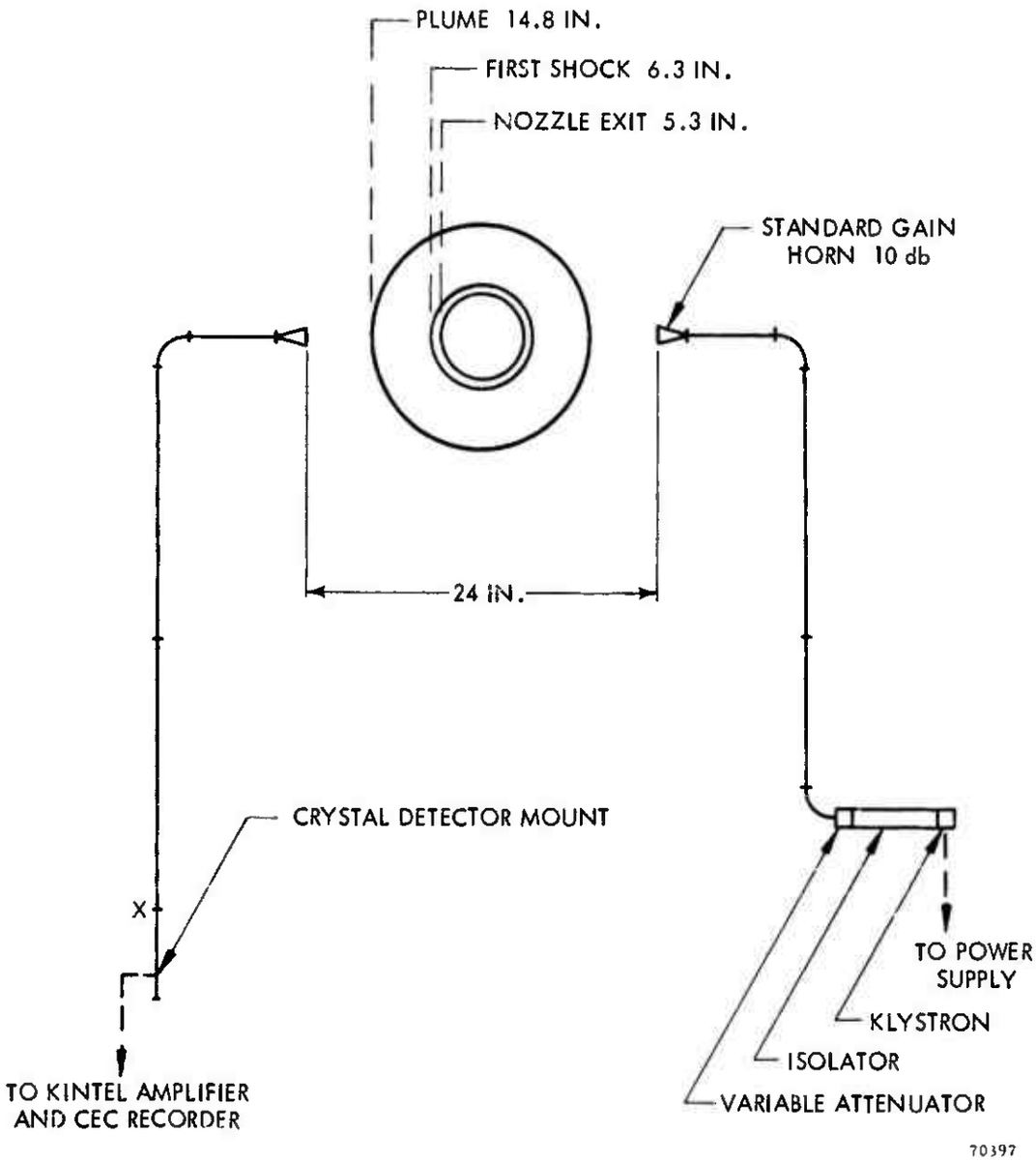

Figure 34. (U) Test Apparatus Schematic

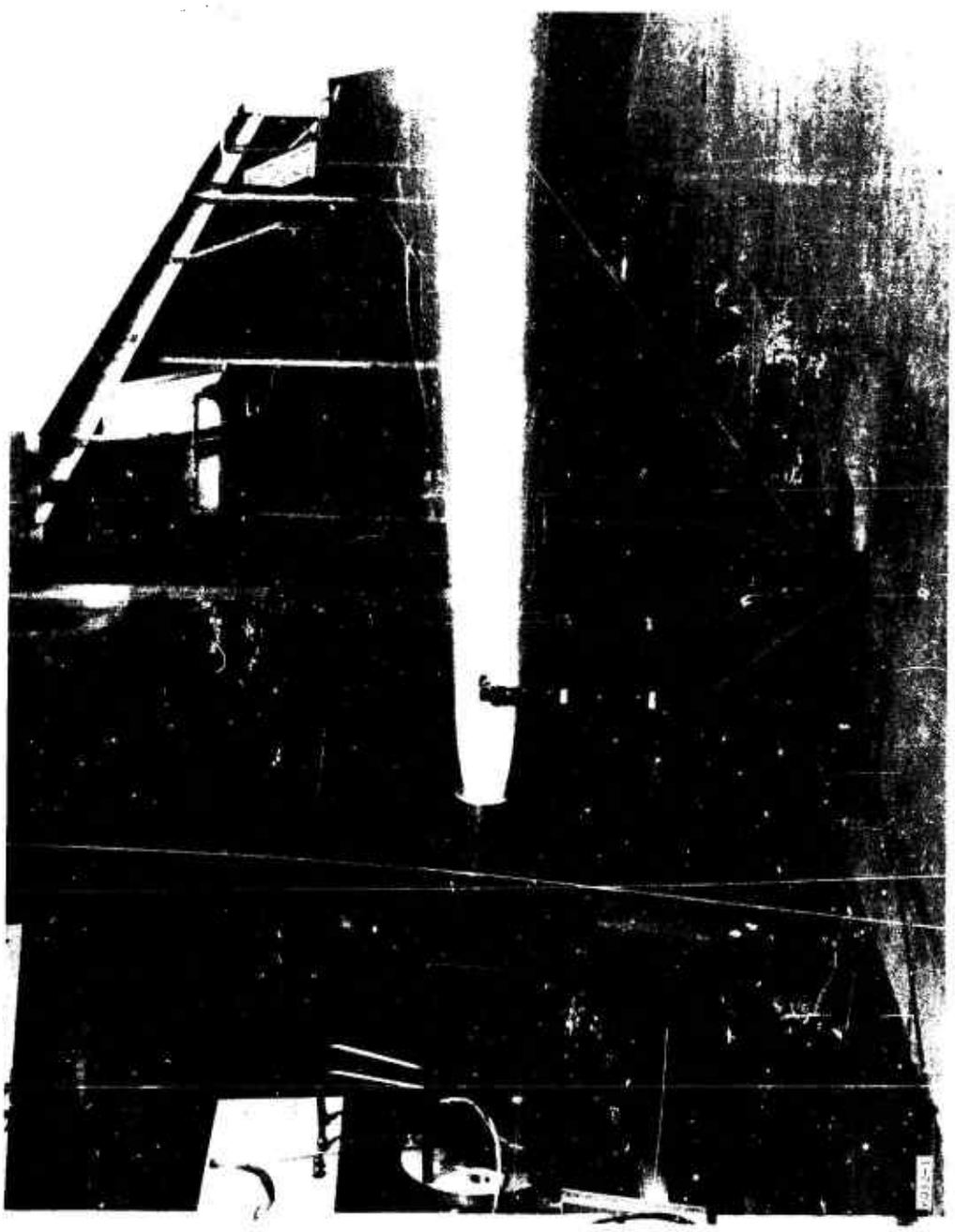

Figure 35. (U) Motor Assembly With Test Apparatus

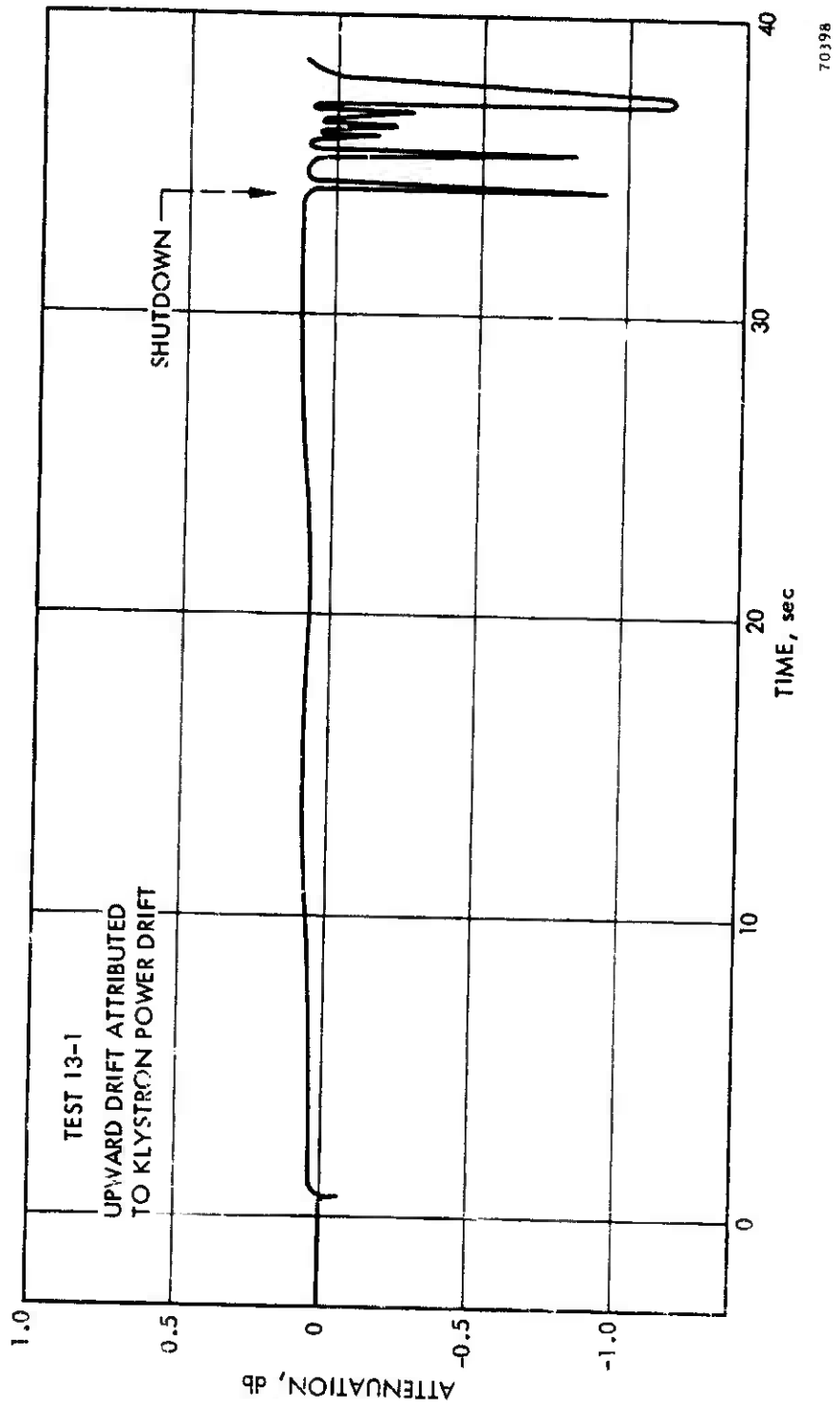

Figure 36. (U) Radar Attenuation

TABLE X

(U) TEST CONDITIONS

Test	Duration sec	Chamber Pressure psia	Mixture Ratio O/F
12-1	10	948	3.37
12-2	40	353	3.91
12-3	10	460	4.96
13-1	34	968	3.02

test reported, the attenuation reached a level of approximately 1 db/cm at 25 exit diameters downstream. It is interesting to contrast this with a 0% aluminum grain firing: approximately 0.3 db/cm near the first shock, nearly zero between shocks, and zero at 25 exit diameters.

(C) The tests described herein confirm expectations of low radar attenuation in the types of hybrid propellants tested. This desirable characteristic may be a result of using boron in the fuel which has been shown to substantially decrease radar attenuation in propellants containing AP (a major source of electron producing alkali metals). These results may also be influenced by the high O/F ratio used, giving rise to free halogens in the exhaust. In either case, the ability to minimize or reduce radar attenuation problems through appropriate propellant formulation in hybrid systems is evident and indicates an area for future investigation.

PRECEDING PAGE BLANK-NOT FILMED

APPENDIX III

MOTOR DRAWINGS

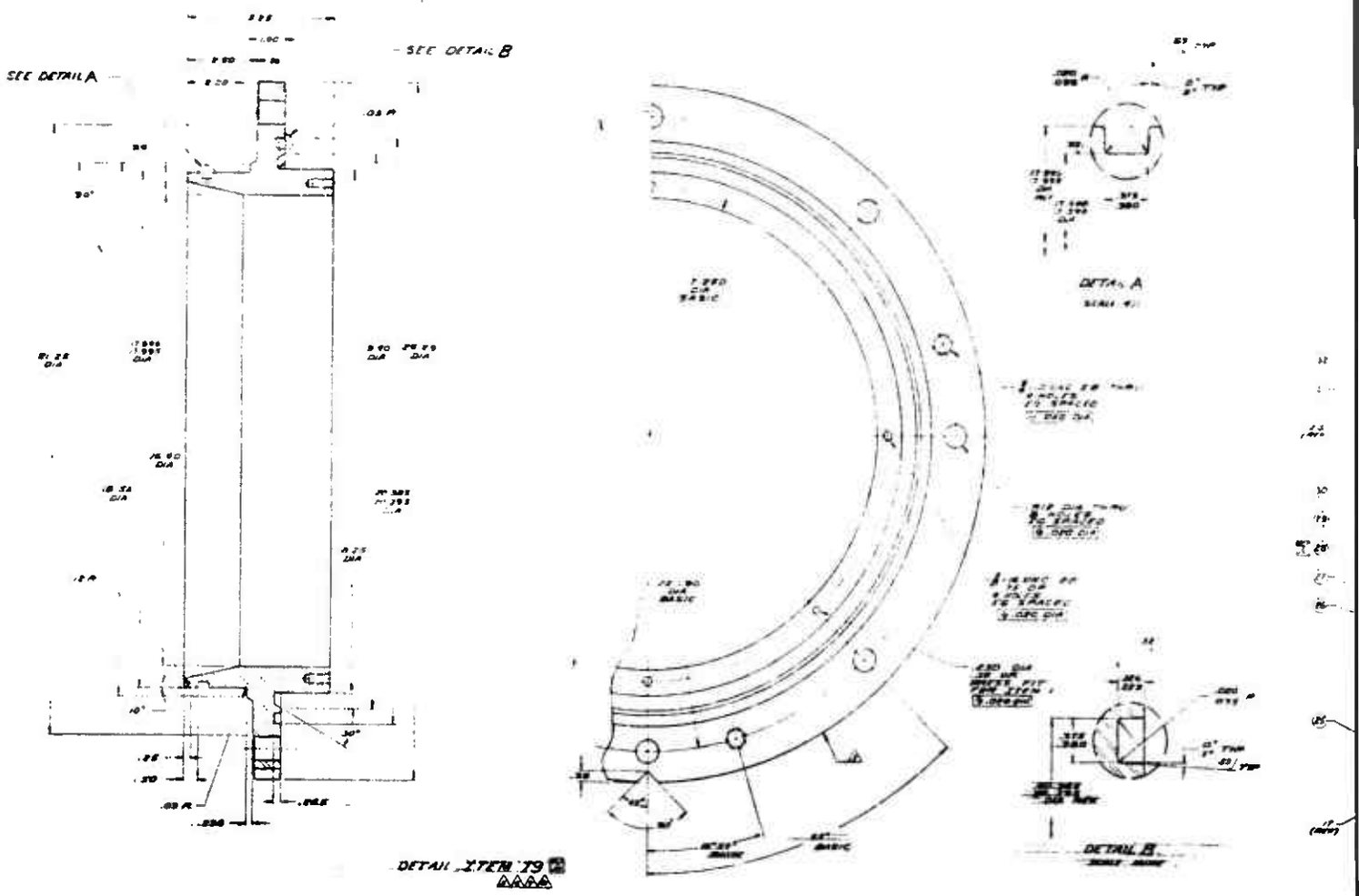

UNCLASSIFIED

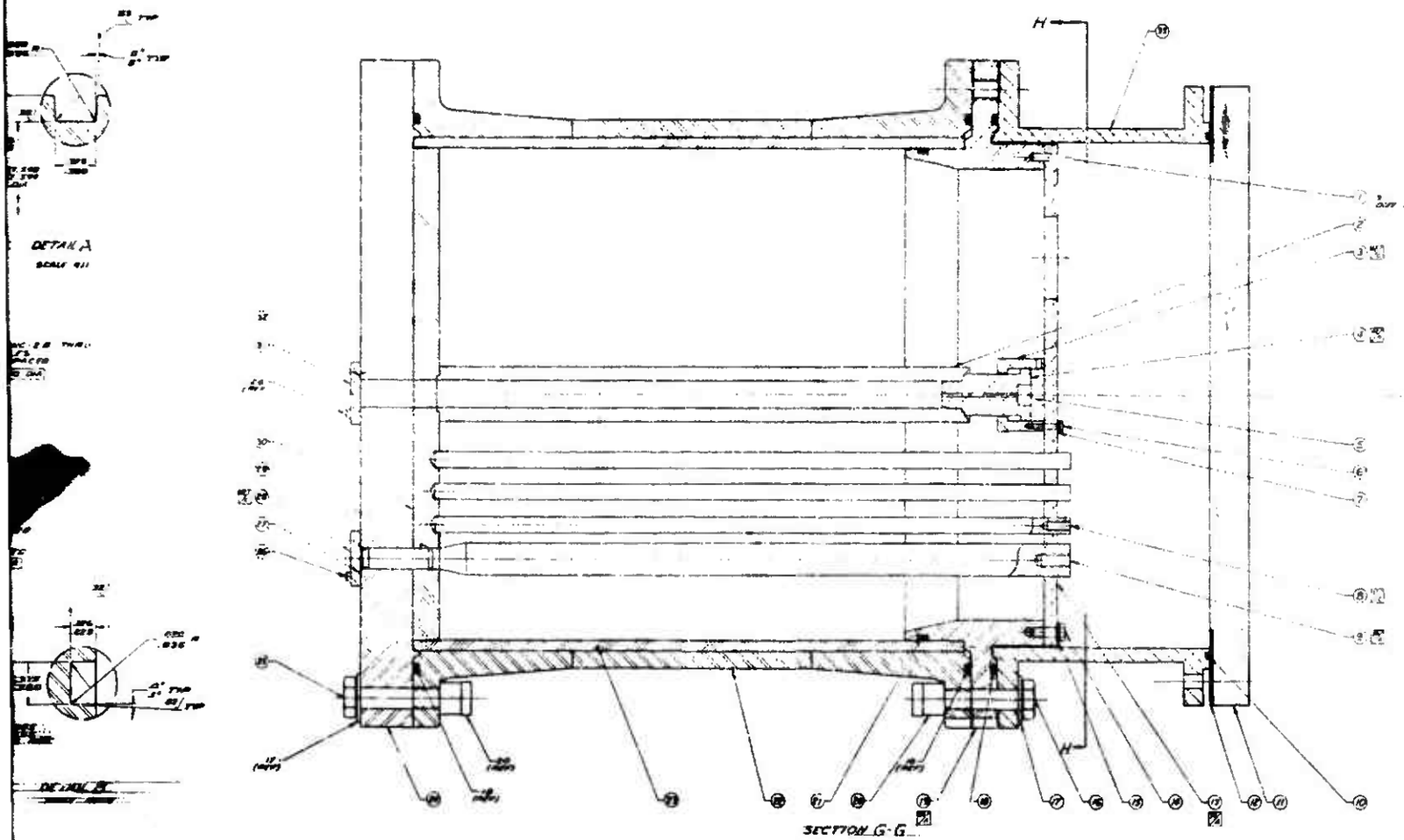

1

2

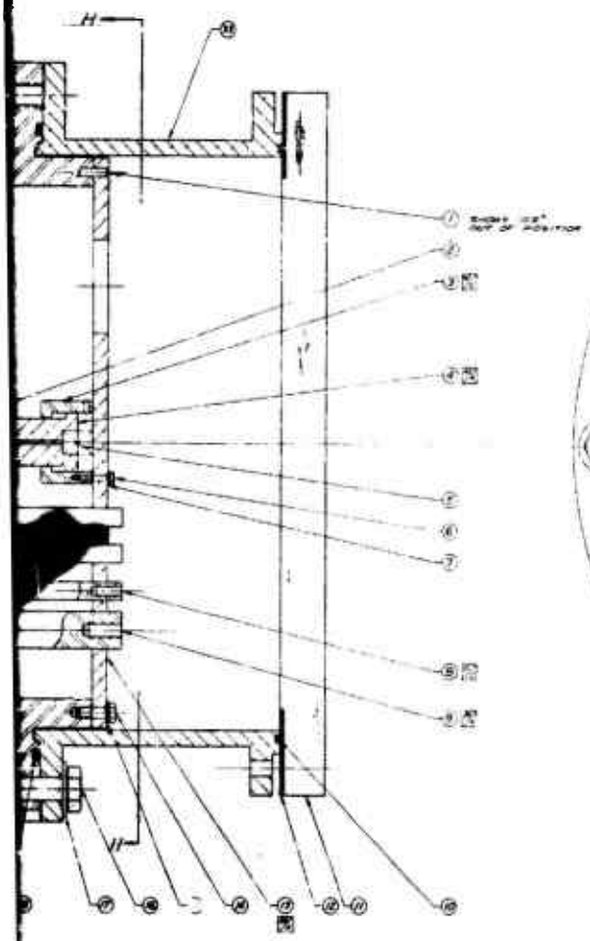

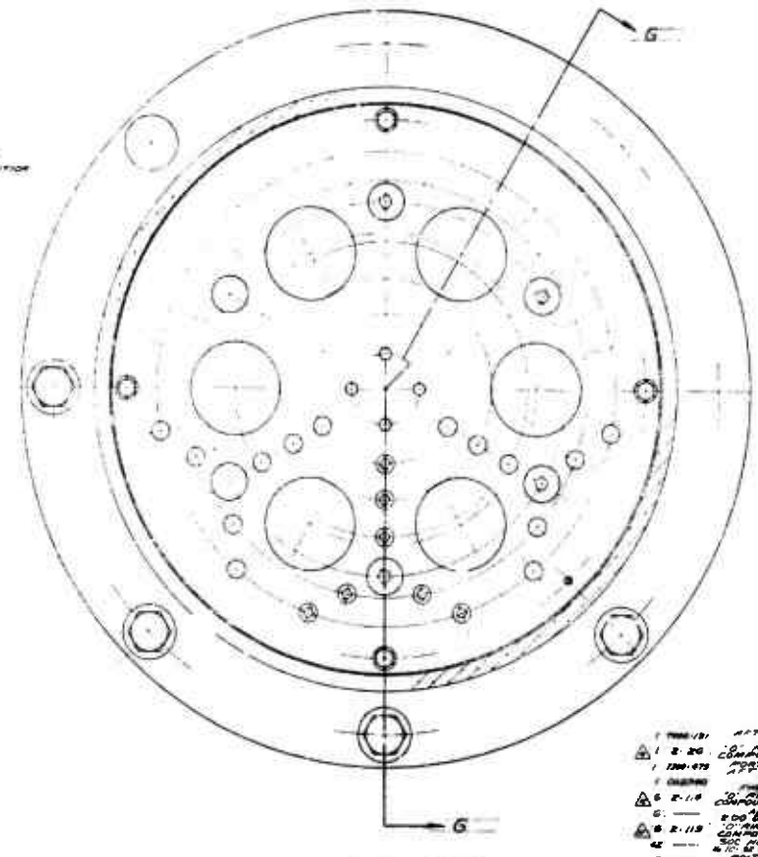

SECTION H-H

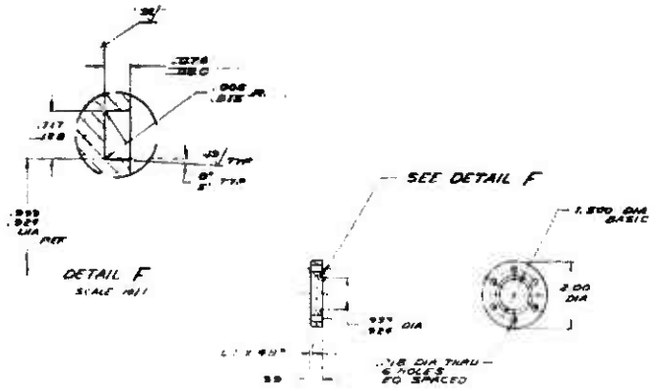

DETAIL ITEM 28

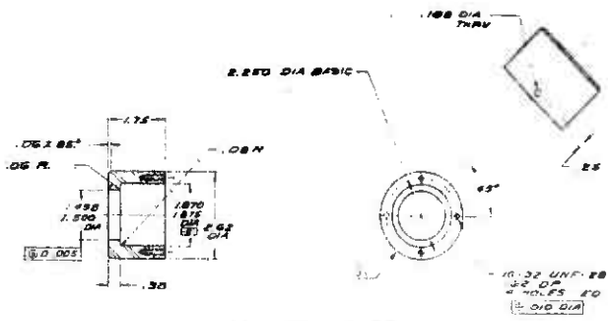

DETAIL ITEM 3

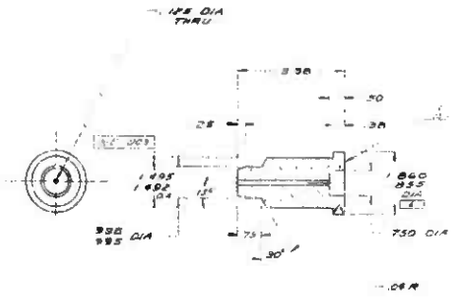

DETAIL ITEM 4

UNCLASSIFIED

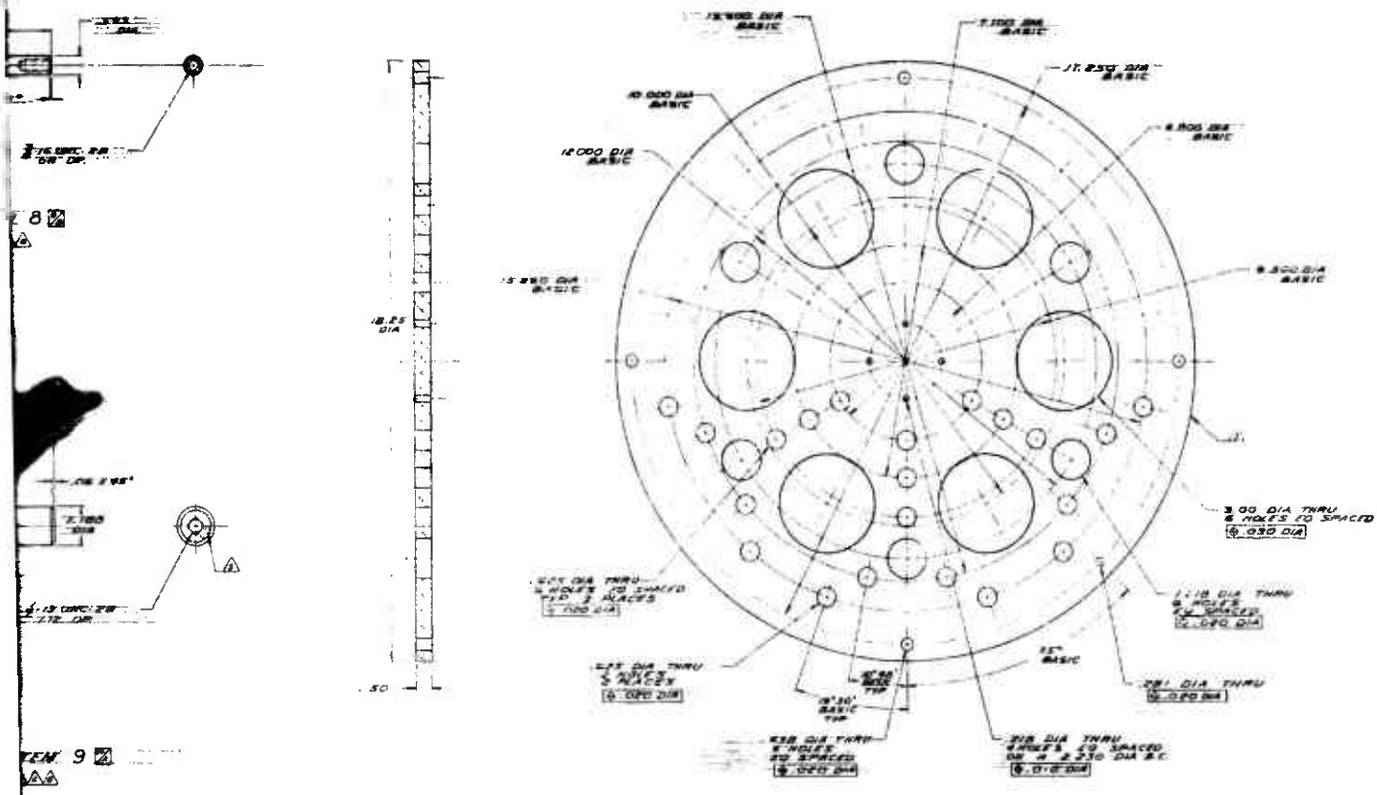
DETAIL ITEM 13

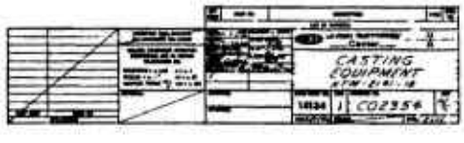
CASTING
EQUIPMENT
C02356

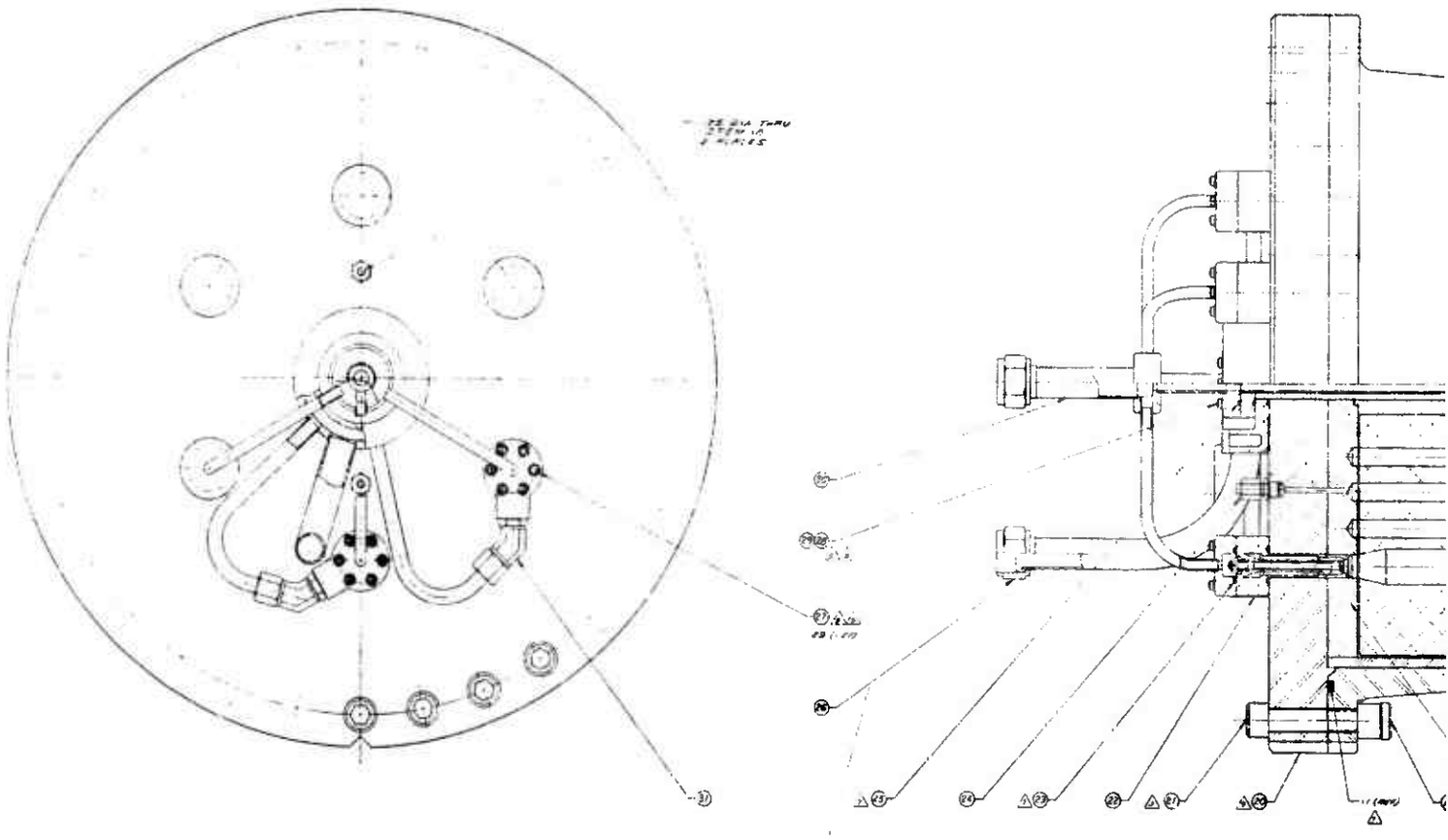

UNCLASSIFIED

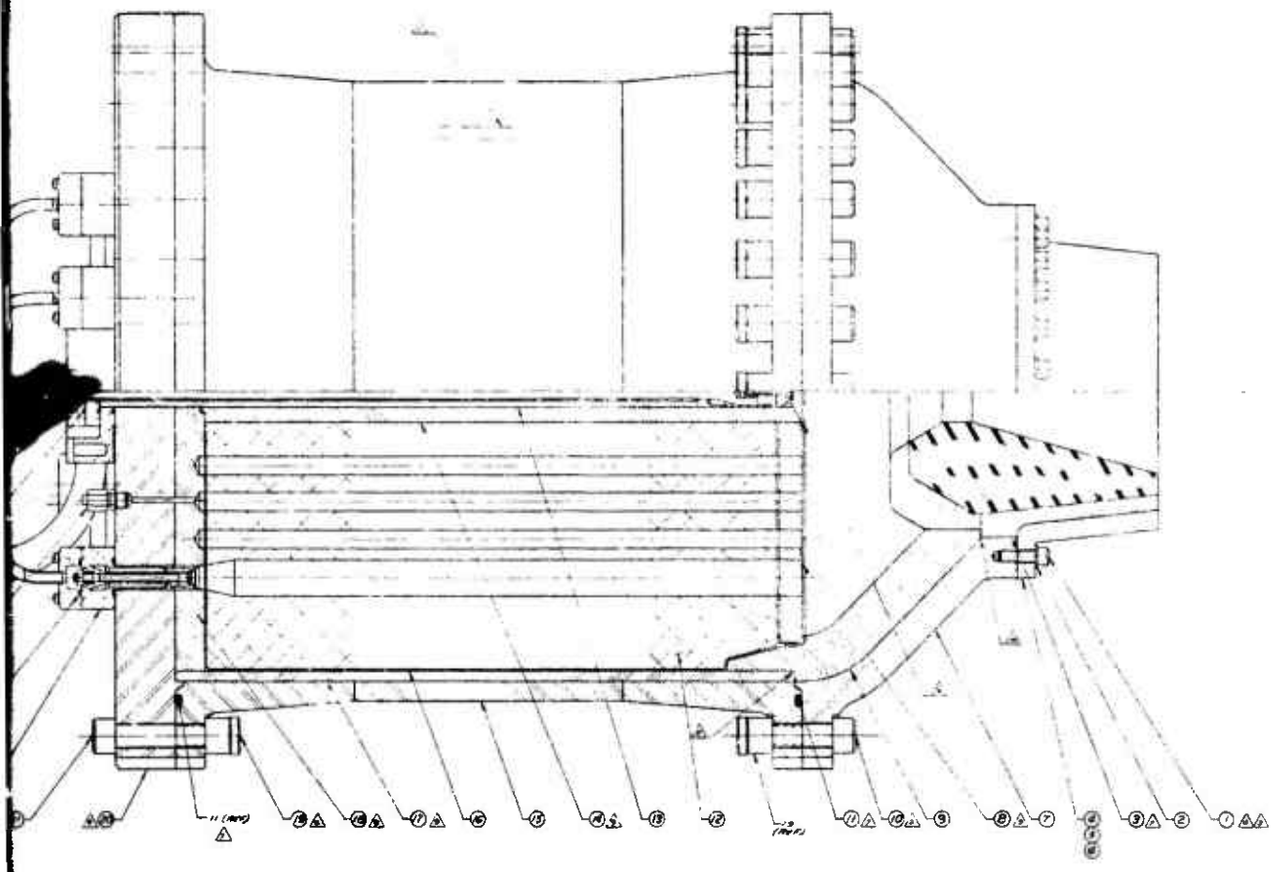

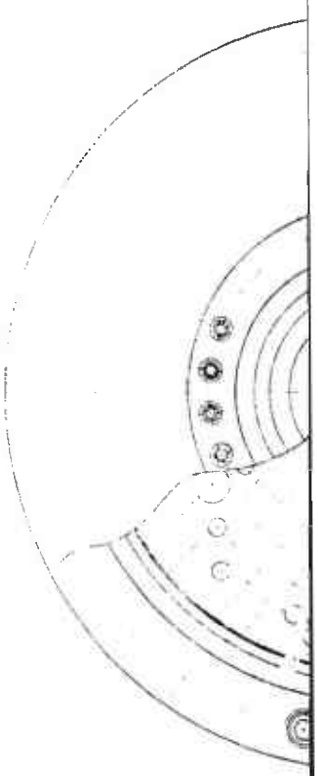

1

2

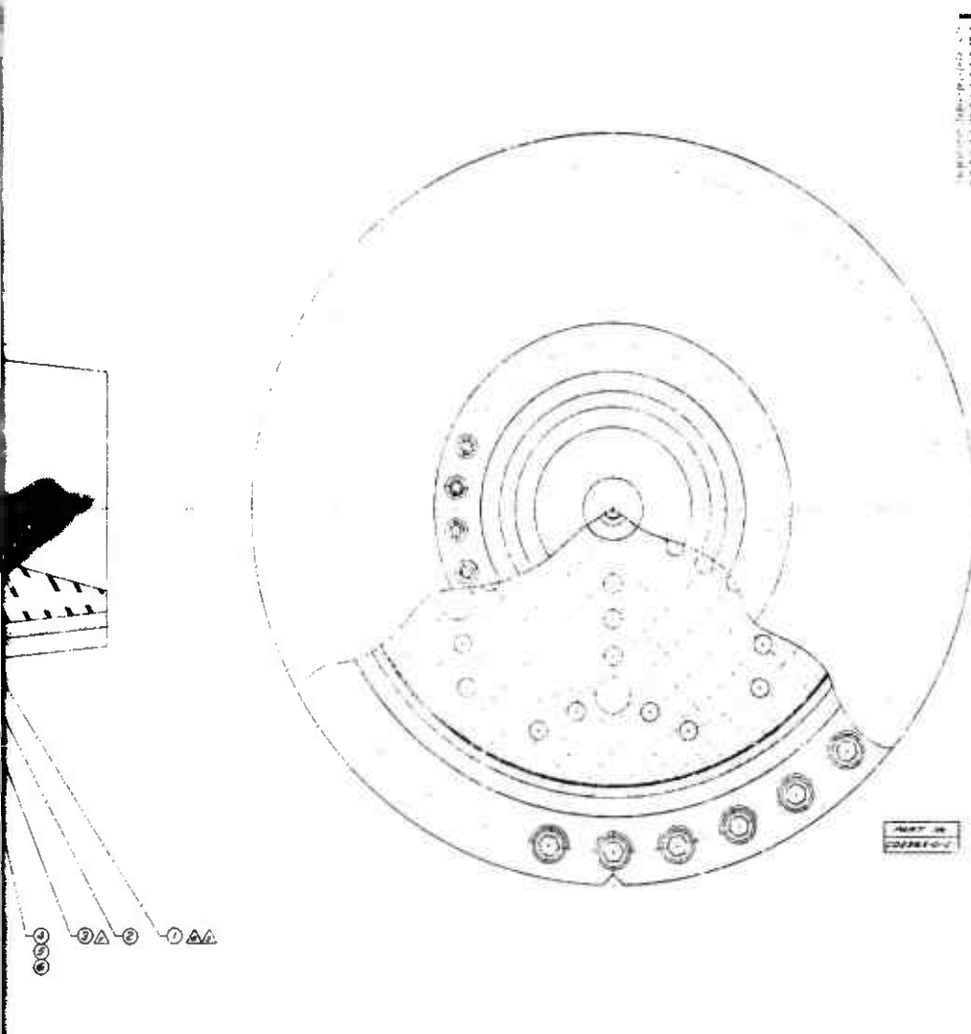

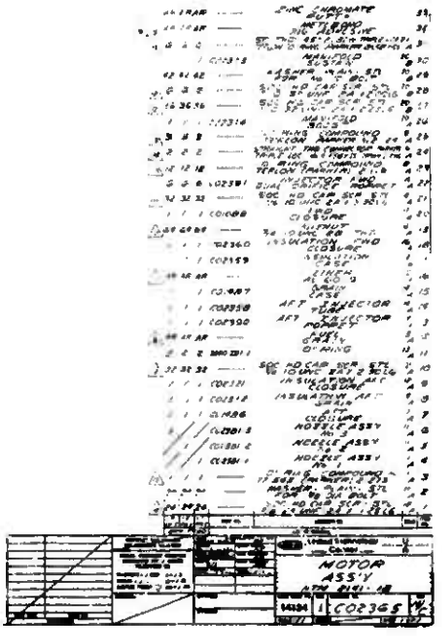

Contract AF 04(611)-10789, Full-Scale
Heavyweight Motor Assembly

2

3

④ BOND ITEM 5 TO ITEM 4 USING ITEM 7. ALTERNATE FOR ITEM 7 ADHESIVE EPON No 422, SHELL CHEMICAL CO. PITTSBURG CALIF (OR EQUIV)

⑤ NARMCO MATERIALS DIV OF TELECOMPUTING CORP COSTA MESA, CALIF (OR EQUIV)

⑥ WESTERN BACKING CORP 3512 - 20 HELMS AVE, CULVER CITY, CALIF

⑦ TAPE WRAP AT 10" TO NOZZLE CENTERLINE CURE PER NOTE 8

⑧ OR EQUIV

⑨ LAMINATE ITEMS 1, 2 & 3 AT 90° TO ℄ OF PART AND CURE AT :

TEMP	PRESSURE	TIME
160°F	0 PSI	30 MIN
325°F	2000 PSI	1 HR
375°F	200 PSI	1 HR
385°F	2000 PSI	1 HR

⑩ PREPARE MATING SURFACE BETWEEN ITEMS 4 & 5 AS FOLLOWS:
a. DEGREASE
b. ETCH FOR 2 MINUTES (MIN) AT 180°F WITH A SOLUTION OF 891 ml 35 % HYDROCHLORIC ACID 89 ml 85 % PHOSPHORIC ACID & 43 ml 60 % HYDROFLUORIC ACID
c. RINSE WITH DISTILLED WATER.
d. SURFACE AIR DRY FOR 30 MINUTES (MIN)

NOTES:
1. UNLESS OTHERWISE SPECIFI ALL SHARP BREAK ALL SHARP .005 - .015. ALL FILLET RADII
2. DIMENSIONS GIVEN ARE FINIS
3. RUBBER STAMP PART NO WITH HIGH CHARACTERS APPROX
4. CHANGES OR SUBSTITUTIONS AFFECTING FUNCTION OF PA MADE UPON APPROVAL OF PRO
5. CRACKS AND DELAMINATIONS NOT
6. LAMINATE ITEM 3 PARALLEL OUTSIDE SURFACE OF ITEM CURE AT 310°-325°F, 10 FOR A MIN OF 3 HOURS.
7. MOLD AT 275°-325°F, 200 FOR A MIN OF 8 HR. POST AT 300°F, ROOM PRESSURE 24 HR. AIR COOL TO RO

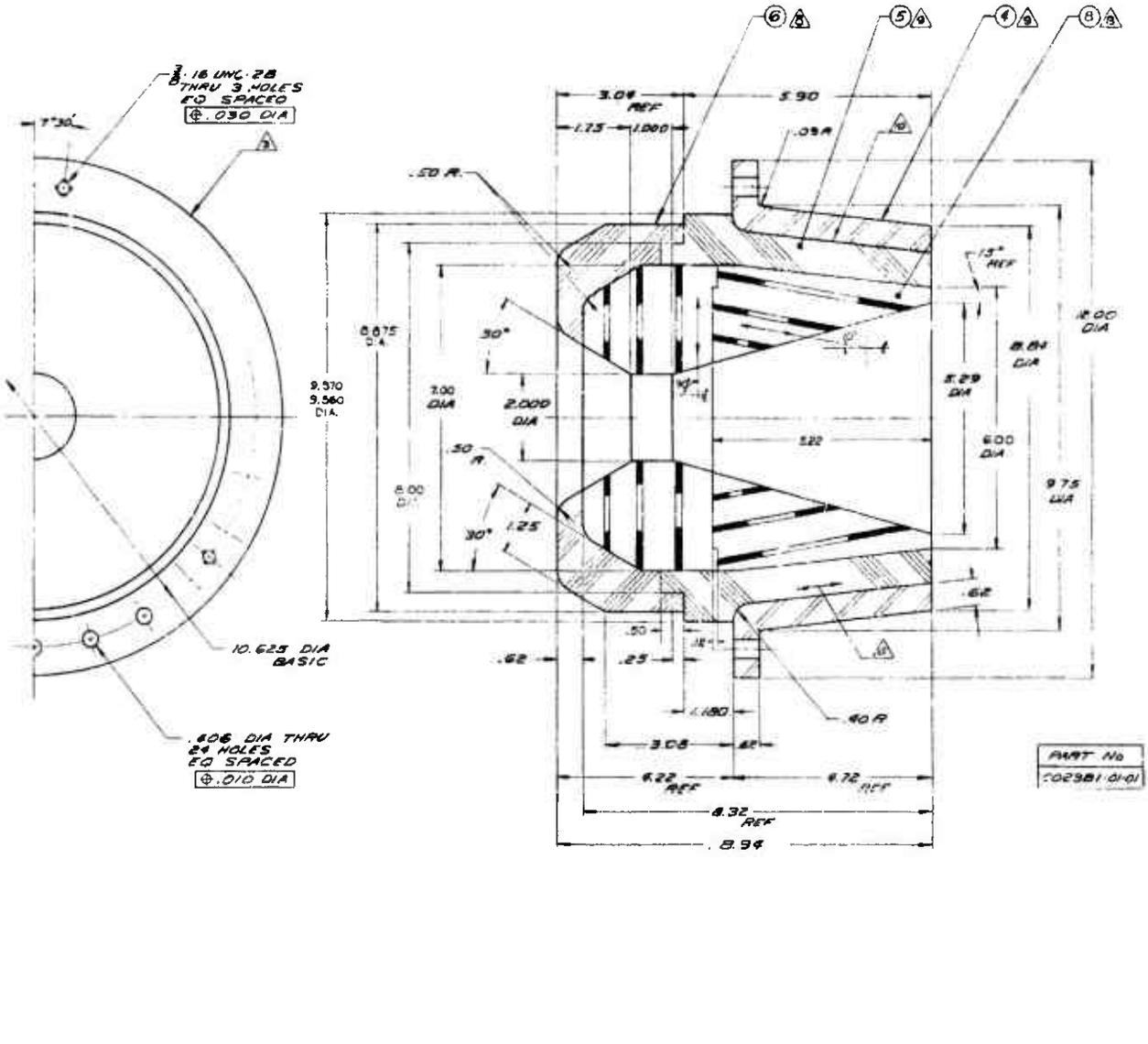

PART No
7023811-01-01

UNCLASSIFIED

(3) LAMINATE ITEMS 1, 2 & 3 AT 90° TO ℄ OF PART AND CURE AT:

TEMP	PRESSURE	TIME
AMB° F	0 PSI	30 MIN.
115° F	2000 PSI	1 HR.
670° F	2000 PSI	1 HR.
325° F	2000 PSI	1 HR.

(4) PREPARE MATING SURFACE BETWEEN ITEMS 4 & 5 AS FOLLOWS:
A. DEGREASE
B. ETCH FOR 3 MINUTES (MIN) AT 180°F WITH A SOLUTION OF: 89 ml 35% HYDROCHLORIC ACID, 89 ml 85% PHOSPHORIC ACID & 43 ml 60% HYDROFLUORIC ACID
C. RINSE WITH DISTILLED WATER.
D. FORCE AIR DRY FOR 30 MINUTES (MIN)

NOTES:
1. UNLESS OTHERWISE SPECIFIED: REMOVE ALL BURRS, BREAK ALL SHARP EDGES .005 - .015. ALL FILLET RADII .020 R.
2. DIMENSIONS GIVEN ARE FINISHED SIZES.
3. RUBBER STAMP PART No WITH .12 (MIN) HIGH CHARACTERS APPROX AS SHOWN.
4. CHANGES OR SUBSTITUTIONS NOT AFFECTING FUNCTION OF PART MAY BE MADE UPON APPROVAL OF PROJECT ENG.
5. CRACKS AND DELAMINATIONS NOT PERMISSIBLE.
6. LAMINATE ITEM 5 PARALLEL TO THE OUTSIDE SURFACE OF ITEM 4 AND CURE AT 310°-325°F, 1000 PSI FOR A MIN OF 3 HOURS.
7. MOLD AT 275°-325°F, 2000 PSI FOR A MIN OF 2 HR. POST CURE AT 300°F, ROOM PRESSURE FOR 24 HR. AIR COOL TO ROOM TEMP.

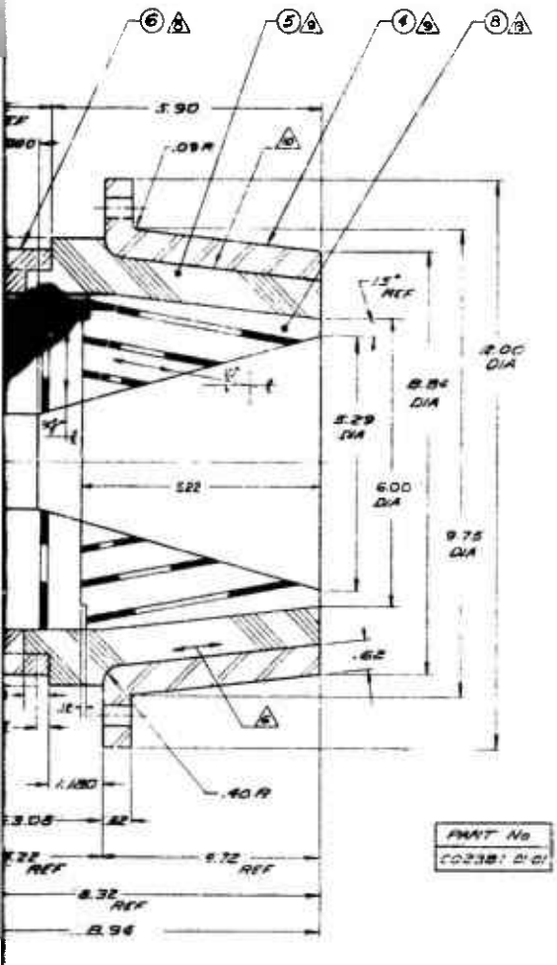

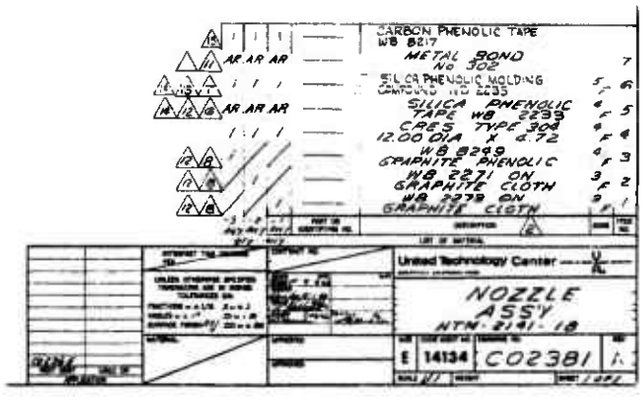

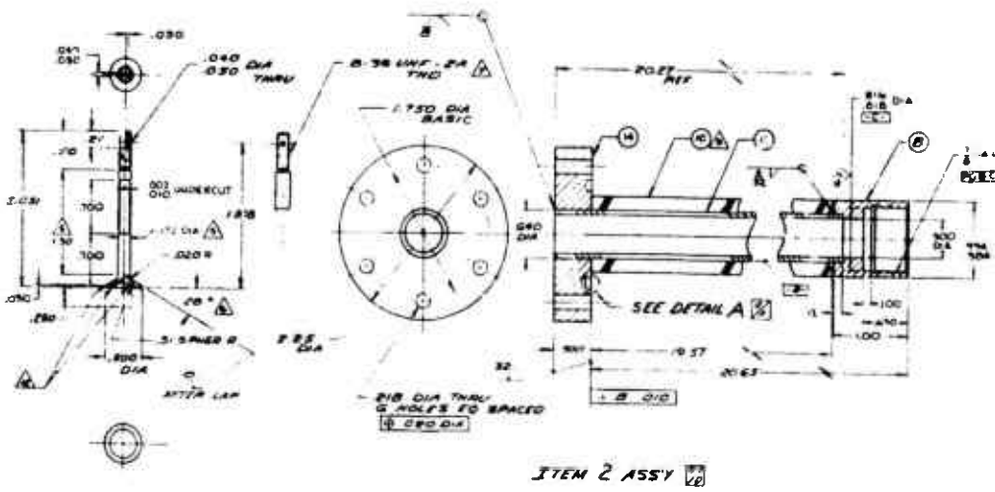

ITEM 2 ASS'Y

DETAIL ITEM 15

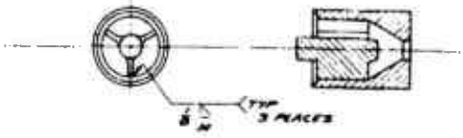

DETAIL ITEM 5
(ALTERNATE METHOD OF CONSTRUCTION)

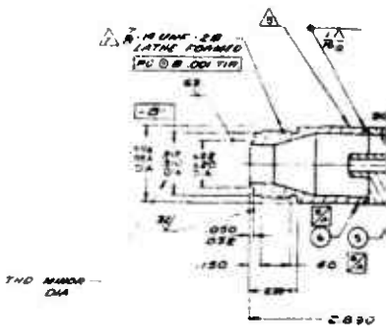

ITEM 1 ASS'Y

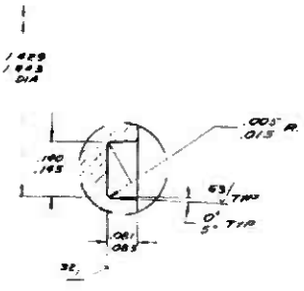

DETAIL A
SCALE 1/1

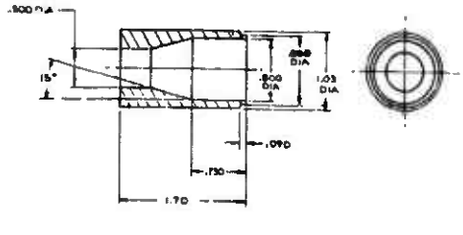

DETAIL ITEM 6

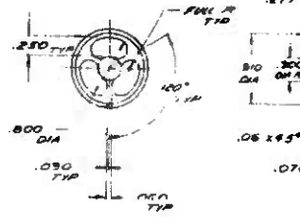

DETA

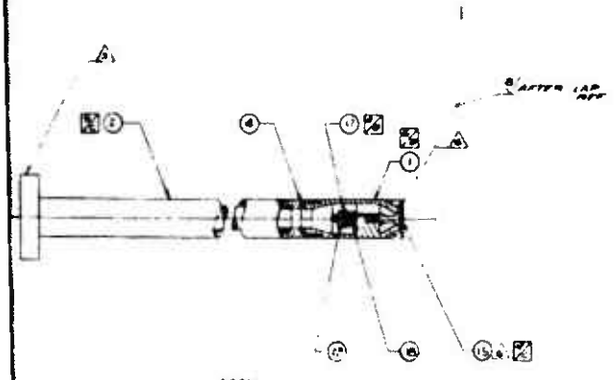

ASSY

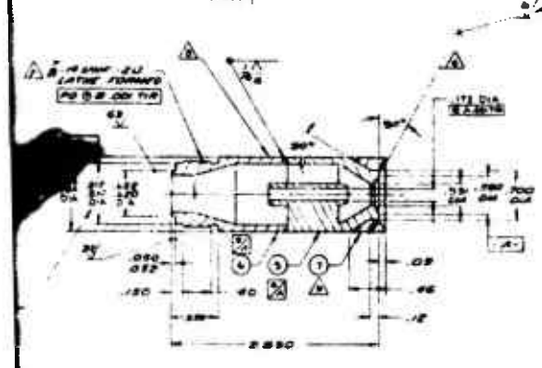

ITEM 1 ASSY

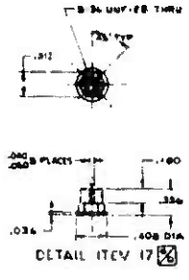

DETAIL ITEM 17

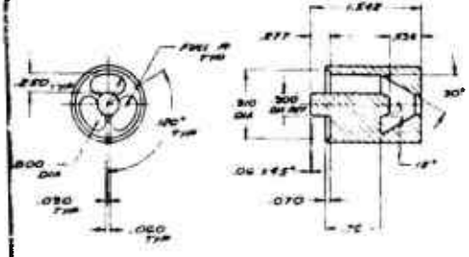

DETAIL ITEM 5

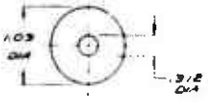

NOTES:

1. UNLESS OTHERWISE SPECIFIED: REMOVE ALL BURRS, BREAK ALL SHARP EDGES .005/.015, ALL FILLET RADII TO BE .010/.030 R.
2. DIMENSIONS GIVEN ARE FINISHED SIZES
3. RUBBER STAMP PART NO WITH .12 MIN HIGH CHARACTERS.
4. CHANGES OR SUBSTITUTIONS NOT AFFECTING FUNCTION OF PART MAY BE MADE UPON APPROVAL OF THE PROJECT ENGR.
5. HARD ANODIZE - SANFORD PROCESS: THIS AREA .0010 - .0015 THK & POLISH TO 16 CLEARANCE BETWEEN ITEM 5 & 15 TO BE .0010 - .0012 ON DIA AFTER COATING
6. LAP SEAT AT ASSY 360° CONTACT WITH 8 FINISH
7. CLEAR ANODIZE THREADS
8. WELD PER MIL-W-87248 CLASS 2
9. BOND ITEMS 7 TO 8 & 10 TO 12 WITH EPON No 422, SHELL CHEMICAL CO. PITTSBURG CALIF
10. SEABOARD - PACIFIC DIV, 15001 SO BROADWAY, GARDENA CALIF
11. PORTER SEAL CO, 88 W JACKSON ST HAYWARD, CALIF.
12. HARD ANODIZE - SANFORD PROCESS - THIS AREA .0010 - .0015 BUILD UP
13. TAYLOR CORP, SAN CARLOS CALIF
14. THIS PART MUST PASS A HYDROTEST TO 1500 PSI TO BE PERFORMED AT U.T.C.

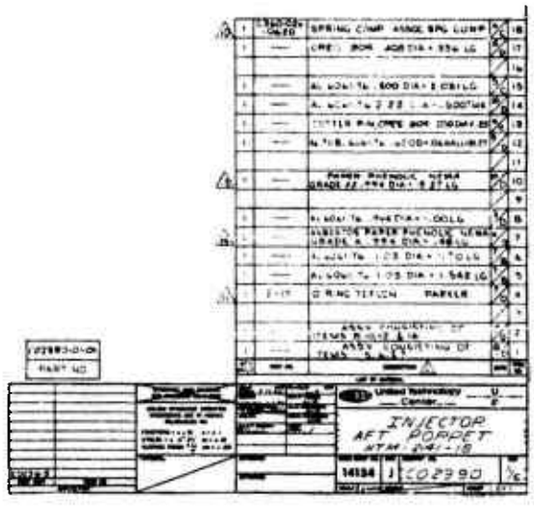

INJECTOR AFT POPPET ASSY (M) - 18

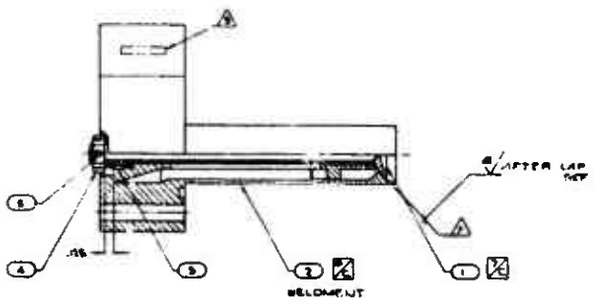

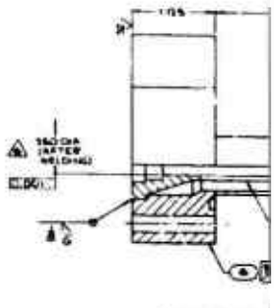

WELDMENT

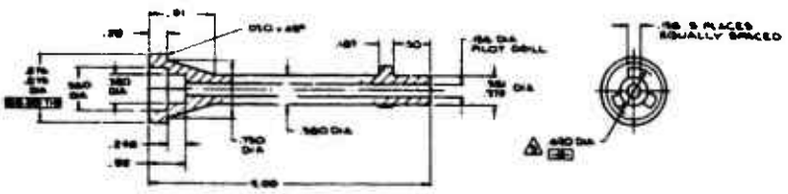

DETAIL ITEM 7

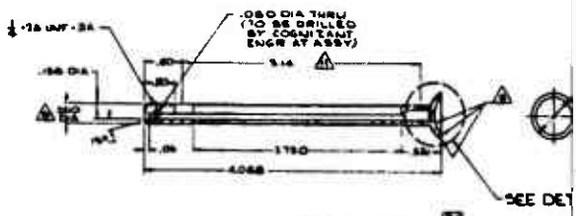

DETAIL ITEM 1

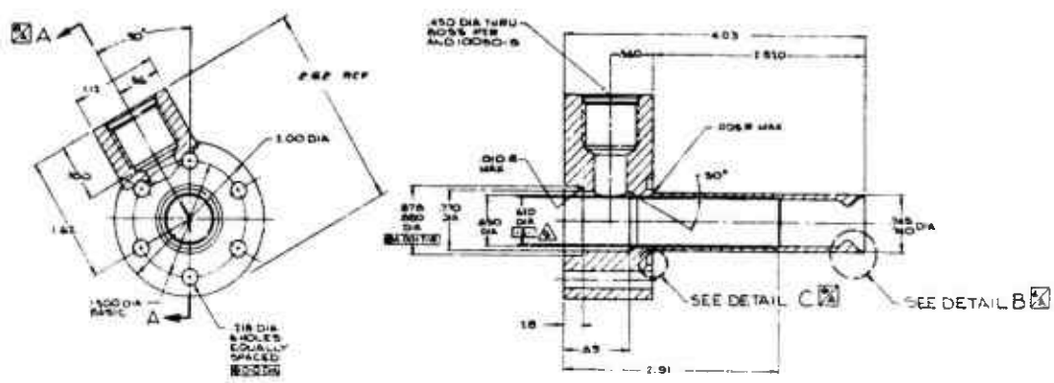

DETAIL ITEM 6

SECTION A-A

DETAIL C

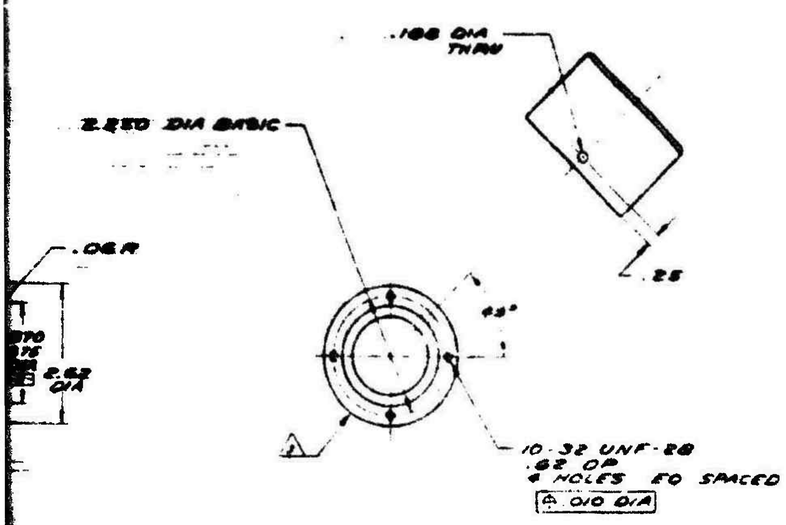

DETAIL ITEM 3

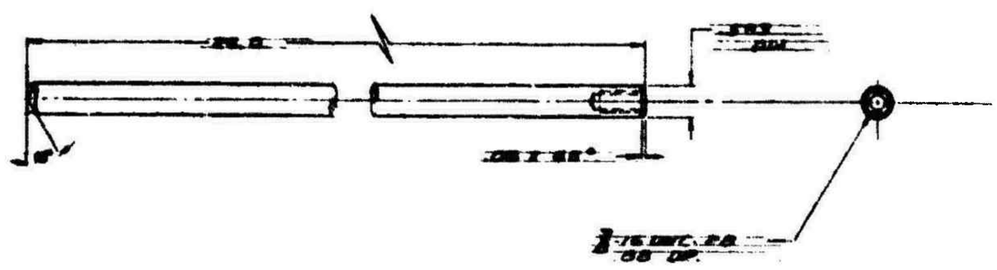

DETAIL ITEM 8

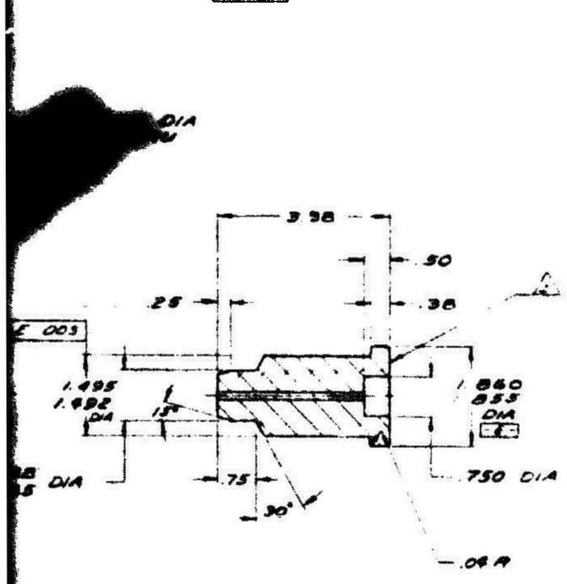

DETAIL ITEM 4

DETAIL C
SCALE 10/1

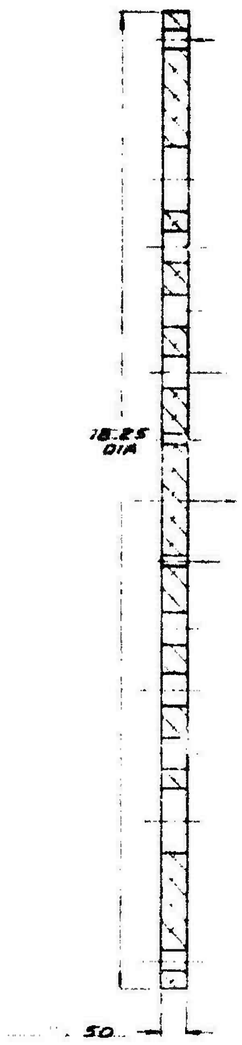

DETAIL ITEM 9

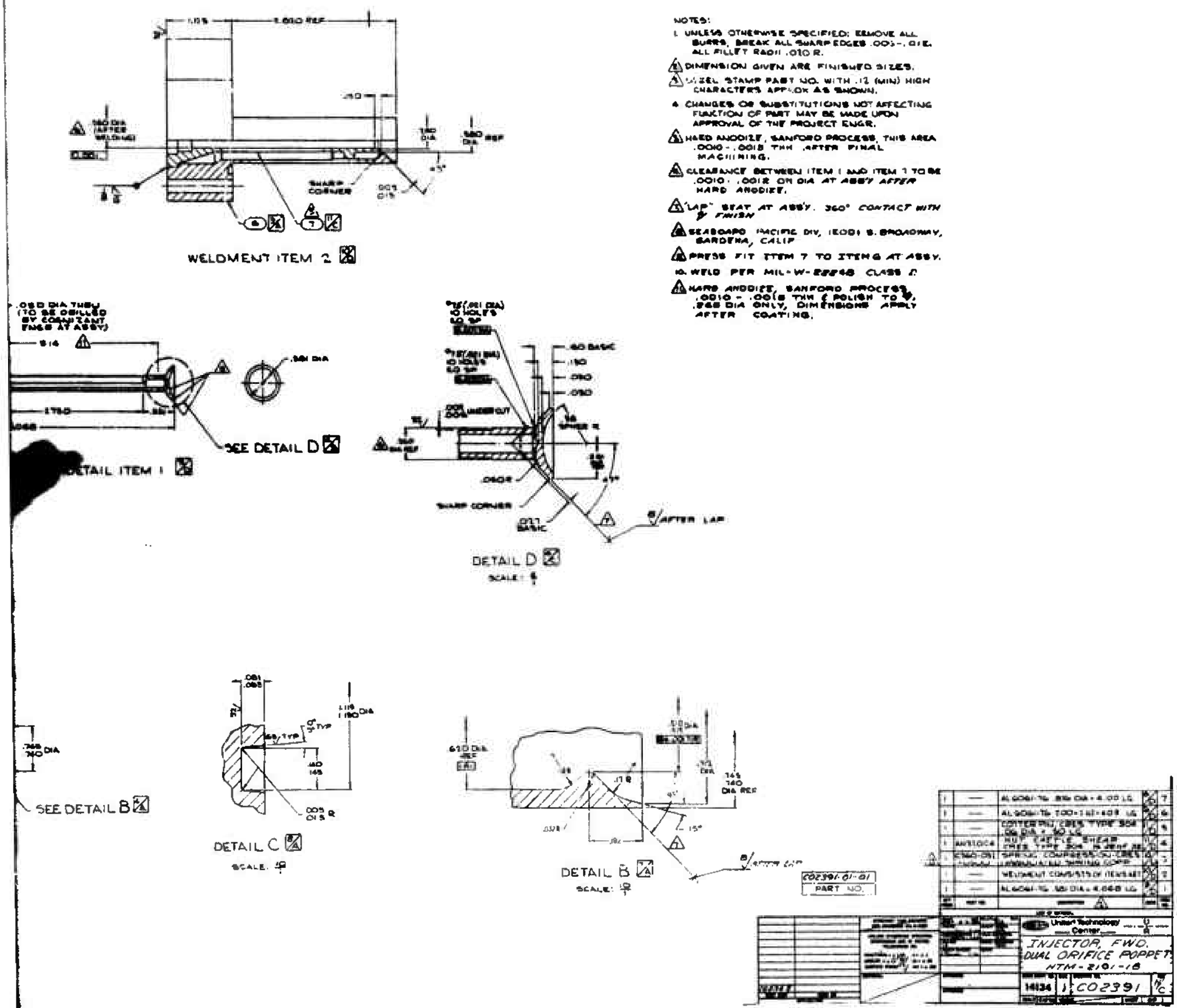

NOTES:
1. UNLESS OTHERWISE SPECIFIED: REMOVE ALL BURRS, BREAK ALL SHARP EDGES .005-.015. ALL FILLET RADII .010 R.
2 DIMENSION GIVEN ARE FINISHED SIZES.
3 VIZEL STAMP PART NO. WITH .12 (MIN) HIGH CHARACTERS APPROX AS SHOWN.
4. CHANGES OR SUBSTITUTIONS NOT AFFECTING FUNCTION OF PART MAY BE MADE UPON APPROVAL OF THE PROJECT ENGR.
5 HARD ANODIZE, SANFORD PROCESS, THIS AREA .0010-.0015 THK, AFTER FINAL MACHINING.
6 CLEARANCE BETWEEN ITEM 1 AND ITEM 7 TO BE .0010-.0012 ON DIA AT ASSY AFTER HARD ANODIZE.
7 "LAP" SEAT AT ASSY. 360° CONTACT WITH FINISH
8 SEABOARD PACIFIC DIV, 16001 S. BROADWAY, GARDENA, CALIF
9 PRESS FIT ITEM 7 TO ITEM 6 AT ASSY.
10. WELD PER MIL-W-
11 HARD ANODIZE, SANFORD PROCESS, .0010-.0015 THK & POLISH TO, .266 DIA ONLY, DIMENSIONS APPLY AFTER COATING.
WELDMENT ITEM 2
DETAIL ITEM 1
SEE DETAIL D
DETAIL D
SHARP CORNER
SEE DETAIL B
DETAIL C
DETAIL B
C02391-01-01
PART NO.
WELDMENT CONSISTS OF ITEMS
United Technology Center
INJECTOR, FWD. DUAL ORIFICE POPPET
HTM-2101-16
14134
C02391

DOCUMENT CONTROL DATA - R & D

(Security classification of title, body of abstract and indexing annotation must be entered when the overall report is classified)

1. ORIGINATING ACTIVITY (Corporate author) United Technology Center Division of United Aircraft Corporation Sunnyvale, California	2a. REPORT SECURITY CLASSIFICATION CONFIDENTIAL 2b. GROUP 4

3. REPORT TITLE

Experimental Investigation of Prepackaged Hybrid Propellant Systems (U)

4. DESCRIPTIVE NOTES (Type of report and inclusive dates)

Preliminary Final Report UTC 2141-FR, September 1966 through March 1967

5. AUTHOR(S) (First name, middle initial, last name)

Hamers, J. W.

6. REPORT DATE	7a. TOTAL NO. OF PAGES	7b. NO. OF REFS
May 1967	126	3

8a. CONTRACT OR GRANT NO	9a. ORIGINATOR'S REPORT NUMBER(S)
AF 04(611)-10789 b. PROJECT NO. 3058 c. Element No. 62405184 d. BPSN 623148	UTC 2141-FR 9b. OTHER REPORT NO(S) (Any other numbers that may be assigned this report)

10. DISTRIBUTION STATEMENT

In addition to security requirements which must be met, this document is subject to special export controls and each transmittal to foreign governments or foreign nationals may be made only with prior approval of AFRPL (RPPR/STINFO), Edwards, California 93523.

11. SUPPLEMENTARY NOTES	12. SPONSORING MILITARY ACTIVITY
	Air Force Rocket Propulsion Laboratory United States Air Force Edwards Air Force Base, California

13. ABSTRACT (Unclassified)

An applied research and development program has been conducted on prepackaged hybrid propellant systems suitable for application to advanced tactical missile requirements.

An 18-in.-diameter flight configuration hybrid motor has been designed, fabricated, and tested. A high density, high specific impulse, hybrid propellant combination has been formulated; and a fuel grain geometry has been developed which will provide nearly constant fuel flow rate and permit nearly complete fuel utilization. Dual-thrust oxidizer injectors have been developed and successfully tested. A simple thrust control system has been designed, which will control the motor thrust at two levels and will permit multiple starts at either thrust level.

The results of the program indicate that high density impulse hybrid propulsion systems are feasible for application to advanced tactical missiles.

DD FORM 1 NOV 65 1473

14. KEY WORDS	LINK A		LINK B		LINK C	
	ROLE	WT	ROLE	WT	ROLE	WT
PREPACKAGED						
HYBRID						
PROPELLANT						